BONDED LAMINATES FOR RETROFITTING

OF

REINFORCED CONCRETE BEAMS

A

thesis

Submitted in fulfilment of the requirement

for the award of the degree of

DOCTOR OF PHILOSOPHY

by

PREM PAL BANSAL

Under the supervision of

Dr. S.K. Kaushik
Formerly, Professor & Head
Department of Civil Engineering
Indian Institute of Technology
ROORKEE - 247667

Dr. Maneek Kumar
Professor & Head
Department of Civil Engineering
Thapar University
PATIALA – 147004

DEPARTMENT OF CIVIL ENGINEERING
THAPAR UNIVERSITY, PATIALA – 147004
PUNJAB - INDIA
JANUARY-2008

Dedicated

to

My Parents

CERTIFICATE

Certified that the work presented in the thesis entitled "**BONDED LAMINATES FOR RETROFITTING OF REINFORCED CONCRETE BEAMS**" which is being submitted by Mr. Prem Pal Bansal (Regn. No. 9030251) in fulfillment of the requirement for the award of the degree of 'Doctor of Philosophy' in the Department of Civil Engineering, Thapar University, Patiala, is an authentic record of the candidate's own work carried out during the period from June 2004 to December 2007 at this University under our supervision. The matter presented in this thesis has not been submitted for the award of any other degree in any University.

Dr. S.K. Kaushik
Formerly, Professor & Head
Department of Civil Engineering
Indian Institute of Technology
ROORKEE - 247667

Dr. Maneek Kumar
Professor & Head
Department of Civil Engineering
Thapar University
PATIALA – 147004

ACKNOWLEDGEMENTS

Time has provided me cherished opportunity to express feelings of gratefulness and submit my acknowledgements for those who helped me earning this day in my life.

First of all, I take this opportunity to express my profound sense of indebtedness and heart felt gratitude to my guides **Dr. S.K. Kaushik**, Formerly Professor and Head, Department of Civil Engineering, IIT Roorkee, and **Dr. Maneek Kumar**, Professor and Head, Department of Civil Engineering, Thapar University, Patiala under whom this research work has been completed. I shall ever remain indebted to them for their meticulous guidance, constructive criticism, clear thinking, constant encouragement, moral support and forbearance right from beginning of this research to its completion. Without their tireless efforts and outstanding knowledge of the subject, it would not have been possible for the investigation to take the shape of this thesis.

I am also thankful to Prof. (Dr.) Rafat Siddique, Prof. (Dr.) O.P. Pandey, Dr. Naveen Kwatra, Mr. Rajesh Pathak, Mr. Rajeev Gupta, Dr. Arindam Sarkar, Sh. Gurbinder Singh, Mr. Rajesh Bhatia, Sh. Om Prakash, and other faulty members for constantly encouraging me and providing cheerful support during my tenure of work.

The moral support of my friends Er. Rajesh Gupta, Er. Rajesh Kumar, Er. Sandeep Gupta, Er. Ravi Goel, Er. V.K. Garg, Er. Rajiv Bhandari, Er. Adesh Gupta, is sincerely appreciated. I express my sincere thanks to Mr. Yadvinder Behal, Mr. Rajesh Behal, Mr. Rakesh Behal and all the staff members of the Behal communications for providing those moments of relaxation after whole days work.

Special word of appreciation goes to Sh. Ram Simran, Sh. Amarjit Singh, Sh. Satya Narayan, Sh. Roop Chand, Sh. Avtar Singh and other laboratory colleagues, who helped me in my experimental work.

I would like to thank M/s ACC Cements Ltd., and M/s FEFY Co. for providing cement and GFRP lamination respectively, for the research work free of cost.

I would also like to thank authorities of the University for providing me financial assistance, which helped me to complete the work timely.

Above all, I thank my parents, Sh. Harbans Lal Bansal, Smt. Kamlesh Bansal, whose love and affectionate blessings have been a constant source of inspiration in making this

manuscript reality. The encouraging words from my sisters Mrs. Neelam Singla, Mrs. Gagan Kansal, and my brother-in-laws Sh. Pankaj Singla, Er. Satish Kansal are thankfully acknowledged.

My wife, Ekta, has borne the pains and distress of daily routine. My son Sahir and daughter Ishita always kept my morale high with their ever smiling and cheerful faces. They deserve all admiration.

Last but not the least, I wish to express my thanks to all those who remained behind the screen but whose work has been consulted and quoted in the present research.

In the end, I am thankful and grateful to the Almighty for bringing this day in my life.

(Prem Pal Bansal)

ABSTRACT

The RCC structures constructed these days suffer damage due to a large number of factors like improper design, faulty construction, overloading, change in codal provisions, non-engineered construction, explosions, wear and tear, earthquake, fire etc. A major part of the funds used in the construction industry is being spent on repair, retrofitting and rehabilitation of such structures.

Retrofitting is different from repair or rehabilitation. It is basically a process of strengthening and enhancement of the performance of deficient structural elements in a structure or of the structure as whole. The extent of damage to a structure can be assessed with the help of modern non-destructive testing techniques and methods. Once it is established that a structural member is unable to resist the design loads, the structure has to be repaired/strengthened to make it functional.

The repairing or strengthening of existing structures poses higher challenge to a civil engineer in comparison to design and construction of new structures. Specific technology has to be designed and developed to rehabilitate the damaged structures, and to improve the performance for new functions, of old undamaged structures. Thus, the technique to be used should be simple in execution; offer better performance when handled by less experienced workers, and must use materials that are readily available, durable, strong and economical.

Retrofitting of deficient buildings can be done by increasing the strength, stiffness and/or ductility of its specific constituent elements or of the whole building. For any building, depending upon the requirement, a combination of the above may also be selected. Retrofitting of individual members or elements is referred to as local retrofitting. This retrofitting technique is normally adopted when, after the evaluation, only a few of the building's elements are found to be deficient.

For local repair and retrofitting a large number of techniques are being used. These include injection techniques, shotcreting, removal and replacement technique, external pre-stressing, plate bonding etc. Of all the above techniques plate bonding has been found to be the most effective and a very convenient method. In the plate bonding

technique too, use of Fibre Reinforced Polymer (FRP) laminates has gained lot of popularity in the last decade or so. But FRP lamination requires a lot of skill and its initial cost is very high. As a substitute various authors have suggested the use of ferrocement jacketing as a more attractive option in place of FRP plate bonding due to its easy application, improved tensile strength, lesser weight, economical use, higher impermeability, and long life of the treatment.

In the present study, an effort has been made to study the effect of ferrocement jacketing on the strength of retrofitted beams. The studies have been carried out for various combination's of parameters like type of bonding agents, orientation and type of wire mesh, number of layers of wire mesh in the ferrocement jacket, initial stress level, and type of beam sections (under reinforced or balanced section). The effect of these parameters on the strength of reinforced concrete beams initially stressed in flexure to pre-determined levels, and subsequently retrofitted with jackets was investigated. A design methodology for the retrofitting of stressed beams, using a mathematical model developed based on the limit state design procedure, is provided and verified with the data generated from testing.

A similar set of beams was also retrofitted using the GFRP jackets with orientation of fibres at 0^0 and 45^0 to the longitudinal axis of the beam, to study the behaviour of such beams.

Some of the major conclusions drawn based upon the study are as follows:

1. GFRP jackets used for retrofitting of the under reinforced beams perform better with fibres at forty-five degree to the longitudinal axis of the beam.
2. The strength of the section decreased with increase in initial stress level. The maximum load carrying capacity of the retrofitted beams decreased due to decrease in stiffness of section with increase in initial stress level.
3. GFRP jacketing leads to improvement in energy absorption capacity of all the type of beams irrespective of the type of section (under reinforced or balanced) and orientation of fibres in the jackets.
4. Cement slurry is the most efficient plate bonding agent due to its low cost to strength ratio.

5. Welded wire mesh with forty-five degree orientation to the longitudinal axis significantly improves the load carrying capacity of the retrofitted reinforced concrete beams.
6. Woven wire mesh used for ferrocement jacketing of beams should be preferred over welded wire mesh due to larger improvement in load carrying capacity, ductility ratio and energy absorption.
7. Ferrocement jacketing leads to an improvement in the energy absorption capacity of all type of beams irrespective of the type of section (under reinforced or balanced) and reinforcement in the jackets.
8. The percentage increase in the load carrying capacity of beams retrofitted using ferrocement jackets, increase with an increase in percentage reinforcement in the jackets.
9. The percentage increase in the load carrying capacity of beams retrofitted using ferrocement jackets, decreases with an increase in the initial stress level and with increase in tension reinforcement in the unretrofitted beam.
10. The mathematical procedure proposed in the study can be efficiently used to predict the maximum and safe load carrying capacities of the initially stressed retrofitted beams.

CONTENTS

LIST OF TABLES

LIST OF FIGURES

LIST OF PLATES

CHAPTER -1
INTRODUCTION

1.1 GENERAL

Reinforced concrete is one of the most abundantly used construction material not only in the developed world, but also in the remotest parts of the developing world. The RCC structures constructed in the rural areas of the developing world, pose threat due to its abuse rather than use, due to non-transference of expertise and technology. The majority of the houses are still being constructed in the traditional manner using indigenous techniques following simpler and economical procedures. Unfortunately, such non-engineered constructions are mostly prevalent in earthquake prone areas of the developing world e.g. Turkey, Pakistan, India and Iran. The rural populations in the developing world have to mostly rely on local skill, material and technology. The transformation of non-engineered construction into an engineered one, therefore, needs to be such that it is sustainable.

The RCC structures constructed in the developed world are also often found to exhibit distress and suffer damage, even before their service period is over due to several causes such as.

- Improper Design
- Faulty Construction
- Change of usage of the Building
- Change in Codal Provisions
- Overloading
- Earthquakes
- Explosion
- Corrosion
- Wear and tear, Flood, fire etc.

Such unserviceable structures require immediate attention, enquiry into the cause of distress and suitable remedial measures, so as to bring the structure back to its functional use again.

In the last few decades or so, several attempts have been made in India and abroad to study these problems and to increase the life of such structures by suitable retrofitting and strengthening techniques.

1.2 RETROFITTING

Retrofitting is basically a process of strengthening and enhancement of the performance of deficient structural elements in a structure or structure as whole. It is different from repair or rehabilitation. Repair refers to partial improvement of degraded strength; it's only a cosmetic enhancement. Rehabilitation is a functional improvement, wherein the aim is to achieve the original strength of the structure, after it has deteriorated and suffered damage. Retrofitting means structural strengthening of the building to a pre-defined performance level irrespective of whether the structure is damaged or not. Thus, the goals of the retrofitting can be enumerated as (*IS:13935:1993, White 1995*)

- Removing the weak points, where stress concentration is possible.
- Increasing the lateral load carrying capacity and stiffness of the building
- Improving the energy absorption and energy dissipation capacity of the building
- Achieving the desired performance most effectively and economically.

1.2.1 Retrofitting Program

A typical retrofitting program includes the following steps (*Basu, 2002*)

(a) Evaluation

It means checking the suitability of an existing building for the desired purpose as per the latest codal provisions and, analysis and design techniques. The evaluation process involves collection of data for the existing buildings, preparation of architectural drawings as per site, collection of structural drawings and verifying/modifying them according to as built information, visual inspection of the building, performing non-destructive and destructive tests as per site requirement. After the collection of the data the building is analyzed and designed as per current methods and codes. If the demand-to-capacity ratios of the components are greater than one or if the building fails to achieve the target performance level, then retrofitting becomes necessary.

(b) Decision to Retrofit

Based upon the extent of deficiency, the economic viability, and the expected performance after retrofitting, a decision is taken whether to repair, retrofit or demolish and reconstruct the building.

(c) Selection and Design of Retrofit Scheme

After the evaluation and decision to retrofit, the type of retrofit scheme is selected depending upon the deficiencies in the building and the members to be strengthened. The various retrofit schemes possible are discussed in the succeeding section.

(d) Verification of Retrofit Scheme

The selection of a particular retrofitting scheme is justified with the help of proper structural analysis and design of the structure to be retrofitted. The possible modes of failure after retrofitting need to be studied and an increase in strength at the cost of a ductile failure mode changing to brittle is not desirable.

(e) Construction

The effectiveness of the retrofit scheme greatly depends on the quality and effectiveness of execution. So, the selected scheme should be such that it can be easily executed at the site.

(f) Monitoring

Monitoring the performance of the retrofitting scheme is necessary to detect any defect or remaining deficiency. This will lead to refinement of the design guidelines and specifications for future retrofit projects.

1.2.2 Retrofitting Strategies

Retrofitting of a building can be done by increasing the strength, stiffness and/or ductility of the elements or of the whole building. Depending upon the requirement of a building a combination of the above may be selected. Retrofitting strategies may be broadly classified into the following categories:

(a) Global Retrofitting

(b) Local Retrofitting

(c) Base Isolation and Energy Dissipation

(a) Global Retrofitting

The retrofitting of the building as a whole is termed as global retrofitting. This is undertaken to improve the overall behavior of the building. If the evaluation of the building indicates large demand-to-capacity ratios in the components throughout the structure, then normally global retrofitting strategies are adopted. This may involve providing additional elements like shear walls and braced frames, reduction in the plan and vertical irregularities, reduction in the mass and improving the connections between elements.

(b) Local Retrofitting

Retrofitting of individual members or elements is referred to as local retrofitting. This retrofitting technique is normally adopted when after the evaluation only a few building elements are found to be deficient. The local retrofitting includes the strengthening of beams, columns, joints, walls and footings and connections to resist the predicted demand. The various local retrofitting strategies are discussed in detail in the succeeding section.

(c) Base Isolation and Energy Dissipation

The behavior of the buildings during an earthquake can be improved by providing energy dissipation or base isolation devices.

The energy imparted to a structure during an earthquake can be dissipated by special devices such as viscous fluid dampers, yielding plates or friction pads. These are called energy dissipation devices. A tuned mass damper is one such device consisting of a mass, spring and viscous damper attached to a vibrating main system in order to attenuate any undesirable vibrations. Because the natural frequency of the damper is tuned to a frequency near the natural frequency of the main system, it causes the damper to vibrate in resonance, dissipating the vibrating energy through the damping in the tuned mass damper *(Tsai and Lin 1993)*.

Base isolation produces a system with a fundamental response that consists of nearly rigid body translation of the structure above the bearings. Most of the displacement included in the isolated system by the ground motion occurs within the compliant bearings, which are specifically designed for the large displacements. Most bearings also have excellent energy dissipation characteristics.

1.2.3 Local Repair and Retrofitting Techniques

A large number of local repair and rehabilitation techniques are being used now-a-days. Some of these are as discussed below.

(a) Epoxy Injection Technique

This technique involves injection of high strength epoxy into cracked concrete, filling the voids and rebinding the fractured structure. Depending upon the viscosity of the epoxy, low or high, it can be used for the repair of fine cracks and surface coating or filling large cracks, respectively. This technique generally involves drilling holes at

close intervals along the cracks, in some cases installing entry ports, and injecting the epoxy under pressure.

The basic steps needed in epoxy injection are as follows:

1. Cleaning the Cracks: Remove any contamination by flushing with water or some specially effective solvent. Then blow out the solvent with compressed air, or allow adequate time for air drying.
2. Sealing the surfaces: This keeps the epoxy from leaking out before it has polymerised. A surface can be sealed by brushing any epoxy over the surface of the crack and allowing it to harden. If high injection pressures are needed, prepare the crack in a V-shape, fill with epoxy, and strike off flush with the surface.
3. Installing entry ports: This is done by drilling a hole into the crack, penetrating below the bottom of the V-grooved section
4. Mixing the epoxy in batch mixing: The adhesive components are pre mixed as per the manufactures instructions, usually with a mechanical stirrer like a paint mixing paddle.
5. Injecting the epoxy: This is done using hydraulic pumps, paint pressure pots, or air-actuated caulking guns. The pressure should be selected carefully because too much pressure can extend existing cracks and cause more damage.
6. Removing the surface seal: This is carried out after injected epoxy has cured. Surface seal is removed by grinding or some other appropriate means.

(b) Mortar Injection Technique

In this method repairing is done by injecting pre-mixed mortar. It is mainly used to repair old works where conventional placing of concrete is difficult. It is used for large repair jobs, in under water placements, piers and retaining walls. It consists of injecting grout into the voids of compacted mass of clean and well-graded aggregates. The injection of the grout should be smooth with uninterrupted operation and positive head should be maintained in the grout lines after the forms have been filled and grout is set.

(c) Epoxy Mortar Filling Method

In this method, epoxy of low or high viscosity is mixed with fine aggregate to form epoxy mortar. Epoxy mortar has higher compressive and tensile strengths and lower

modulus of elasticity as compared to cement concrete. It is used for filling the larger voids.

(d) Shotcreting

The cast in place ready mix concrete or air placed concrete is commonly called shotcrete. The shotcrete is placed either by a dry mix or a wet mix process. If specified, fibres of steel, polypropylene or other material may be used together with the admixture to modify the structural properties of concrete/mortar to be placed in position. Shotcrete is ideally suitable for repair works that require concrete to be placed between existing elements where an intimate surface is needed.

(e) Removal and Replacement Technique

This technique involves replacing loose and damaged concrete with new concrete. Additional reinforcement can be provided by welding it to existing steel. The other replacement material used is epoxy sand mortar.

(f) Repair Using Steel Fibrous Concrete

In this method damaged portion of concrete in beams is removed, and this portion is recast using concrete mixed with steel fibers. Steel fibrous concrete exhibits ductile behavior, better stiffness and better shear strength as compared to conventional concrete.

(g) External Prestressing

Post tensioning is often a good solution when a major portion of the member has to be strengthened or when cracks must be closed. Prestressing strands or bars are used to apply compressive force to the ailing member. This technique needs adequate anchorage for the prestressing steel, analysis of the effect of the tensioning force and eccentricities on stresses in the structure.

(h) Concrete Replacement Technique

This technique is used to repair large and deep patches, which occur during the repair of deteriorated portion of a concrete structure. This is basically used in the repair of walls, parapets, piers and kerbs. This method can be applied either as dry packing, or as grouting.

Dry packing: is a method in which a mortar of low water content is hand placed on the prepared surface followed by tamping or ramming it into place, so as to produce an intimate contact between the mortar and existing concrete.

Grouting: is a method in which deep and wide cracks are repaired by filling them with cement grout. The grouting is done under high pressure and after the crack is filled, the pressure is maintained for sometime to ensure good penetration.

(i) Plate Bonding Technique

The idea of plate bonding technique is mainly based on the fact that concrete is a building material with high compressive strength and poor tensile strength. A concrete structure without any form of reinforcement subjected to tension or bending will crack at a relatively small load. Thus, in order to increase the strength of the concrete/structure, plates of different materials are bonded on the soffit or web faces of the flexural elements using any of the following bonding agents.

(i) Cement Slurry.

(ii) Epoxy Adhesives

(iii) Shear Connectors, or

(iv) Combination of (i) or (ii) with (iii) above

Three types of plates are commonly used in this technique, namely

(i) Steel plates.

(ii) Fiber Reinforced Polymer (FRP) Plates.

(iii) Ferrocement Plates

The salient features of each of the technique are explained below:

(i) Steel Plates

Steel plate bonding technique has its origin in South Africa, wherein steel plates were used to strengthen a concrete beam as some of the reinforcement had been accidentally omitted in the construction. It substantially increased the strength, ductility, stability and stiffness of the beams and also, reduced the crack width. The addition of steel plates is simple and rapid to apply, does not reduce the clear height of the storey significantly and can be applied even when building is in use. The plating may be done either on the tension face or on the side faces of the beams as shown in Fig. 1.1 The tension face plates accomplish the highest increase in flexural strength and stiffness. Side-face plating mainly increases the shear capacity and the flexural strength to a limited extent. A combination of above two methods is also done in the form of U-shaped jackets. Technically this method performs well but it has some drawbacks, like the risk of corrosion and also the steel plates might need lengthening by welding due to limited transportation length.

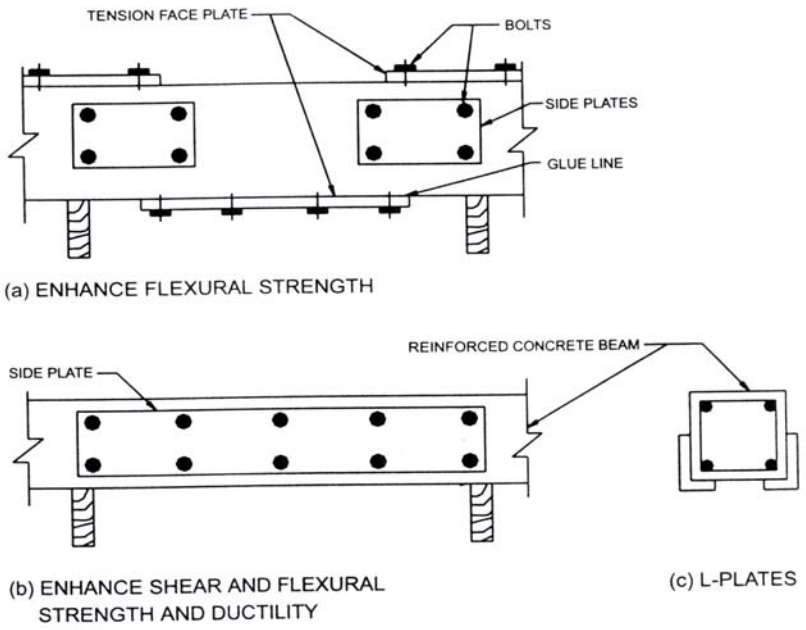

Fig. 1.1 Strengthening of Beams Using Steel Plates

(ii) Fiber Reinforced Polymer Plates

The term Fibre Reinforced Plastics describes a group of materials composed of inorganic and organic fibres embedded in a resin matrix. FRPs possess excellent properties such as high tensile strength and stiffness; are lightweight and non-magnetic, and offer good resistance to corrosion and chemicals, which make them particularly suitable for the rehabilitation and strengthening works. One such application in columns is shown in Fig. 1.2. In the construction industry, the most commonly used FRPs are Glass fibre reinforced plastics (GFRPs), Carbon fibre reinforced plastics (CFRPs) and Aramid fibre reinforced plastics (AFRPs).

FRP is mechanically different from steel since it is anisotropic, is linearly elastic and has usually high strength with lower modulus of elasticity than steel. FRP sheets are thin, light and flexible enough to be inserted behind the pipes, electrical cables, and other service ducts thus facilitating their installation.

The main drawback of FRP sheets is their high cost. The other disadvantages are susceptibility of FRP to moisture and degradation of properties at high temperatures, as in case of fire and damage due to ultraviolet exposure.

FRP has not only been used as sheets, but also as reinforcing bars. FRP bars can also be attached to web of a beam for shear strengthening (*Lorenzis and Nanni,*

2001,2002). These near surface mounted bars can be anchored to the flange of the beam. The failure occurs due to debonding of the bars due to splitting of the epoxy paste in the grooves.

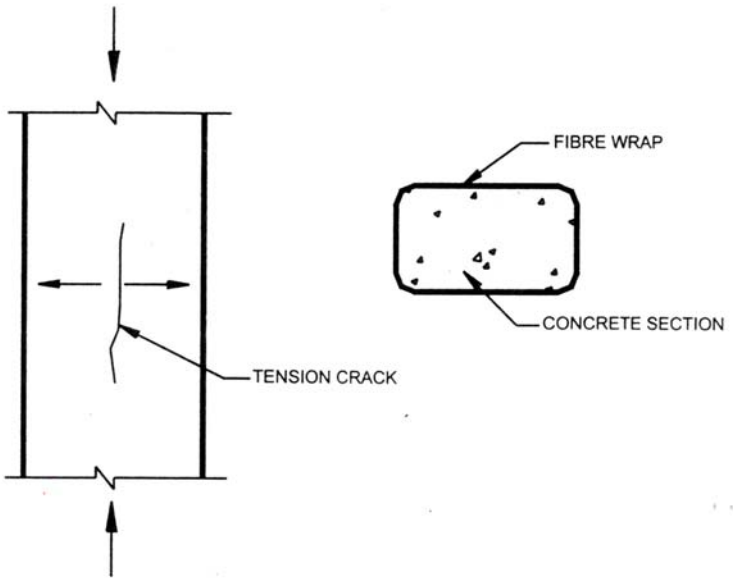

Fig. 1.2 FRP Wrapping Technique

(iii) Ferrocement Plates

Ferrocement is a type of thin walled reinforced concrete commonly constructed of hydraulic cement mortar reinforced with closely spaced layers of continuous and relatively small size wire mesh. Ferrocement is capable of resisting high tensile, shear, impact, and fatigue stresses coupled with excellent resistance to corrosion and ingress of water. Ferrocement plates can be used to increase the load carrying capacity of concrete elements, provide permanent formwork to the concrete structures, glued to the surface or cast-in-situ and bonded to the structural element using suitable bonding agents. Also, ferrocement has a lower cost as compared to steel and FRP. Therefore, ferrocement plates can be an excellent alternative to steel and FRP plates.

Of the afore discussed techniques plate-bonding is one of the most effective and convenient methods of retrofitting. Among the plate bonding techniques FRP plates are quite popular now-a-days. But it is observed that the use of FRP is restricted to developed countries or urban areas of the developing countries due to higher initial cost and requirement of skilled labour for their application. Thus, there is a need to

develop an alternative technique, which is economical and can be executed at site with the help of semi-skilled labour available at site. Ferrocement jacketing is found to be one such attractive technique due to its properties such as good tensile strength, lightweight, overall economy, water tightness, easy application and long life of the treatment.

It is proposed to use ferrocement jackets for carrying out the current study due to its advantageous properties of being lightweight, durable and having low thermal conductivity material, and can be cast into any shape at site. It is economical and does not require any specifically skilled labour for execution. It is also proposed to use GFRP jackets for comparison purpose. A review of the work earlier carried out using ferrocement and FRPs is presented in the succeeding chapter.

1.3 OBJECTIVES AND SCOPE OF THE WORK

The main objectives of the present work are follows:

- Study the effect of retrofitting on beams stressed to different levels.
- Study the effect on the maximum load, safe load and ductility of the (under reinforced and balanced) beams retrofitted with ferrocement jackets with variation in following parameters.
    (a) Type of wire mesh,
    (b) Number of wire mesh layers,
    (c) Orientation of mesh.
- To develop a technique and methodology for designing and using ferrocement jackets for retrofitting of stressed RCC beams using conventional RCC theory.
- To compare the data, with beams retrofitted with GFRP jackets having different orientation of fibres (0^0, 45^0)

The scope of the present work includes studying first of all, the effect on maximum and safe load carrying capacity, ductility and toughness, of the orientation of fibers on the beams retrofitted using GFRP jackets. In the second part the effect of various parameters such as type of bonding agent, type of wire mesh, number of wire mesh layers, and orientation of the wire mesh, on the maximum and safe load carrying capacity, ductility and toughness, of the beams retrofitted using ferrocement jackets. To achieve this firstly, with the help of pilot studies parameters are finalized for the final study. Various pilot studies undertaken are as follows:

(i) Effect of type of bonding agents on the Strength of the beams retrofitted using ferrocement jackets.

(ii) Effect of wire mesh orientation on the strength of the beams retrofitted using ferrocement jackets.

(iii) Effect of type of wire mesh on the strength of the beams retrofitted using ferrocement jackets.

From the pilot studies an efficient bonding agent, orientation of wire mesh, and type of wire mesh is finalized for the final study. In the final testing program the effect of type of section (under reinforced or balanced), initial stress level, and number of wire mesh layers, on the maximum and safe load, ductility and toughness is studied on the prototype beams.

In the end efforts has been made to develop a mathematical model for calculating the maximum and safe load carrying capacity of initially stressed beams, retrofitted using ferrocement jackets. The mathematical model so developed is validated with the experimental results obtained from the test programme undertaken and also compared with work done by earlier researchers.

1.4 ORGANIZATION OF THESIS

The thesis is presented in the seven chapters as detailed below:

Chapter – 1 introduces the retrofitting of structures, need of retrofitting, and various methods of retrofitting and different materials used now-a-days for local retrofitting of elements. At the end of the chapter objectives and scope of the study are given.

Chapter – 2 on literature review presents the work done by various researchers in the field of ferrocement, application of ferrocement, retrofitting of structures using ferrocement and FRP laminates and jackets.

Chapter – 3 details the materials used, techniques adopted for casting, curing, testing, retrofitting of the beams, the pilot studies undertaken for the finalization of parameters for further detailed study along with their results and conclusions.

Chapter - 4 details the scheme of experimentation, variables involved, for retrofitting of the beams using GFRP and ferrocement jackets.

Chapter- 5 deals with the analysis and discussion of the results obtained from the experimental data of the beams retrofitted using ferrocement jacketing. The results are presented both in tabular as well as graphical form.

Chapter – 6 deals with the retrofitting of stressed beams using GFRP jacketing. The results obtained from the experimental program of the control and retrofitted beams are presented and discussed.

Chapter – 7 The mathematical model developed and validation of the model with the test results obtained is presented in this chapter.

Chapter – 8 gives the major conclusions of the study.

A list of references, referred in the work and appendices are presented after chapter-8. The notations and symbols have been defined where they appear first in the text.

CHAPTER-2
LITERATURE REVIEW

2.1 GENERAL

A 30 years record of major Turkish earthquakes show that almost 0.2 million dwellings were destroyed by earthquakes (*Gulkan and Wasti, 1980*), which is about 65% of the destruction caused by all other natural disasters. Dinar earthquake of 1995 and Kocoeli earthquake of 1999 have substantially increased the percentage. Almost all post earthquake studies and damage assessment have led to the conclusion that a building should be designed and constructed such that in the event of the occurrence of an earthquake of probable maximum earthquake intensity: the building does not suffer total or partial collapse; it should not suffer such irreparable damage which would require demolition and rebuilding and in case it sustains such damage it could be repaired quickly and easily to bring it to its usual functioning (*ISET, 1981*).

Although concrete is the most widely used man made construction material in the world it is heterogeneous in nature, brittle in behavior and possesses relatively low tensile strength when compared to its high compressive strength. The low tensile strength of concrete is normally compensated by reinforcing steel, whenever, it is subjected to tensile stress. The use of reinforcement does not improve the inherent low tensile strength and brittle behavior of concrete. But it delays the propagation of the micro cracks, which are invisible to naked eye, and are inherently present in the concrete at the aggregate-cement paste interface. These micro cracks propagate with the application of load, to form visible structural cracks.

Efforts have been made to improve the above stated basic deficiencies of concrete, by evolving two-phase composite materials wherein the presence of one phase improves the basic properties of the other phase and each phase is used to its best advantage.

Ferrocement over the years has gained respect in terms of its superior performance and versatility, and now is being used not only in the housing industry but its use is being continuously explored in retro-fitting and strengthening of damaged structural members (*Singh and Kaushik et al, 1998*). Ductility requirements are the main feature of an efficient earthquake resistant design process, and ferrocement being a highly ductile material has led to its

application in the rehabilitation of houses damaged by earthquakes. The effectiveness of its use has been reported by many researchers (*Desia, 1999, Wasti and Erberik et al, 1998*). Taking the lead from its potential use in enhancing earthquake-resisting abilities, 5 houses were built in Northern area of Pakistan, using indigenous materials and local skills, utilizing ferrocement bands to improve the earthquake resistance of such houses in 1990 (*NED university, 1998*). The houses since then have performed remarkably well and have sustained low to moderate shocks effectively. The details were simple to follow and execute by the local skilled workers, and materials were readily available from near by cities. Composite construction with ferrocement gives more versatility to this delicate looking thin walled construction material. Its path for future as a laminated cementitious composite combining advanced cement based matrices, high performance reinforcing meshes and fibres, and new construction techniques promises to be very bright (*Naaman, A.E. 2001*).

Many experimental studies have been conducted in recent years to strengthen flexural members by using various materials. *Andrew and Sharma (1998)* in an experimental study compared the flexural performance of reinforced concrete beams repaired with conventional method and ferrocement. They concluded that beams repaired by ferrocement showed superior performance both at the service and ultimate load. The flexural strength and ductility of beams repaired with ferrocement was reported to be greater than the corresponding original beams and the beams repaired by the conventional method.

The bonding of fibre reinforced plastic (FRP) laminates to tension face of concrete girders is becoming an attractive solution to the rehabilitation and retrofit of damaged structural systems. *Al-Farabi et al (1993),* while investigating the effectiveness of fiberglass bonded plates for capacity enhancement, reported an increased strength and reduced ductility. Premature failure by plate separation was also identified as a potential problem at the plate curtailment location. Steel plates bonded by epoxy were used to repair shear-cracked beams utilizing various forms of plate bonding by *Basunbul et al (1993)*. The experimental investigation clearly demonstrated that the effectiveness of the repair primarily depends on how effectively the diagonal tension cracks in the shear-damaged beams were trapped. Flexural mode of failure was observed surpassing shear capacity for only those specimens where full encasement of the shear zone was carried.

2.2 FERROCEMENT

J.P. Lambot originally developed ferrocement in the 1870's in the Var region of France as a means for constructing a boat, its main difference from traditional RCC being that reinforcement is subdivided.

Ferrocement is a thin composite material made of cement mortar and reinforced with layers of continuous and relatively small diameter wire mesh, natural fibers like bamboo strips, synthetic fibers like nylon etc which are closely bound together to create stiff structural form. As per *ACI committee – 549 (1988)* ferrocement is a form of reinforced concrete using closely spaced multi layer mesh and /or small diameter rods completely infiltrated with, or encapsulated, in mortar. Due to its excellent tensile strength, durability, lightweight, smaller crack widths as compared to RCC and low thermal conductivity, it is being used in wall elements, roofing, water tanks, silos, boat construction industry and for architectural purposes also.

It is the uniform distribution of the reinforcement in the resulting composite and its different material performance, strength behavior and potential applications, which distinguish ferrocement from conventional reinforced concrete. Generally thin continuous steel wires are used in the form of mesh. The mesh may be of welded or woven type or in any other form as found economically suitable such as slotted steel sheets, expanded metal mesh etc. These thin wires provide very large surface area per unit volume of steel used thus increasing the bond strength, which is assumed to be proportional to the surface area of wires in contact with the mortar. As a result, failure of ferrocement generally takes place by yielding of wires, and not by slippage or bond failure. Thus, there exists a perfect 'composite action' over a certain range of stresses which are much wider than any other composite structural material like concrete, RCC, cement, mortar etc.

It has been reported that ferrocement, even on being subjected to one thousand cycles of wetting and drying, and nine weeks of curing in sodium chloride solution, retains its stiffness and ultimate strength [*Ravinderarajah, R. S. and Parmasivam, P., 1986*]. Steel wire mesh with closely spaced wires is the most commonly used reinforcement in ferrocement. Its presence in ferrocement improves its crack resistance, impact strength, and toughness [*Ravinderarajah, R. S. and Parmasivam, P.,1988*]. Expanded metal mesh, welded wire fabric, wires or rods, prestressing tendons, and discontinuous fibres are also being used in special applications or for reasons of performance or economy [*ACI committee – 549, 1988*]. The hexagonal (chicken) wire

mesh and woven square mesh give a better performance for elastic and ultimate design when placed uniformly rather than in-group binding [*Hossain, M.Z. and Hasgawa, T, 1998*].

Ohama and Shirai (1992), compared the durability of polymer-ferrocement with conventional ferrocement. The polymer-ferrocement, using styrene- butadiene rubber latex, was prepared with various polymer-cement ratios, and tested for accelerated carbonation, chloride ion penetration and accelerated corrosion. It was concluded that the carbonation and chloride ion penetration depth of polymer-ferrocement decreases markedly with an increase in the polymer-cement ratio regardless of the exposure and immersion periods, and are strongly affected by polymer-cement ratio and water cement ratio. The corrosion inhibiting property of polymer-ferrocement is remarkably improved with an increase in the polymer-cement ratio.

A brief review of the various properties of the ferrocement is as under:

2.2.1 Ferrocement in Tension

The tensile strength of ferrocement depends mainly on the volume of reinforcement in the direction of the applied force and the tensile strength of the mesh. The tension behavior may be divided into three regions, namely, pre-cracking, post-cracking stage and post-yielding stage. A ferrocement element subjected to increasing tensile stresses behaves like a linear elastic material till the development of the first crack in the matrix. Once the cracks have developed the material enters the stage of multiple cracking and this stage continues up to the point where the wire meshes start to yield. In this stage the number of cracks keeps on increasing with an increase in the tensile stress without any significant increase in the crack width. After the yield of reinforcement, the composite enters the stage of crack widening. The number of cracks remains essentially constant and the crack width keep on increasing. The reinforcement bars primarily control this type of behavior.

The tensile strength of ferrocement is significantly affected by mesh-parameters, strength characteristic of the mortar used, type of mesh and degree of compaction if done manually. Mesh-parameters like orientation of wires relative to loading axis, and specific surface factor are directly responsible for enhancement of the tensile strength of ferrocement.

The tensile strength of ferrocement is significantly affected by the following parameters:

1. Type of mesh,

2. Compressive Strength/Composition of mortar, and

3. Degree of compaction.

The strength of ferrocement in direct tension σ_c can be calculated using the 'rule of mixtures'

$$\sigma_c = \sigma_m V_m + \sigma_f V_f \qquad (2.1)$$

where σ_m and σ_f are stresses in the matrix and fibres, respectively and V_m and V_f are the respective matrix and fibre volume ratios.

An increase in the tensile force cause excessive strains, the matrix cracks and the bond between matrix and steel wires is lost. Thus, at ultimate tensile strength the matrix does not contribute to the tensile strength of ferrocement, and its ultimate tensile strength in direct tension is equal to that of the longitudinal steel wires only [*Rajagopalan, K. and Parameswaran, V.S., 1974*]. Although, the orientation of the reinforcement has no significant effect on the tensile strength of ferrocement [*Johnston, Colin D. and Mattar, Samir G, 1976 & Khanzadi, M.K. and Ramesht, M.H. , 1996*], but it has been reported [*Abdullah and Mansur, M.A . 2001*] that the first crack strength, ultimate strength, effective modulus and efficiency of ferrocement elements decrease as the angle of wire mesh orientation increases from 0 to 45 degree, but arrangement of the reinforcement has no effect . The tensile strength at cracking is directly proportional to specific surface factor (S_f) [*Kamasewara, Rao C.B. and Rao, A. Kamasundara, 1994 & Ravinderarajah, R. S. And Parmasivam, P., 1988*]. Also, the ferrocement elements with evenly distributed reinforcement and minimum cover show reduced crack widths and increased number of cracks at failure.

Johnston & Mattar (1976), studied the effect of mesh type, thickness of mortar and orientation of wires relative to the loading axis and concluded that, orientation of the reinforcement has a marked effect on the absolute strength. It was also concluded that the ultimate load is independent of the type of wire mesh and specimen thickness because the mortar is cracked long before failure and does not contribute to the ultimate strength of the composite. The specimens reinforced with expanded metal mesh shows greater stiffness and almost complete absence of visible cracks prior to failure due to the geometry of wire mesh.

Al-Noury and Huq (1988), investigated the behavior of ferrocement in tension. They proposed expressions for predicting the first crack strength and modulus of elasticity of ferrocement in the un-cracked and cracked range. It was found that the crack

strength of ferrocement in tension can be predicted on the basis of the strain at the limit of proportionality of mortar and the un-cracked modulus of ferrocement. The modulus of elasticity of ferrocement in the cracked range can be predicted on the basis of the behavior of an equivalent model with aligned wires. Beyond the first crack, the crack formation mechanism in ferrocement in the cracked range is related to the matrix-wire interfacial bond.

Akhtaruzzaman and Pama, (1988), performed an analytical and experimental investigation on the crack spacing and crack width of ferrocement in direct tension. The theoretical investigation showed that the slip modulus, ultimate bond strength and modulus of elasticity of mortar have negligible influence on the crack spacing while the ultimate tensile strength of the mortar and the volume fraction and modulus of elasticity of steel have significant influence on the crack spacing. The crack width was found to be greatly influenced by the volume of steel fraction, modulus of elasticity of steel and ultimate bond strength of mortar.

Abdullah and Mansur (2001), have shown that first crack, ultimate strength, effective modulus and efficiency of ferrocement elements decreases as the angle of wire mesh orientation increases from 0 to 45 degrees. They also showed that first crack strength increased as the specific surface, diameter and spacing of transverse reinforcement increased.

2.2.2 Ferrocement in Compression

The behavior of ferrocement in compression is influenced by the type of mesh and strength characteristics of cement mortar used as reported by various researchers.

ACI committee 549 (1988) has proposed following equation to calculate the ultimate compressive strength of ferrocement sheet

$$P_{ult} = 0.85 C_r \phi f_c \qquad (2.2)$$

Where $C_r = 1 - \left(\frac{l}{40r}\right)$, for wall elements

$C_r = 1 - \left(\frac{l}{60r}\right)$, for columns and wall elements with $1/r > 40$

Johnston and Mattar (1976), showed that the welded wire mesh is much superior to expanded metal mesh as compression reinforcement. From the failure patterns of the specimens they concluded that the geometry of the expanded metal mesh promotes an

expansive scissors action in the lateral direction which renders the reinforcement ineffective as the restraint required to exploit the triaxial strength of the mortar within. It was also concluded that the orientation of the reinforcement has a relatively minor effect in compression due the scissor action in either direction and the lateral reinforcement influences the strength much more strongly than the longitudinal reinforcement. The lateral steel carries 17-42 percent of the total load and the longitudinal steel carries only 5-14 percent. Therefore, rectangular mesh with a large amount of steel deployed in the lateral direction should give a better strength- cost effectiveness than square meshes.

Kameswara Rao and Kamasundra Rao (1986) investigated the stress-strain curve and Poisson's ratio of ferrocement in axial compression. It was found that the specific surface is the only factor, which controls the behavior of ferrocement in axial compression. The ferrocement behaves linearly up to 50-60 percent of the ultimate strength in compression; beyond this limit the behavior becomes non-linear. The value of strains at ultimate strength and young's modulus increases with the specific surface area.

Mansur and Abdullah (1998) studied the behavior of ferrocement panel subjected to biaxial tension-compression and found significant reduction in strength as well as stiffness of ferrocement in compression, due to presence of tensile strain in the perpendicular direction. However, the extent of such reduction was not as large as in ordinary reinforced concrete panels

The number of layers, with a minimum of two, also increases the load carrying capacity of compression members. Its better impact resistance also makes it useful for application in pre-cast ferrocement slender piles [*Chockalingam S. et al 1988*].

It was observed that ferrocement plates subjected to edge wise compression fail in buckling for slenderness ratio greater than 100 and in crushing/splitting for slenderness ratio less than 100 [*Kaushik, S.K., Singh, K.K. and Prasad, Rajinder, 1994*].

Ferrocement has also been used as a casing to existing masonry, concrete and RCC columns. The load carrying capacity of masonry columns encased with ferrocement has been observed to be 2 to 2.5 times as compared to uncased columns. The strength increase is manily due to additional strength contributed by the ferrocement casing. The failure of encased columns is due to failure of casing under combined bending and tension in the lateral direction and pre-mature failure can occur if mesh is not

wrapped properly and plaster does not penetrate into it fully. In most of cases local failure occurs near the end of the specimens due to platen effect [*Singh, K.K., Kaushik, S.K. and Prakash, Anand, 1988*, *Ahmed, T., Ali, Sk.S. and Choudhury, J.R., 1994*].

This significant increase in compressive strength and ductility has also been observed in case of ferrocement encased concrete columns for both axial and eccentric loading. However, the effectiveness of the confinement reduces with an increase in the slenderness ratio. At slenderness ratio values above 100 there is little difference in the strength and ductility due to confinement. The ratio of the core area to the total area and shape of the column is also significant for the strength increase. Confinement is less effective in case of rectangular columns than for circular sections [*Kaushik, S.K. , Prakash, A. and Singh, K. K., 1994, Singh, K.K., Kaushik, S.K. and Prakash, Anand, 1988]*.

Similar types of results are reported by various authors for RCC columns, either encased or repaired using ferrocement. *Nedwell, P.J. et al (1994)* reported that repair behaved, to a large extent, independently of the column but that the restraint provided by the ferrocement casing adds significantly to the ultimate strength.

Takiguchi, K. and Abdullah (2001) repaired and strengthened RC columns with inadequate shear strength, using ferrocement jacket and tested the repaired columns under cyclic lateral forces and constant axial load. From the test results it was found that the proposed repair and strengthening technique is very effective. It was also reported that the regardless of the number of layers of wire mesh, condition of original column before being strengthened, and the shape of the jacket, all the strengthened columns exhibit superb ductility performance. For the columns with lean cores, ferrocement casing with large volume fraction of mesh can contribute to large percentage strength increase due to beneficial effect of confinement [*Singh, K.K., Kaushik, S.K. and Prakash, Anand, 1988*]. Thus, ferrocement is an economical and a viable option for jacketing and repairing of columns.

2.2.3 Ferrocement in Flexure

Ferrocement has excellent tensile strength, as reported by a number of researchers, almost comparable to the compressive strength of the cement mortar used. As a result, ferrocement specimens remains crack free over a wide range of loading. Also the cracks produced in the post-cracking range are very fine, and are not capable of

affecting the flexural behavior. Thus, a whole section can be taken to be effective in resisting the imposed loading till attainment of ultimate strength in the mesh wires.

Johnston and Mowat (1974) have reported that the strength of ferrocement in flexure is mainly affected by the type of reinforcement, orientation of wire mesh and distribution of reinforcement across the depth. The high degree of subdivision of reinforcement and its uniform distribution in the matrix of the ferrocement results in narrow and uniformly spaced cracks under loading, rather than wide more random cracking that is symptomatic of conventional reinforced concrete. They compared the strength behavior of expanded metal mesh, welded mesh and woven mesh and concluded that the expanded metal mesh offers the best performance in terms of uniaxial bending. However, in biaxial bending the expanded metal mesh imparts considerable weakness in the second direction, and bars do not contribute any strength in this direction. To improve the behaviour in biaxial bending, expanded metal mesh should be placed with the orientation altering between the consecutive layers. Whereas, the welded wire mesh, offers equal strength in both the directions and is more effective than the woven wire mesh. So, two-dimensional fixity, elimination of bond failure, and restraint offered by the lateral component of reinforcement make the expanded metal mesh and welded wire mesh superior than the woven wire mesh. The performance of the ferrocemnt beams is optimal when the reinforcing layers are spaced uniformly throughout the depth of the section.

It has been observed that the crack width decreases but number of cracks increase in ferrocement beams as compared to RCC beams. Consequently, the impermeability, stiffness and durability of the beams improve. Also a higher-grade matrix and volume fraction of wire mesh reinforcement increases the first crack strength and the ultimate moment of resistance. However, a lower grade matrix gives more cracks due to its higher ductility but higher volume fraction has been observed to provide effective control of crack width by formation of a larger number of well-distributed cracks. The ultimate moment increases with an increase in either the volume fraction of the reinforcement or the grade of matrix [*Mansur, M.A. and Paramasivam, P., 1986, Onet, Train et al, 1992*]. The transverse reinforcement is beneficial with respect to crack development in ferrocement beams and it also plays an important role in improving the ultimate moment of ferrocement elements. It was reported that both yield strength and ultimate strength improves with increasing the number of layers of the wire mesh, but no significant improvement was noted with increase in number of

wires in single layer [*Ramesht, M.H., Nedwell, P.J., 1994*]. The first crack strength of ferrocement bundled and placed near the top and bottom surfaces is about 16 per cent higher than those having evenly distributed reinforcement [*Ravinderarajah, R. S. And Parmasivam, P., 1988*]. The number of layers and thickness of ferrocement affect significantly on the first crack strength and ultimate load. However, the arrangement of wire mesh do not affect significantly [*Hossain, M.Z. and Hasgawa, T., 1998*]. The performance of ferrocement in flexure has also been observed to improve if stainless steel wire mesh and 10 per cent silica fume by weight of cement is added to it [*Nedwell, P.J. and Nakassa, A.S., 1999*]. *Karasudhi, P. et al (1977)* studied the fatigue strength of ferrocement in flexure with three different types of wire meshes. Viz. chicken wire mesh, welded square mesh, and expanded metal. Test results reveled that the fatigue strength of ferrocement is dependent on the fatigue properties of the reinforcement as in case of reinforced and prestressed concrete. Among the three wire meshes used, chicken wire mesh imparted greater fatigue strength over the others. The behavior of ferrocement beams in long-term loading reveals that ferrocement being a flexible material; it is necessary to first consider deformability of the ferrocement member, then the proper selection of cross-sectional shape etc. [*Onet, T. and Magureanu, C., 1993*]

The ferrocemnt members are fabricated in thin section thus their relatively large deflections may constitute an important design limitation. *Balaguru, Perumalsamy et al. (1977)* carried out an investigation to predict deflections and crack widths for ferrocement structures subjected to flexure, for different amount of volume fractions of the reinforcement. It was observed that the specific surface area does not have a strong influence on the cracking behaviour in flexure and the crack width in the ferrocement elements in flexure can be calculated using the following expression:

$$w_{cal} = \varepsilon_s SR \qquad (2.3)$$

where

w_{calc}	=	Average crack width
ε_s	=	Tensile strain in extreme layer of steel
S	=	Spacing of transverse wires
R	=	ratio of distances to the neutral axis from the extreme tension fibre and from the centriod of steel

Karunakar Rao, P. and Jagannadha Rao, V. (1988) proposed the following equation for the calculation of ultimate moment in a ferrocement flexural element.

$$M_R = M_{SU} + M_{fU} \qquad (2.4)$$

Where $M_{SU} = A_S f_y \left(d - t_s - n/2\right)$

and $M_{fU} = \left(KA_m f_{cr}\right)\left(d - t_m - n/2\right)$

A_s is area of steel reinforcement,

f_y is yield strength of reinforcement,

d overall depth of FC section,

t_s depth of bottom steel from bottom of specimen

n depth of neutral axis

K is factor which accounts for the mobilization of zone of resistance and its value is dependent upon the cracking characteristics.

A_m is area of mortar matrix constituting the stress intensive area in the tensile zone.

f_{cr} is stress in mortar at first crack. All the parameters can be obtained from flexural studies on laboratory specimens,

t_m depth to the centriod of stress intensive area in the tensile zone, from the bottom of the specimen.

Sehgal, V.K. et al. (1988) studied the behaviour of simply supported ferrocement box girder subjected to uniformly distributed load on the entire top flange and also on half of the flange width. It was concluded that irrespective of the mode of load application, the first crack load was practically constant. Also the maximum deflection at mid span at first crack load was nearly the same, demonstrating the large load distribution, which the box section can bear. It was also concluded that serviceability for box girder elements is governed by the maximum crack width and not the deflection. The recommended value of maximum crack width was 0.1 mm.

Mansur, M.A. et al (2000) presented the flexural strength results of thin walled ferrocement channels with different volume fraction of reinforcement. The test results indicated the existence of considerable ductility for such panels suggesting that the "rigid-plastic' concept is applicable to predict the ultimate moment capacities of the structural sections. The same was also verified from the data available for the I-sections in the literature. Using the method, typical design charts were developed for

typical thin walled panels. These charts are equally applicable to inverted U, U, and box sections respectively.

Beams rehabilitated with ferrocement jackets show better performance in terms of ultimate strength, first crack load, crack width, ductility and rigidity of the section. It was observed that the cracking and ultimate strength increases by 10 percent and 40 percent in case of rehabilitated beams, whereas these increases were 10-30 percent and 40-50 percent in case of composite sections. The jacketing increases the rigidity of the beams and lead to 37 percent and 29 percent reduction in deflection. The crack width of the composite beams and rehabilitated beams decreases on an average by 42 percent and 36 percent respectively [*Kaushik, S.K. and Dubey, A.K., 1994*].

The addition of thin layer of ferrocement to a concrete beam enhances its ductility and cracking strength. Composite beams reinforced with square mesh exhibit better overall performance compared to composite beams reinforced with hexagonal mesh. An increase in the number of layers improves the cracking stiffness of the composite beams in both cases. [*Nassif, H.H et al, 1998, Vidivelli, B. et al, 2001, Nasif, N.H. et al 2004*].

The higher number of wire mesh used show more increase in strength in shallow beams than those in deep beams, although with a single layer of mesh sufficient increase in ultimate strength has been obtained [*Kabir, A. and Ali, S., 1996*].

A ferrocement shell improves the flexural behaviour of RCC beams, although there is no increase in the moment carrying capacity of under reinforced beams. However, the moment carrying capacity increased by 9 per cent and 15 per cent for balanced and over reinforced sections respectively [*Seshu, D.R., 2000*].

S.K. Kaushik et al (1987) investigated the behaviour of ferrocement plates in flexure by varying the length of mesh overlaps. It was observed that as the first crack and ultimate load approaches the value corresponding to that of a continuous mesh, when the overlap is sufficient to develop the required strength through bond for same amount of steel. When mesh-overlap is insufficient, bond failure occurs due to slippage at overlap and the first crack load is much lower than the ultimate value. The authors suggested a minimum mesh overlap of 100mm. Alternatively, it should be calculated from conventional approach.

The ultimate strength of the reinforced concrete beams, which failed due to overloading and were repaired using ferrocement laminate, is affected by the level of damage sustained prior to repairing. However, ultimate strength ductility ratio and

energy absorption have been reported to improve after the repair in all cases. The steel ratio used in the repair layer has a great influence on the amount of gain in the resisting moment, ductility ratio and energy absorption. The higher the steel ratio the higher the gain in resisting moment and energy absorption; conversely, the ductility ratio was found to be decreased with increase in steel ratio [*Fahmy, Ezzat H. et al, 1997*].

However, *Paramasivam, P. et al (1994)* has observed that beams with higher volume fraction of reinforcement exhibit localized horizontal cracks at the concrete/ferrocement interface and delamination of ferrocement from the concrete substrate. The increase in the flexural capacity, therefore, depends on the preservation of composite action until failure to fully utilize the ferrocement laminate at the beam soffit. It is also reported that cyclic loading with a maximum load applied and restricted to 50 percent of the theoretical static ultimate load capacity, did not seem to have any adverse affect on the performance of the strengthened beams after 150,000 cycles of load applications [*Paramasivam, P. et al, 1998*].

In normal conditions all the bonding agents used to develop composite structural behaviour give reasonably good results, but resistance to chloride penetration in accelerated aging tests improved by using SBR or acrylic bond coats [*Mays, G.C. and Barnes, R.A., 1995*]. Composite beams with shear connectors carried about 12 per cent higher load and had 10 per cent reserve flexural strength compared to control beams. They also show lower deflection when subjected to the same load as applied to to RCC beams without shear connectors [*Kadir, Mohamand Razali Abdul et al., 1997*].

Nasif, N.H. et al (2004) reported that composite action can not be attained based on rough surfaces without shear studs and minimum five studs are needed for full composite action. Beams with shear studs with hooks exhibit better pre-cracking stiffness as well as cracking strength than those with L-shaped studs.

One single coat of cement slurry gives composite action between ferrocement overlay and original beam upto failure load [*Kabir, A. and Ali, S., 1996*], but in case of unbonded repaired beams stiffness and ductility of beams decrease considerably [*Kaushik, S.K. and Garg, V.K., 1994*].

Paramasivam, P. et al (1994) studied the flexural behavior of reinforced concrete T-beams strengthened with thin ferrocement laminate attached to the tension face using L-shaped mild steel round bars as shear connectors. From the experimental

investigation it was concluded that after strengthening the performance of the beam improved substantially in terms of strength, flexural rigidity and first crack load, provided the connectors are adequately spaced and the surface to receive the laminate roughened to ensure sufficient bond strength for composite action.

Anwar, Nimityongsku,. Pama and Robels-Austriaco (1991) investigated the rehabilitation technique for reinforced concrete structural beam elements using ferrocement. The technique involved strengthening of the reinforced concrete beams by application of hexagonal chicken wire mesh and skeletal steel combined by ordinary plastering. The basic parameters involved were the number of wire meshes applied, its geometrical configuration and the degree of distress in the beams. The test results were in good compliance with the original design capacity of the beams. From the test results, a design chart was developed to determine the parameters for rehabilitation of the beams elements.

Thus, ferrocement is a viable alternative material for repair and strengthening of reinforced concrete structures. It has been accepted by the local building authority in Singapore for use in upgrading and rehabilitation of structures. The National Disaster Mitigation Agency (NDMA), Government of India, also accepted the use of ferrocement for this purpose.

2.2.4 Ferrocement in Shear

Cracking shear strength of ferrocement is not a unique-value unlike tensile strength which can be precisely defined in terms of specific surface factor as done by most of researchers, rather it is controlled by strength characteristics of cement mortar, mesh parameters in addition to shear-span to depth ratio which changes the mode of failure even if all other factors remain the same. Thus, most of the researchers have tried to correlate shear strength to each of the parameters individually and have recommended that the equation giving the least value should be considered for design.

Mansur, M.A. and Ong, K.C.G (1987), studied the behavior of ferrocement in shear, when reinforced with welded wire mesh. It was concluded that the shear strength of ferrocement depends upon the shear-span to depth ratio (a/h), volume fraction of reinforcement, strength of mortar and the amount of reinforcement near the compression face. It was concluded that the shear force at ultimate load increased with a decrease in the a/h ratio and the ultimate shear failure occurred in beams with relatively high volume fraction of reinforcement and low compressive strength of mortar. An increase in the amount of reinforcement near the compression face also

increased the diagonal cracking strength of the beam. The diagonal cracking strength of ferrocement beams can be calculated using the following expression:

$$\frac{V_{cr}}{bd} = 6.8\left(f'_c \; p\frac{d}{a} \right)^{0.75} \qquad (2.5)$$

Where V_{cr} = Shear force at diagonal tension cracking

b = Width of the beam

d = Effective Depth of the beam

f'_c = compressive strength of mortar Cylinder

p = A_{st}/bd

a = Shear span

A similar trend was also reported by *Al-Kubaisy, M.A. and Nedwell, P.J. (1999), T*he following equation for calculating the critical shear force in ferrocement beams was proposed.

$$\frac{V_{cr}}{bh} = 0.1\sqrt{f'_c} + 55.5\frac{V_f h}{X_c} \qquad (2.6)$$

where $X_c = \dfrac{198(a/h)}{\sqrt{f'_c}} - 14$

f'_c cylinder compressive strength of mortar (N/mm^2),

b, width of the beam

h, overall depth of the beam

V_f volume fraction of reinforcement in longitudinal direction

Mansur, M.A. and Ong, K.C.G (1991), carried out similar type of study on I-beams and concluded ferrocement I-beams provide highly efficient crack control characteristics under short term loading. The ultimate shear strength of the beams increases with decrease in a/h and increase in strength of mortar, reinforcement in longitudinal and transverse direction. The beams fail in shear only when the a/h ratio is less than or equal to 1.5. Beyond this value failure occurs in flexure. The beams failing in flexure exhibit considerable ductility before failure.

Al- Sulainanu, G.J. and Basuisbu,l I.A. (1991), investigated the behavior of ferrocement under direct shear by conducting axial compression test on Z-shaped specimens reinforced with woven wire mesh producing pure shear on the shear plane. From the experimental results they concluded that ferrocement under direct shear exhibits two stages of behavior (cracked and un-cracked) while under flexure it

exhibits, a third stage (plastic stage) in addition. The cracking and ultimate shear stress increases with mortar strength and volume fraction of mesh, while the shear stiffness in the untracked stages not significantly affected by the amount of reinforcement; it is mainly affected by the mortar strength. Ductility of ferrocement material under direct shear increases with increasing wire mesh reinforcement and decreases with higher mortar strength. The authors had proposed following equation to predict the cracking and ultimate shear stress:

$$\tau_{cr} = \sigma_{mt} + 450V_f \qquad (MPa) \qquad (2.7)$$

$$\tau_{ult} = \sigma_{mt} + 900V_f \qquad (MPa) \qquad (2.8)$$

where τ_{cr} = Cracking shear stress

$\tau_{ult.}$ = Ultimate shear stress

σ_{mt} = Mortar tensile strength, and

V_f = Volume fraction of wire mesh reinforcement

Desayi, Prakash et al (1994), had performed an experimental investigation on the shear strength of ferrocement. They have studied different variables like number of layers of wire mesh, two mesh layouts, and strength of the mortar and shear span-to-depth ratio. They have noticed two types of shear cracking and failure, namely those due to flexure-shear and web-shear. Test results indicate that for both of the mesh layouts considered, the shear strengths of ferrocement at cracking and at failure due to flexure-shear and web-shear increase as the shear span-to-depth ratio are decreased and the volume fraction of mesh wires is increased. They have concluded that the shear stresses at which the web-shear crack and web-shear failure occurred were higher than the shear stresses at which the flexure-shear crack and flexure-shear failure occurred.

Al-Kubaisy, M.A., (1998), studied the location of critical diagonal cracks in ferrocement beams with change in shear span to depth ratio (a/h), volume fraction and compressive strength of the mortar. It is reported that location of critical diagonal crack as measured from the nearest support increases as the a/h ratio is increased and, to a lesser extent as compressive strength of mortar decreases. The effect of the volume fraction is not clearly defined

Shear strength enhancement provided by a circular and square ferrocement jacket can be conservatively estimated by considering the jacket acting as a series of independent spiral reinforcement with the amount of hoop reinforcement equal to the volume

fraction of wire mesh. It is found necessary to limit the yield stress of the wire mesh in jacket, fy to less than equal to 0.4fy to avoid premature yielding of the wire mesh which could lead to fracture of jacket within the plastic region.

The shear distressed RCC beams when strengthened with ferrocement pre-cast plates bonded with original beams using epoxy, simple bolting, epoxy with bolting, and cement sand mortar with bolting yielded an increase of 20 per cent, 19 per cent, 35 per cent, and 25 per cent strength respectively. When cement sand mortar alone is used as the bonding agent no improvement in strength is there. [*Xiong, Guangjing, et al., 2000*].

Lim, C.T.E. et al (2001), used push out test to study different methods of attachment of ferrocement components used to strengthen reinforced concrete elements and transfer shear across such interfaces. The ferrocemnt is attached to the concrete surface by cast in-situ epoxy resin, pre cast with epoxy resin. Three types of mechanical anchorages used as shear connector, viz. anchor bolts, power actuated nails, and mild steel bars were examined. It was concluded that surface preparation significantly increase cohesion between the surfaces in contact at the ferrocement-concrete interfaces. Specimens pre-cast and bonded with epoxy behaved monolithically with the adjoining surface and mild steel bars with an suitable anchorage length is found to be suitable for use a shear connector.

Abdullah A, Katsuki Takiguchi (2003), had strengthened reinforced concrete columns with ferrocement jackets. They had used circular and square ferrocement jackets for strengthening square reinforced concrete columns with inadequate shear resistance. They had concluded that by providing external confinement over the entire length of the RC columns, the ductility is enhanced tremendously. They had also concluded that ferrocement jacket can be used to strengthen RC column with inadequate shear strength to enhance its ductility and also less number of layers of wire mesh within the center portion of the circular ferrocement jacket could be adopted in strengthening shear failure type RC column.

Nassif, Hani H., Husam Najm, (2004), had performed an experimental study to examine a shear transfer between composite layers. They have concluded that in order to provide a full composite action between both the layers a minimum of five studs are needed. They also concluded that beams having shear studs with hooks exhibited better pre-cracking stiffness as well as cracking strength than those with L-shaped

studs and also beams specimens with square mesh exhibited better cracking capacity than the control beam as well as beams with hexagonal mesh.

Mohammad Taghi Kazemi et al (2005), undertook a study to evaluate a retrofit technique for strengthening shear deficient short concrete columns. Ferrocement jacket reinforced with expanded steel mesh was used for retrofitting in the study. It was concluded that expanded meshes were more effective than lateral ties in the shear strengthening of concrete columns. The specimens strengthened with expanded meshes showed finely distributed shear cracks even at large displacements.

Rafeeqi, S.F.A. et al (2005), studied the behavior of the beams strengthened in shear by providing complete ferrocement wrap and equally spaced strips, with one and two layers of woven square mesh in the shear span. It was concluded that after the strengthening the increase in the shear capacity is not substantial. However, brittle shear-compression failure is transformed into ductile shear failure, thus giving ample warning before failure.

2.2.5 Ferrocement as Roofing Material

Ferrocement can be used as a roofing material. Thin slabs of ferrocement covered by a layer of lightweight mortar topping, which is assumed to be non load bearing, perform well within the serviceable limits [*Prakhya, K.V.G., 1988*]. The first crack load and ultimate load increases by 16 –24 per cent and 13.2 – 11.7 per cent respectively when mesh arrangement consisting of twin layers with the two meshes orthogonally oriented and placed in contact are used compared to all the meshes oriented in one direction or the alternative layers equally spaced with orthogonal orientation [*Al-Rifaie, W.N., 1990*].

The toughness of ferrocement slabs decreases with changing orientation pattern of the meshes. Reinforced brick reinforced slabs strengthened with wire mesh at the tension face show an improvement in the strength, ductility, water proofing quality and crack arrest properties of the slab. The ductility, number of cracks, first crack load and ultimate collapse load increases, but the crack width decreases with an increase in the number of wire meshes [*Kaushik, S.K., 1991*]. The same type of results were observed for RCC slabs reinforced with ferrocement sheets at the bottom also [*Kaushik, S.K., 1991*].

The distressed RCC slabs if strengthened with ferrocement laminates show improvement in strength, ductility ratio and energy absorption properties of the slab.

The improvement in ultimate strength depends upon the level of damage sustained prior to repair [*Fahmy, Ezzat H., 1997*].

Clarke, R.P. et al (1991), studied the effect of through the thickness, orientation pattern of meshes, stacking sequence of meshes, span to thickness ratio and in-plane orientation angle on the strength, toughness and mid point deflection characteristics of ferrocement slabs. It was concluded that changing the orientation pattern of the meshes in the slab from constant to alternate increases the strength but decreases its toughness if number of layers of mesh was an odd number, however both toughness and strength decrease if the number of layers of mesh was an even number. For square ferrocement slabs under biaxial bending maximum strength is achieved if the angle of orientation of the meshes relative to the edges is of the slab was 45 degree, however it was minimum at zero degree orientation. The maximum toughness was achieved if through the thickness orientation pattern of the meshes was constant and it was minimum when the orientation pattern was anti symmetrical.

Hussin, Mohd. Warid (1991), presented extensive data on the cracking and strength behavior of thin ferrocement sheets of 10mm thickness in flexure. Cement replacement by 50% to 70% fly ash and inclusion of super plasticizer can produce mixes of excellent flow characteristics and adequate early strength that can further ease the construction process and enable incorporation of short discrete fibers without difficulties of fabrication. The inclusion of fibers increases stiffness, decrease deflection and shows large ductility at failure. Small opening meshes exercise better cracking control than large opening meshes. However, incorporation of fibers in the mix modifies this pattern as large result in substantial reduction in crack spacing and crack widths compared with conventional ferrocement. For structural application s of ferrocement, deflection is a major design limitation. Fiber ferrocement along with layers of mesh can increases stiffness of the composite and reduces deflection at all stages of loading. The measured crack spacing and crack width can be satisfactorily predicted by the method proposed in this work.

Kaushik et al (1991), used galvanized iron sheets and corrugated ferrocement sheets at bottom layer to represent lost formwork. The formwork provides the support to the fresh concrete during the service stage and strength in the hardened stage. They conclude that CGI formwork fail by shear bond of failure where as ferrocement fails in the flexural mode. And also the ferrocement exhibits better performance to the CGI composites in terms of load carrying capacity, energy absorption capacity, and

ductility and recovery in unloaded condition. They have observed that the cost is reduced by 20 percent by using ferrocement formwork to RCC with the increase in first crack, yield and ultimate load carrying capacity.

The behavior and performance of composite ferrocement brick reinforced slab without ferrocement panels especially to be shaped into simple geometric forms was studied by *Mattone (1992)*. It was reported that there are numerous advantages afforded by this building technique. Prefabrication ensures product quality by optimizing aggregate grain, the water cement ratio binder and addictive quantities and may entail a reduction in cost, while the simplicity of the operation to be performed to obtain a structural element from the semi-finished product make the process ideally suitable for self-help activities, enabling even unskilled workers to participate in the construction of their homes.

Anwer, A.W. (1993) presented the advantages and application of ferrocement for low-cost housing especially in Pakistan. Ferrocement roof and wall system provide a cheaper but durable solution. At the same time, they give a more permanent look to the structure as compared to other low-cost materials. There is a reasonable amount of economy achieved by using ferrocement. The economic analysis shows, that the housing ferrocement wall panels and brick masonry roofing units are 40% cheaper than the reinforced concrete roofs.

Formwork is that integral part in the construction of concrete structures. It is a temporary structure used to form fresh concrete to the desired shape, size, position and finish, and to support the dead and live loads during construction without the collapse or danger to workmen or the structure. Permanent formwork is that type of formwork, which becomes the integral part of the structure. It saves the striking time and activities related to it.

Ferrocement permanent formwork provides protection to reinforced concrete and gave an increase in strength of 15 percent over the conventional reinforced concrete *(G.C Mays and R.A. Barnes, 1995)*. It saves considerable time and money in the construction of floor slab of a building and provides eco friendly construction by conservation of Natural Resources *(Karunakar Rao et al, 1996)*.

Analytical and experimental investigation of hollow ferrocement units were studied by *Mathews et, al (1998)* the system consists of top and bottom flanges connected by webs, there by leaving hollow spaces in between. The hollow section is selected mainly the passage of heat from outside. Based on the investigation the load

deflection of the developed section is quite similar to that of a typical ferrocement element. There appears to be good potential for the use of these elements for roof/floor in residential buildings for span up to 3.5m

2.3 FIBRE REINFORCED PLASTICS

The term fibre reinforced plastics describes a group of materials composed of inorganic and organic fibres embedded in a resin matrix. FRPs possess excellent properties such as high tensile strength and stiffness; are lightweight and non-magnetic, and offer resistance to corrosion and chemicals, which make them particularly suitable for the rehabilitation and strengthening works. In construction industry, the most commonly used FRPs are Glass fibre reinforced plastics (GFRPs), Carbon fibre reinforced plastics (CFRPs) and Aramid fibre reinforced plastics (AFRPs). The conventional reinforced concrete (RC) beams strengthened in flexure with externally bonded fibre reinforced polymers have shown strength increase of 50 percent or more in combination with a considerable increase in the deflection capacity [*Bonacci, J.F. and Maalej, M, 2001*]. The beams strengthened with CFRP unidirectional sheets show significant static capacity increase (approximately 150 percent), load at first crack and post cracking stiffness when compared to un-strengthened beams [*Kachlakev, D and McCurry, D.D., 2000*].

RC beams strengthened with externally bonded FRPs when subjected to monotonically increasing loading exhibit three fundamental failure modes that can be identified as flexure, de-bonding and shear [*Colotti, Vincenzo, 2001*]

2.3.1 Flexural Members

The beams strengthened with FRP sheets bonded to the tension face exhibit significant improvement in flexural strength in both wet/dry environmental conditions and at room temperature. However, the specimens subjected to cycles of wet/dry conditions show less improvement than those kept at ambient indoor or outdoor enviornment. However, it was also observed that none of the specimen failed due to FRP rupture but rather due to the de-bonding between FRP sheet and the concrete interface [*Toutanji, Houssam A. and Gomez, William, 1997, Jia, Junhui et al. 2005*].

Saadatmanesh, Hamid et al (1991), studied thee effect of strengthening of beams by gluing GFRP plates to their tension face. The study indicates that significant increase in the flexural strength can be achieved; the gain in the ultimate flexural strength was more significant in beams with lower steel reinforcement ratios. In addition plating

reduced crack size in the beams at all the load levels. It is reported that cambering the beams resulted in improved cracking behavior, but it was suggested that before application, further studies must be conducted to examine the creep behavior of the epoxy joint subjected to sustained cambering stresses. *An, Wei. et al , 1991*, proposed the analytical model based on the compatibility of deformations and equilibrium of forces for the same beams and it was observed that proposed model give reasonably approximate behavior of the strengthened beams and the composite plate, bonded to the tension face of the beam, increases the stiffness, yield moment, and ultimate moment of the beam and reduces the curvature at failure.

Philip, A. Ritchie et al (1991), studied the effectiveness of external strengthening of beams using glass, carbon, and aramid fibre plates bonded to tension side of the beams. An increase stiffness of beams (over the working load range) from 17 to 99 percent and ultimate strength from 40 to 97 percent was achieved after strengthening. After the strengthening the crack pattern shifted from several widely spaced and large width cracks to many more closed spaced narrower cracks. The FRP plates used demonstrated brittle behavior, despite their brittle behavior, through proper design, fibre reinforced plastics can develop enough ductility to be utilized as effective concrete reinforcement.

Nanni, Antonio (1993), suggested that the use of FRP rod-type reinforcement in RC (non pre-stressed) construction would not result in material savings. However, its justification would be based on factors such as durability or magnetic permeability. A more efficient use of FRP reinforcement may be in pre-stressed concrete construction because high strength and low modulus characteristics of FRP can be better exploited. The flexural design of RC type members can be done using working stress method more appropriately, because FRP is linear elastic up to failure, its rigidity is considerably lower than that of steel, and nominal moment capacity is highly variable as it depends on concrete maximum strain and reinforcement bond.

GangaRao, Hota V.S. (1998), investigated the effect on flexural strength, of wrapping the beams with carbon fabrics. It was reported that strength and stiffness both improves after the strengthening of the beams. The percentage increase in ultimate strength capacity of the wrapped beams is a function of number of longitudinal layers of the carbon fabric. For a particular fabric layer, increase in ultimate strength is greater for wrapped beams with lower percentage of steel reinforcement than those with higher percentage of steel reinforcement. Damaged beams rehabilitated with

carbon wrapping exhibit ultimate strength and stiffness performance similar to undamaged wrapped beams.

Saadatmanesh, H. and Malek, A.M. (1998), suggested that the bonding composite plates to reinforced concrete beam is an effective technique of repair and retrofit. The ultimate capacity of the strengthened beam is controlled either by compression crushing of concrete, rupture of plate, local failure of concrete at the plate end due to stress concentration, or debonding of the plate. The authors had suggested a simple guidelines using limit state design theory using above failure modes. However, they suggested conducting further experimental works to validate and refine the suggested equations.

Buyukozturk, Oral, and Hearing, Brain (1998), FRP laminates bonded to the tension face of concrete is attractive method of rehabilitation and retrofitting of the beams. This method enhances the flexural strength of the beams but the failure behavior of the system can become more brittle, often involving delamination of the composite and shear failure of the beams. The authors reviewed the parameters affecting the failure modes and techniques used in analysis of these modes. These models have concluded that the section will fail in compression when the steel and/or FRP reinforcement ratio is large and the concrete strain exceeds 0.003 and the shear capacity of FRP strengthened concrete beams does not change significantly from those for unretrofit beams. However, the application of the laminate to the soffit of the concrete beams introduces shear transfer to the concrete/epoxy interface. At the termination of the laminate, a change in stiffness and the discontinuity of beam curvature create stress concentration in the concrete, often initiating cracks that can lead to debonding.

Teng, J.G. et al (2000), studied the feasibility of strengthening deficient RC cantilever slabs by bonding GFRP strips/sheets on the tension side and effectiveness of different anchorage system. The test results have demonstrated that a significant increase in the ultimate load and ductility can be achieved if the slot anchorage system is used to anchor the strips into the supporting wall. The effect of this strengthening method is even better if fibre anchors are installed or the free ends of GFRP composite strips are wrapped around the free edge and onto the soffit of the slab.

Papakonsatantinou, Christos G. et al (2001), investigated the effects of glass fibre reinforced polymer (GFRP) composite rehabilitation system on the fatigue performance of reinforced concrete beams. The results indicate that beams failed

primarily due to fatigue of steel reinforcement. Debonding of the GFRP composite sheet was a secondary mechanism in the strengthened beams. Since, the fatigue mechanism does not indicate a failure of the FRP, the role of the GFRP composite sheet is to increase the strength and stiffness of the beam and thus reduce the stress in the steel. Therefore, the fatigue life of strengthened beams is increased as compared with the non-strengthened beams for the same applied load. The ultimate deflection under fatigue loading conditions is same as the ultimate deflection under static loading conditions. This indicates that the failure mechanism is same under static and fatigue loading conditions.

Teng, J.G. et al (2002), proposed the model for calculating ultimate moment of resistance of the beams strengthened in flexure bonding FRP laminates. The proposed model is based on B.S. 8110 (1997). According to the existing model, the moment carrying capacity of the reinforced concrete beams strengthened with FRP plates in flexure is given by:

$$M_u = k_1 \frac{f_{cu}}{\gamma_c} b_e x\left(\frac{h}{2} - k_2 x\right) + \sum_{i=1}^{n} \sigma_{st} A_{st}\left(\frac{h}{2} - d_{si}\right) + \sigma_{frp} A_{frp}\left(\frac{h}{2} - d_{frp}\right) \qquad (2.9)$$

where

k_1 = mean stress factor

$$= 0.67\left(\frac{\varepsilon_{cf}}{\varepsilon_{co}} - \frac{\varepsilon_{cf}^{\,2}}{3\varepsilon_{co}^{\,2}}\right) \quad \text{if} \quad 0 \le \varepsilon_{cf} \le \varepsilon_{co}$$

$$= 0.67\left(1 - \frac{\varepsilon_{co}}{3\varepsilon_{cf}}\right) \quad \text{if} \quad \varepsilon_{co} \le \varepsilon_{cf} \le 0.0035$$

k_2 = Centroidal Factor

$$= \frac{\frac{1}{3} - \frac{\varepsilon_{cf}}{12\varepsilon_{co}}}{1 - \frac{\varepsilon_{cf}}{3\varepsilon_{co}}} \quad \text{if} \quad 0 \le \varepsilon_{cf} \le \varepsilon_{co}$$

$$= \frac{\frac{\varepsilon_{cf}}{2} + \frac{\varepsilon_{co}^{\,2}}{12\varepsilon_{cf}} - \frac{\varepsilon_{co}}{3}}{\varepsilon_{cf} - \frac{\varepsilon_{co}}{3}} \quad \text{if} \quad \varepsilon_{co} \le \varepsilon_{cf} \le 0.0035$$

f_{cr} = Concrete cube compressive strength

b_e = width of beam

x = Depth of neutral axis

h = depth of beam

σ_{st} = stress in steel at i level

A_{st} = Area of steel in tension zone at i level

d_{si} = Distance of steel at level I from extreme compression fibre

σ_{frp} = stress in FRP

A_{frp} = area of FRP

d_{frp} = Distance of FRP from extreme compression fibre

γ_c = Partial safety factor for concrete

Sheikh, Shamim A. (2002), done extensive study on application of FRP in concrete structures for enhancing their structural performance both in terms of strength and ductility. Author concluded that FRP reinforcing was very effective in enhancing flexural strength of the damaged slabs, shear resistance of the damaged beams and seismic resistance of columns. Both carbon and glass composites provide significant enhancement (approximately 150%) in flexural strength. But as the shear mode of failure is not acceptable, therefore a caution is required to limit the increase in flexural capacity due to FRP reinforcement.

Wang, Y.C. (2003), used FRP plates for strengthening of reinforced concrete beams with beams cut-off designed according to the earlier codes, such as ACI 318-71. From the experimental and analytical results it was concluded that flexural enhancement, which ensures that a strain limit of 0.4% imposed on GFRP plate, may be used to enhance the strength at the bar cut-off points. The U-shaped GFRP strips bonded to the sides of a beam were ineffective in resisting shear unless they are properly anchored at their ends.

Pham, Huy, and Al-Mahaidi, Riadh (2004), the beams strengthened with FRP to enhance its flexural capacity can experience several failure modes, namely flexural failure, end debond, and mid span debond. The authors identified various models to predict such failures and assessed the model with reported literature and beams tested by the authors. It was concluded that beam theory is able to predict the full composite action of beams strengthened with FRP. For a simple and conservative design, mid span debond can be avoided by limiting FRP stress level to

$$f_f \leq \sqrt{\frac{2G_f E_f}{n_f t_f}} \qquad (2.10) \quad (\textit{Maruyama and Ueda's Model})$$

End debond (or anchorage failure) can be avoided by limiting the interfacial bond stress between FRP and concrete to the concrete shear stress (0.3 f_{ct} as recommended by *Shehata et al*.). For more accurate prediction of debond failure loads. Nebauer and Rostasy's models as recommended in fib 14 can be used for end debond and mid span debond respectively.

Pisani, Marco A. (2006), discussed and compared an exact and an approximate approach to the computation of flexural load-carrying capacity of the strengthened beam. The two approaches differ from one another in the way they take into account the extent of the load already acting throughout strengthening operation. It was concluded that load already acting throughout strengthening operation only slightly (less than 5%) affects the flexural load carrying capacity of a beam strengthened with CFRP. Which is much lower than maximum extent of the second order effects that can be ignored in structural analysis according to Euro code 2.

2.3.2 Strengthening of Beams in Shear

Bonding of FRP plates to the RC members, which are deficient in shear, is now a days very popular. Strengthening of RC members in shear using FRPs increases its ultimate displacement by more than ten folds, and toughness by a factor of more than 26 [*Sheikh, Shamim A, 2002*].

Triantafillou, Thanasis C. (1998), studied the effect of area fraction and fibre configuration on the shear capacity of the beams strengthened with CFRP laminate. It was concluded that strength contribution increases almost linearly with a product of fibre elastic modulus and fibre area, for values up to 0.4 GPa, beyond which the effectiveness of FRP ceases to be positive. It was also concluded that effectiveness of FRP increases as the fibres direction becomes closer to the perpendicular to the diagonal crack.

Khalifa, Ahmed et al (1998), presented two design approaches to calculate the contribution of externally bonded CFRP sheet to the shear capacity of the RC beam. The first approach was based on the effective FRP stress, as a function of FRp stiffness and ultimate strain. This design approach s valid for CFRP continuous sheets or strips and for any fibre orientation angle and is suitable only if the failure is controlled by FRP sheet rupture. The second approach was based on the bond mechanism between CFRP sheet and the concrete. The effective width of the FRP sheet at delamination is addressed. This design approach is valid only for CFRP

continuous sheets or strips and is suitable if the failure is controlled by CFRP sheet delamination.

Khalifa, Ahmed, and Nanni, Antonio (2000), investigated the effect of wrapping scheme, CFRP amount, $90^0/0^0$ ply combination, and CFRP end anchorage, on the shear capacity of the beams strengthened with externally bonded CFRP. An increase in shear strength of 35 to 145 percent was achieved, after strengthening of the beams. From the study it was concluded that there are optimum FRP quantities, beyond that the strengthening effects is questionable. But still it was recommended that for field applications continuous sheets are safer than strips because the damage to an individual strip would have more of an impact on the overall shear capacity. The U-shaped laminations are more effective than lamination on the side only and U-shaped laminate with proper anchor still perform better. The laminate with fibre at 0^0 to the longitudinal axis of the beam, had no contribution to the shear strength.

Kachlakev, D. and McCurry, D.D. (2000), studied the effect of varying configuration of CFRP, and GFRP composites on shear capacity of the beams. Results from study showed that the addition of GFRP alone for shear was sufficient to offset the lack of steel stirrups and allow conventional RC beams failure by yielding of the tension steel. This allowed the ultimate deflection to be 200 percent higher than pre-existing shear deficient beam.

Colotti, Vincenzo, and Spadea, Giuseppe (2001), proposed a truss model capable of describing the ultimate behaviour of externally bonded beams in shear. The model is based on the theory of plasticity and differs from the current truss models, since it explains some important failure modes, such as those influenced by bond slip. The accuracy of the model was verified with the experimental results and proved that the proposed model predicts the shear capacity with sufficient accuracy.

Hadi, M.N.S. (2003), studied the effect of amount and types of FRP used on the shear capacity of beams retrofitted using FRP. It was concluded that beams retrofitted with E-glass wrap had 17 percent higher shear capacity as compared to the original beam.. The beams wrapped with E-glass failed in shear with the critical inclined crack making an angle of about 45 degree to the horizontal axis. The failure was due to the rupture of the E-glass sheets. In comparison, the beams wrapped with CFRP failed in flexure due to much higher ductility being available. The results confirmed that, under the same amount and configuration, the CFRP material out performs the E-glass material in structural external strengthening.

Razaqpur, A. Ghani, and Isgor, O. Burkan (2006), proposed an improved method for evaluating the shear resistance of FRP reinforced concrete members. The effect of shear and moment interaction at a section and the effect of the member size on its shear strength was studied. It was hypothesised that the total shear resistance of a member V_c, which is not subjected to axial force, is a combination of a contribution from the un-cracked (plain) concrete V_{c1} and the contribution from the aggregate interlock mechanism V_{c2}

$$V_c = V_{c1} + V_{c2} \leq 0.2k_s\sqrt{f_c' b_w d} \qquad (2.11)$$

Where $V_{c1} = 0.0035k_m k_s k_a \sqrt{f_c' b_w d}$

and $V_{c2} = 0.0035k_m k_s k_r \sqrt{f_c' b_w d}$

Where k_m represents the effect of interaction between the factored moment and the factored shear at a section on its shear strength; k_r represents the effect of reinforcement rigidity $E_f \rho_f$, and k_a and k_s represent the effects of the arch action in concrete and the beam size, respectively. Based on the regression analysis, it was concluded that for all beams regardless of their a/d, V_c varies almost linearly with the cubic root of the longitudinal reinforcement axial rigidity, but some contribution is made by plain concrete, regardless of the amount of longitudinal reinforcement. The existing ACI committee 440 recommended method, which assumes a linear relationship between V_c and $E_f\rho_f$, is highly conservative and its predicted value differs significantly from the corresponding experimental results.

CHAPTER –3

PILOT STUDIES FOR FERROCEMENT JACKETS

3.1 GENERAL

The literature review shows that the behaviour of ferrocement in flexure depends upon various parameters like cement-sand mortar ratio, water-cement ratio, type and orientation of wire mesh, number of wire mesh layers etc. Thus, the behaviour of beams retrofitted using ferrocement jackets will also be dependent upon these parameters. To understand and fix the parameters for further investigation three pilot studies were carried out using ferrocement jackets to retrofit the stressed beams.

The effect of following parameters was investigated.

1. Type of Bonding agent
2. Type of Wire Mesh
3. Wire Mesh Orientation

3.2 MATERIALS

Similar sets of materials were used in the pilot study for casting the beams. Relevant tests in accordance with Indian standard codes of practice were conducted to determine the physical properties of the materials used in the study. The details of the materials used along with their properties are presented in the subsequent sections.

3.2.1 Cement

ACC Surkasha make Portland Pozzolana Cement confirming to *IS:1489 (Part 1)-1991* available in the local market was used for the study. The physical properties of cement obtained from various tests conducted in accordance with relevant IS standards are given in Table 3.1.

3.2.2 Fine Aggregates

IS: 383-1970 defines the fine aggregates, as those passing 4.75mm IS sieve. The fine aggregates are often termed as sand size aggregates. Locally available riverbed sand was used in the present study. The properties of the same are give in Tables 3.2 and 3.3.

As the percentage of fine aggregates passing 600 microns sieve is 59, it indicates that the sand conforms to grading zone-II as per *IS: 383-1970.*

Table 3.1: Physical Properties of Portland Pozzolana Cement

Sr. No	Characteristics	Test Values	Values as per IS:1489 (Part 1)
1	Standard consistency	34	-
2	Fineness of cement as retained on 90-micron sieve (%)	0.5	< 10
3	Setting time (mins) 1. Initial 2. Final	 84 300	 > 30 < 600
4	Specific gravity (Specific gravity bottle)	3.07	-
5	Compressive Strength (MPa) 1. 7days 2. 28 days	 30.0 43.0	 22.0 33.0
6	Soundness (mm) (by Le-Chatelier's method)	2.0	< 10 (Fresh Cement) < 5 (Old Cement)

Table 3.2: Physical Properties of Fine Aggregates

S. No.	Characteristics	Value
1.	Specific gravity (oven dry basis)	2.52
2.	Bulk density loose (kN/m^3)	14.8
3.	Fineness modulus	2.36
4.	Water Absorption (%)	2.67
5.	Grading Zone	Zone II

Table 3.3: Sieve Analysis of Fine Aggregates

Weight of Sample = 1000gm

Sr. No.	Sieve Size (mm)	Weight Retained (gm)	Percentage Weight Retained	Percentage Weight Passing	Cumulative Percentage Weight Retained
1.	4.75	29.5	2.95	97.05	2.95
2.	2.36	12.0	1.2	95.85	4.15
3.	1.18	74.0	7.4	88.45	11.55
4.	0.600	294.5	29.45	59	41
5.	0.300	393.0	39.3	19.7	80.3
6	0.150	155.5	15.55	4.15	95.85
7.	Pan	38.0			
					Σ = 235.80

Fineness Modulus = 235.80/100 = 2.35

3.2.3 Coarse Aggregates

The aggregates retained on 4.75 mm IS sieve are termed as coarse aggregates. Two types of crushed aggregates with different sizes were used in the present study as detailed below:

CA-I Aggregates passing through 20 mm sieve and retained on 10 mm sieve

CA-II Aggregates passing through 10 mm sieve and retained on 4.75 mm sieve

The properties of these aggregates are listed in Tables 3.4 to 3.6.

3.2.4 Water

Fresh and clean potable water was used for casting and curing of the specimens in the present study. The water was relatively free from organic matter, silt, oil, sugar, chloride and acidic material as per Indian standard *IS:456-2000*.

3.2.5 Reinforcing Steel

HYSD steel of grade Fe-415 confirming to *IS:1786-1985* was used in the present study. 12mm and 10mm diameter bars were used as tension reinforcement and 8mm bars were used as compression steel in the beams, whereas, 6mm diameter mild steel bars were used as shear stirrups. The properties of these bars are presented in Table 3.7

Table 3.4: Sieve Analysis of Coarse Aggregate CA-I

Weight of Sample = 3 kg

Sr. No.	Sieve Size (mm)	Weight Retained (kg)	Percentage Weight Retained	Percent Weight Passing	Cumulative Percentage Weight Retained
1.	20	-	-	100	-
2.	12.5	1813.5	60.45	39.55	60.45
3.	10	783	26.1	13.45	86.55
4.	4.75	357.5	11.92	1.53	98.47
5.	Pan	41.5	-		
					Σ = 245.47

Fineness Modulus = (500 + 245.47)/100 = 7.45

Table 3.5: Sieve Analysis of Coarse Aggregate CA-II

Weight of Sample = 3 kg

Sr. No.	Sieve Size (mm)	Weight Retained (kg)	Percentage Weight Retained	Percent Weight Passing	Cumulative Percentage Weight Retained
1.	20	-	-	100	-
2.	12.5	165	5.5	94.5	5.5
3.	10	684	22.8	71.7	28.3
4	4.75	1694.5	56.48	12.22	87.78
5.	Pan	450	-	-	
					Σ = 121.58

Fineness Modulus = (500 + 121.58)/100 = 6.216

Table 3.6: Physical Properties of Coarse Aggregates

Sr. No.	Characteristics	Value	
		CA-I	CA-II
1.	Type	Crushed	Crushed
2.	Maximum Nominal Size (mm)	20	10
3.	Specific gravity	2.68	2.70
4.	Total water absorption (%)	1.45	1.643
5	Fineness modulus	7.45	6.21

Table 3.7 Physical Properties of Steel Bars and Steel Mesh Wires

Sr. No.	Diameter of bars/ mesh wire (mm)	Yield-Strength (N/mm^2)	Ultimate Strength (N/mm^2)	Elongation (percent)
1.	12	452.00	584.00	23.00
2.	10	470.00	580.0	20.0
3.	8	445.00	555.0	23.0
4.	6	442.42	612.7	32.9
5.	2.4 GI	451	612	4.0

3.2.6 Steel Mesh

MS welded steel wire mesh of 40 mm x 40 mm square grid and 2.4 mm diameter wire, and GI woven wire mesh of approximately 30 mm x 25 mm rectangular grid and 2.4 mm diameter wire were used in the ferrocement jacket. The salient properties of the wire meshes used are given in Table 3.7.

3.2.7 Concrete Mix

M20 grade concrete mix was designed as per Indian Standard recommended guidelines IS: 10262-1982, using the materials with properties given in Tables 3.1 to 3.6. The water-cement ratio used in the proportioned mix was 0.52. The mix proportion of material adopted was 1:1.53:3.22 by weight (cement: sand: aggregate).

The quantities of material per cum of concrete along with the strength results of 150 mm cubes cast for the proportioned mix are listed in Table 3.8(a) and (b), respectively.

Table 3.8(a) Mix Proportions for M20 Concrete Mix (kg/m^3)

Water	Cement	Fine Aggregates	Coarse Aggregate – I (20mm)	Coarse Aggregate – II (10mm)
185.0	359.2	549.57	578.31	578.31

Table 3.8(b) Compressive Strength of Cubes for M20 Concrete

S. No.	Age (Days)	Compressive Strength (N/mm^2)
1.	7	22.75
2.	28	26.8
3.	56	28

3.2.8 Mortar Mix for Ferrocement Jackets

The range of mix proportion (Cement: Sand) by weight, recommended for common ferrocement application is between, 1:1.5 to 1:2.5, but not greater than 1:3 in any case, and water cement ratio (by weight) ranging between 0.35 to 0.5 (*ACI Committee 549 Report*). The higher the sand content the higher is the required water content for a constant workability. The fineness modulus of the sand, water-cement ratio and sand-cement ratio were varied and trial batches cast to ensure a mix that can infiltrate the mesh and develop a strong and dense matrix. For the present study, the proportion of cement–sand mortar used for applying ferrocement jackets was 1:2 (cement: sand). The water-cement ratio for mortar was 0.40 to ensure a homogenous mix and desired workability.

3.3 CASTING OF REINFORCED CONCRETE BEAMS

The prototype beams of size 127 mm x 227 mm x 4100 mm were cast for pilot testing purposes in the first stage, in order to finalize the parameters like type of bonding

material, type and orientation of wire mesh. The beam moulds used are shown in Plate 3.1(d).

The beams were designed as under-reinforced sections and balanced sections using the limit state design theory as per *IS:456-2000*. The under reinforced sections were reinforced with two bars of 8 mm diameter in compression (at top) and two bars of 10 mm diameter in tension (at bottom), while balanced sections were reinforced with two bars of 8 mm diameter in compression (at top) and three bars of 12 mm diameter in tension (at bottom) as shown in Figs. 3.1 and 3.2. In both type of sections, 6 mm diameter rings at a spacing of 150 mm c/c were provided as shear stirrups.

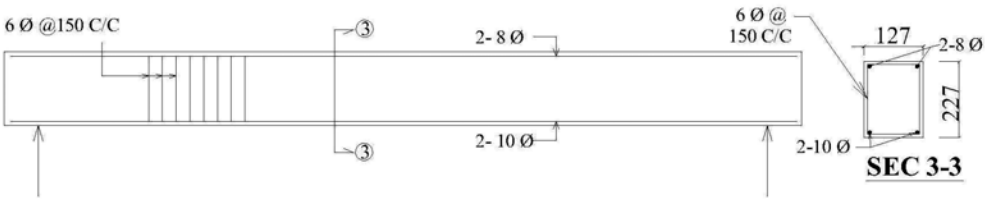

Fig. 3.1 Longitudinal and Cross-Section of Unretrofitted Under Reinforced Beams
(All Dimensions are in mm)

The steel rebars were cut to size and the reinforcement cage prepared depending upon the type of beam to be cast i.e. an under reinforced or a balanced section. Cover blocks of 25 mm size were provided below the reinforcement to maintain a uniform cover to the reinforcement during casting as shown in Plate 3.1(b). The moulds were oiled before concreting to ease the demoulding process. The concrete mix as proportioned was prepared using a pan type concrete mixer as shown in Plate 3.1(a). The concrete mix was then poured into the moulds and compacted using a needle vibrator as shown in Plates 3.1(d) and 3.1(e). The vibration was done until the mould was completely filled and no voids were left. The beams were demoulded after 48

hours. After demoulding the beams were cured for 28 days using jute bags and sand ponding.

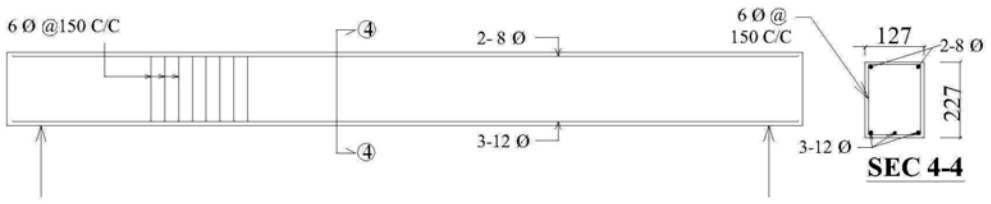

Fig. 3.2 Longitudinal and Cross-Section of Unretrofitted Balanced Beams
(All Dimensions are in mm)

3.4 RETROFITTING USING FERROCEMENT JACKET

The beams were first stressed to a pre-decided level. The beams were then partially destressed (due to self weight only) by putting them upside down. The surface of the stressed beams was chipped creating grooves on surfaces of the beams and cleaned with metallic brush using potable water. One coat of bonding agent was applied on the cleaned surface before placing the wire mesh cage on it without repairing the initial cracks. The cage was properly placed ensuring tight fit with the help of mild steel wire and 1:2 cement mortar with water cement ratio 0.4 was applied. The process is shown in Plate 3.2 and the longitudinal and cross sections of the beam after retrofitting are shown in Fig. 3.3

3.5 TESTING ARRANGEMENT

All the control as well as retrofitted beams were tested under two point loading with simply supported end conditions. The point loads were placed at a distance of 500 mm on either side of the centre of the beam. The load on the beams was controlled through a hydraulically operated jack connected to a load cell. The load was applied in equal increments of 2 kN each and measured using a data acquisition system

having a least count of 0.1 kN, attached to the load cell. The deflection corresponding to the applied load was measured with the help of dial gauges having a least count of 0.01mm. Three dial gauges were used to measure the deflections at the quarter span sections and at the centre of the beams. Fig. 3.4 and Plate 3.3 show the testing arrangement used.

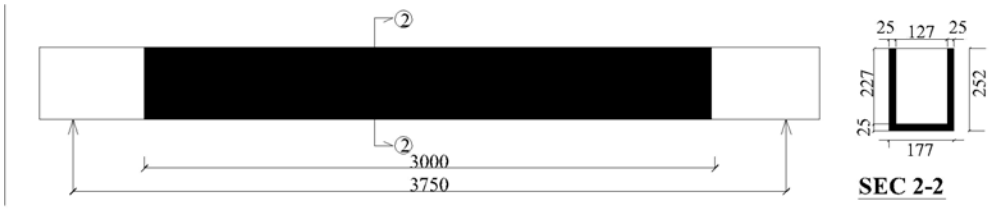

Figure 3.3: Longitudinal and Cross-Section of Retrofitted Beams

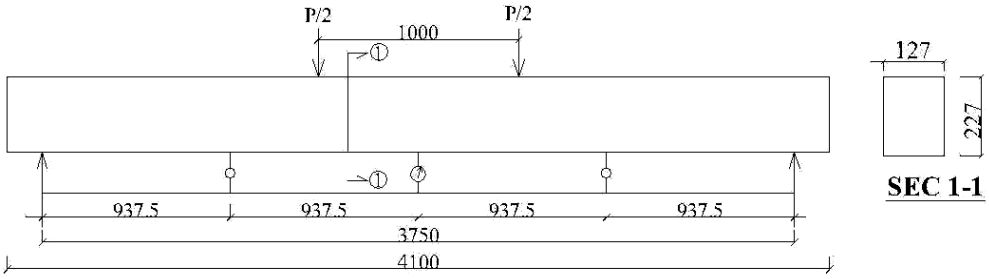

Fig. 3.4 Loading Arrangement for Testing of all Beam Specimens
(All Dimensions are in mm)

3.6 IDEALIZATION OF LOAD DEFLECTION CURVE

The load deflection data obtained from the testing of the beams is plotted and the load deflection curve thus obtained is idealized as quadri-linear curve for the purpose of calculating ductility ratio and toughness of the beam. The ductility ratio is defined as the ratio of deflection at ultimate load (defined as 0.85 of maximum load) to the deflection at yield load. Whereas, toughness is the area under the idealized load deflection curve up to the ultimate load.

The idealized load deflection curve is obtained by linearly joining four points starting from the origin. Each of these four points are located on the curve as explained below.

1. Elastic load point, is the load up to which load deflection curve is linear.
2. Yield load point, is the load at which the yielding of the beam starts, which is obtained by drawing a tangent to the elastic load point and maximum load point on the curve.
3. Maximum load point, and
4. Ultimate load point, defined as the point at which the load drops to 85% of the maximum load.

One such idealized curve is shown in Appendix-C.

(a) Pan Mixer

(b) Cover Block

(c) Preparation of Moulds

(d) Reinforcement Cage in Moulds

(e) Compaction of Concrete Using Needle Vibrator

Plate 3.1 Casting of Beams

(a) Roughened Surface of Beam

(b) Application of Cement Slurry

(c) Fixing of Wire Mesh – 1

(d) Fixing of Wire Mesh - 2

Plate 3.2 Application of Ferrocement Jacket

Plate 3.3 Test Set up for simply Supported Beams Subjected to Two-Point Loading with Dial Gages at Mid-Span and Quarter Span Section

3.7 EFFECT OF TYPE OF BONDING AGENT ON STRENGTH OF BEAMS RETROFITTED USING FERROCEMENT JACKETS

The first of the pilot studies was carried out to study the effect of type of bonding agent on the strength of the beams retrofitted using ferrocement jackets. In this three types of boding agents viz. epoxy, cement slurry and cement slurry with shear connectors were adopted to glue the ferrocement jacket to the distressed beams.

Eight prototype beams of size 127mm x 227mm x 4100mm reinforced with two bars of 10mm diameter in tension and two bars of 8mm diameter in compression as shown in Fig. 3.1 were cast using the proportioned mix. Out of these eight beams, two beams were used as control beams (Type – A) and tested to failure to find out the safe load carrying capacity corresponding to the allowable deflection as per *IS:456-2000* i.e. span/250. The other six beams were stressed to 75 percent of the safe load obtained from the control beam and were then retrofitted with 15 mm thick ferrocement jacket made with 1:2 cement mortar and w/c ratio of 0.40. The jacket was reinforced with a single layer of 40mm x 40mm square welded wire mesh. The three bonding agents mentioned above were used to bond the jacket to the stressed beams. The retrofitted beams were then tested to failure and their behaviour was observed and analyzed.

The sets of two beams each were divided into four categories depending upon the type of bonding agent used. The control beams were designated as type-A. The beams in which cement slurry was used for gluing the ferrocement jacket to the beam were designated as type – B beams as shown in Plate 3.4(a). Epoxy of Nitobond EP make was used for the purpose of gluing the ferrocement jacket to the beam for retrofitting in type – C beams. The same is shown in Plate 3.4(b). The ratio of the epoxy to the hardener adopted was 2:1 as recommended by the manufacturer and properties of the same are provided in Table 3.11.

Screws of 4 mm diameter were used as shear connectors with cement slurry as the bonding agent for the retrofitting of beams designated as type – D beams. The screws were provided in two rows at a spacing of 100 mm c/c as shown in Plate 3.4(c).

3.7.1 Testing of Beams

All the eight beams, control as well as retrofitted, were tested as per arrangement explained in section 3.5 (see Fig. 3.4)

After testing the control beams, the other six beams were stressed to 75 percent of safe load and were subsequently retrofitted using the procedure explained in section 3.4. A set of two beams was retrofitted with each bonding agent. After cleaning the surface, the bonding agent was applied to the surface of the beam and then jacketing of the beam was done with the help of welded wire mesh. Subsequent to that a 15mm thick plaster was applied over the soffit and vertical faces of the beam in U-shape. Following this the beam was cured for a period of 7 days. The retrofitted beams were again tested to calculate the maximum load and corresponding deflections.

3.7.2 Results And Discussion

First, the two control beams were tested to failure. The maximum load corresponding to an allowable central deflection of span/250, i.e. 15 mm was obtained from the load deflection curve as 12.67 kN. The remaining six beams were stressed to 75 percent of this average safe load i.e. 9.5 kN. Subsequently the retrofitting of beams with different bonding agents as mentioned earlier was carried out. These retrofitted beams were then loaded to failure and data was recorded in the form of loads and corresponding deflections. Table 3.9 presents this data for the control as well as beams retrofitted using specified bonding agents. Figure 3.5 shows the load-deflection plots at the mid span point of the control beams and beams retrofitted with different bonding agents.

It is observed from the curves in Fig. 3.5 that with an increase in load there is considerable increase in deflection for all the beams. The average spacing of the cracks was observed to be 80-120 mm for the control beams, whereas it decreases for retrofitted beams. The average spacing of the cracks decreased to 40-60 mm for the retrofitted beams, indicating better distribution of stresses after retrofitting. The primary reason of decrease in spacing of cracks is the closely spaced reinforcement in the tension zone, which acts as a crack arrestor. The failure for the control beams occurred at a load of 21.8 kN with a deflection of 44.85 mm, whereas the retrofitted beams with cement slurry failed at a load of 25.2 kN with a deflection of 39.2 mm at the center. The failure load for retrofitted beam using epoxy as bonding agent was observed to be 25.6 kN at a deflection of 43.25 mm. These values of deflection and load increased to 26.2 kN and 46.28 mm, respectively for beams retrofitted with cement slurry and shear connectors. The above observations clearly indicate that after

retrofitting there is a considerable increase in the load carrying capacity, the highest being for beams using shear connectors.

The load deflection curves are idealized as quadri-linear curves as explained in section 3.6 and using the idealized curves the ductility ratio i.e. ratio of deflection at ultimate load to yield load and energy absorption i.e. area under the curve up to ultimate load is calculated and presented in Table 3.10. It is observed that the ductility ratio increases by 5.34, 9.9 and 10.21 percent and energy absorption increases by 11.02, 14.73, and 21.67 percent for Type-B, Type-C and Type-D beams respectively as compared to the control beams (Type-A).

The results indicate that the beams retrofitted with shear connector, as bonding agent is best among all the three with regards to enhanced maximum load carrying capacity, ductility ratio and energy absorption followed by the epoxy bonded and cement slurry bonded beams, respectively. The increase in ductility ratio and energy absorption of beams using shear connectors as compared to the beams retrofitted with other bonding agents indicates that shear connectors are best for dynamic load applications.

However, a detailed cost analysis to check the economic feasibility of various bonding agents, which is presented in the succeeding section, throws up other different prospective.

3.7.3 Cost Analysis

A comparative analysis of cost for the above pilot study is presented in Table 3.12.

The cost analysis shows that the cost to strength ratio is highest in case of beams retrofitted with epoxy followed by beams bonded with shear connectors and cement slurry. This is primarily due to the fact that cement slurry is easy to apply as compared to shear connectors, which require more time and technical supervision and cost of epoxy is much more than the other bonding agents resulting in a higher cost of retrofitting.

Table 3.9: Load v/s Deflection Data for Control Beam and Beams Retrofitted with Ferrocement Jackets Bonded to the Beam Using Different Bonding Agents

S. No	Control Beam (Type –A^+)			Beam with Cement Slurry (Type –B^+)			Beam with Epoxy (Type –C^+)			Beam with Cement Slurry and Shear Connectors (Type – D^+)		
	Load	Deflection (mm) at		Load	Deflection (mm) at		Load	Deflection (mm) at		Load	Deflection (mm) at	
	(kN)	L/2	L/4	(kN)	L/2	L/4	(kN)	L/2	L/4	(kN)	L/2	L/4
1.	3	2.1	1.20	2	0.263	0.16	2	0.25	0.2	2	0.47	0.26
2.	4	3.0	1.82	4	1.66	0.93	4	1.85	1.19	4	2.42	1.46
3.	6	5.0	3.02	6	3.76	2.24	6	3.68	2.35	6	4.14	2.56
4.	8	8.3	5.00	8	5.25	3.11	8	5.55	3.53	8	5.98	3.74
5.	10	10.98	7.00	10	7.21	4.29	10	7.1	4.55	10	8.03	5.08
6.	12	14.0	9.22	12	9.11	5.39	12	8.51	5.42	12	10.15	6.47
7.	14	17.0	11.2	14	10.85	6.36	14	10.09	6.39	14	12.35	7.88
8.	16	20.0	13.50	16	12.98	7.62	16	11.94	7.51	16	14.88	9.6
9.	20	28.0	19.00	18	16.16	9.55	18	13.87	8.73	18	17.1	11.04
10.	21.8	44.85	33.4	20	18.44	10.96	20	17.72	10.99	20	19.34	12.55
11.	21	61.28		22	23.05	13.48	22	24.39	15.02	22	23.44	14.96
12.	18	76.28		24	30.61	17.57	24	31.99	19.37	24	32.3	19.94
13.				25.2	39.2	22.18	25.6	43.25	24.65	26	45.14	24.22
14.				23.5	58.12	-	24	52.25	-	26.2	46.28	24.5
15.				20	75.10	-	21	74.56	-	25	58.32	-
16.										22	74.78	-

Table 3.10: Test Results of the Beam Specimens Retrofitted Using different Type of Bonding Agents

Sr. No	Beam type	P_{max} (kN)	M_{max} (kN-m)	Ductility Ratio*	Increase in Ductility Ratio (%)	Energy Absorption** (kN-m)	Increase in Energy Absorption (%)
1.	Control Unretrofitted Beam (Type-A^+)	21.8	14.99	2.46	-	1244.27	-
2.	Retrofitted with Cement Slurry (Type-B^+)	25.2	17.32	2.60	5.34	1381.35	11.02
3.	Retrofitted with Epoxy Resin (Type-C^+)	25.6	17.60	2.73	9.9	1427.51	14.73
4	Retrofitted with shear connectors (Type-D^+)	26.2	20.30	2.74	10.21	1513.92	21.67

* *Ductility ratio of the beams is defined as ratio of deflection at ultimate load to the yield load calculated from idealized quadri-linear load deflection curve*

** *Area under the load deflection curve upto ultimate load*

Table 3.11 Material Properties Epoxy Resin

S.No.	Property	Typical Test Value
1.	Pot Life (mins.) at 20^0C	45
2.	Compressive Strength (MPa)	50
3.	Tensile strength (MPa)	20
4.	Flexural Strength (MPa)	35
5.	Shear Strength (MPa)	25

Table 3.12: Cost Analysis of the Beams Retrofitted Using Different Bonding Agents

Material	Rate(Rs.)	Cost (Rs.) of Beam type			
		A^+	B^+	C^+	D^+
Concrete Ingredients					
Cement (kg)	3.30	181.50	181.50	181.50	181.50
Rebars (kg)	32.0	402.82	402.82	402.82	402.82
Coarse Aggregates (cft)	12.0	27.26	27.26	27.26	27.26
Fine aggregates (cft)	7.0	22.95	22.95	22.95	22.95
Labour for control beams	Lump Sum	125.0	125.0	125.0	125.0
Cost of ingredients		*759.52*	*759.52*	*759.52*	*759.52*
Retrofitting Material					
Welded Wire mesh	Lump Sum	-	316.67	316.67	316.67
Epoxy	Lump Sum	-	-	500.00	-
Additional material like cement, Fine aggregates, screws etc.	Lump Sum	-	80.19	65.49	90.49
Labour	Lump Sum	-	100.00	100.00	325.00
Cost of Retrofitting		-	*497.16*	*982.16*	*732.16*
Total Cost	**Lump sum**	**759.52**	**1256.38**	**1741.68**	**1491.68**
Cost Ratio		1.0	1.65	2.29	1.96
Strength Ratio		1.0	1.72	1.75	1.79
Cost/Strength Ratio		1.0	0.96	1.31	1.09

$^+$Beam Type A = Control unretrofitted beam
Beam Type B = Beam retrofitted with welded wire mesh Using Cement slurry as Bonding Agent
Beam Type C = Beam retrofitted with welded wire mesh Using Epoxy Resin as Bonding Agent
Beam Type D = Beam retrofitted with welded wire mesh Using Shear Connectors and cement slurry as Bonding Agent

(a) Cement Slurry

(b) Epoxy Resin

(c) Shear Connectors with cement Slurry as Bonding agent

Plate 3.4 Different Bonding Agents

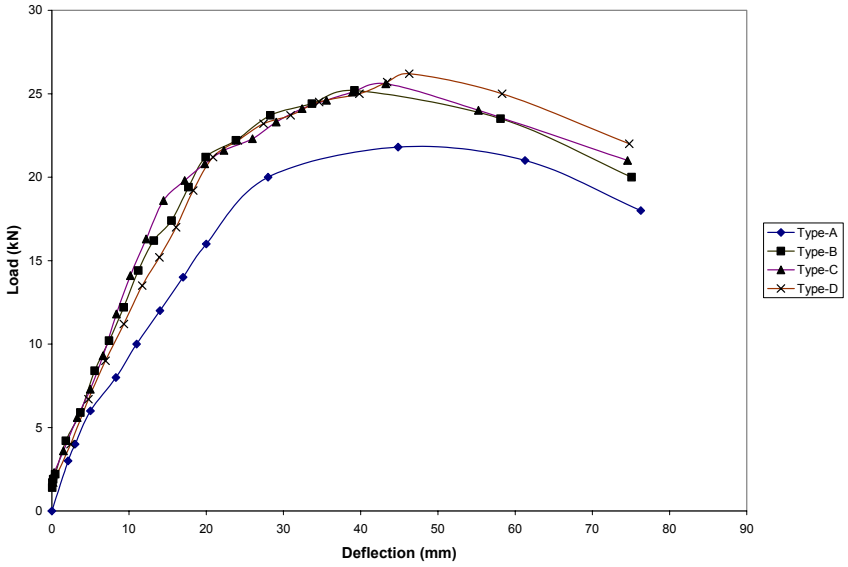

Fig. 3.5 Load v/s Deflection Curve at Mid Span for Control Beam and Beams Retrofitted with Ferrocement Jacket, Bonded with Different Bonding Agents

3.8 EFFECT OF ORIENTATION OF WIRE MESH ON STRENGTH OF BEAMS RETROFITTED USING FERROCEMENT JACKETS

The second pilot study was carried out to study the effect of orientation of wire mesh on the strength of beams retrofitted using ferrocement jackets. Herein, three orientations of wire mesh viz. 0^0, 45^0 and 60^0, to the longitudinal axis of the beam were adopted to reinforce the ferrocement jacket used to retrofit the beams.

In this study too, eight prototype beams of size 127mm x 227mm x 4100mm reinforced with two bars of 10 mm diameter in tension and two bars of 8mm diameter in compression were cast using the proportioned mix. Out of these eight beams, two were used as control beams (Type- A) and tested to failure to find out the safe load carrying capacity corresponding to the allowable deflection as per *IS:456-2000* i.e. span /250. The other six beams were stressed to 75 percent of the safe load obtained from the testing of the control beams and were then retrofitted with 15 mm thick ferrocement jackets made with 1:2 cement sand mortar and w/c ratio 0.40. The jacket was reinforced with single layer of 40mm x 40mm square welded wire mesh. The three wire mesh orientation viz. 0, 45, 60 degree were used in the ferrocement jackets.

The set of beams (two each) were divided into four categories depending upon the orientation of wire mesh in the jacket. Control beams were designated as type-A, whereas, beams retrofitted with welded wire mesh oriented at 0 degree were designated as type – B beams. Retrofitted beams having welded wire mesh oriented at 45 degrees and 60 degrees were designated as type – C and type-D, respectively. The same are shown in Plate No 3.5.

3.8.1 Testing of Beams

All the eight beams, control as well as retrofitted, were tested as per the testing arrangement explained in section 3.5 (see Fig. 3.4)

After testing the control beams, the other six beams were stressed to 75 percent of the safe load and were subsequently retrofitted using the procedure explained in section 3.4. A set of two beams was retrofitted with each wire mesh orientation. After cleaning the surface, the cement slurry was applied to the surface of the beam as a bonding agent and then jacketing of the beam was done with the help of welded wire mesh. Subsequent to that a 15mm thick plaster was applied over the soffit and two sides of the web of the beam in a U-shape. Following this the beam was cured for a

period of 7 days. The retrofitted beams were again tested to obtain the values of loads and corresponding deflections.

3.8.2 Results And Discussion

First, the two control beams were tested to failure. The load corresponding to an allowable central deflection of 15 mm (span/250) was obtained from load deflection curve as 12.67 kN. The remaining six beams were stressed to 75 percent of this average safe load i.e. 9.50 kN. Subsequently the retrofitting of beams using different orientations of wire mesh in the ferrocement jackets was carried out. These retrofitted beams were then loaded to failure and the data was recorded in the form of load and deflection. Table 3.13 presents this data for the control beams and beams retrofitted using specified wire mesh orientations. Fig 3.6 shows the load deflection behaviour at the mid span points of the control as well as beams retrofitted with different wire mesh orientations.

It is observed from the curves in Fig 3.6 that with an increase in load there is a considerable increase in deflection for all the beams. It was also noted that the spacing of cracks was 45mm in case of beams retrofitted with wire mesh at zero degree as compared to beams retrofitted with wire mesh at 45^0, for which it was 85mm. The spacing increased to 108 mm for 60-degree orientation. This shows that the distribution of stress with wire mesh at zero degree is better. It is also observed that corresponding to the serviceability requirement of 15 mm deflection, the load increased from 12.67 kN for the control beam to 14.15 kN, 13.25 kN, 15.41 kN for type B, C and D retrofitted beams, respectively.

It is also observed from the curves that the deflection at the centre at maximum load is maximum in the case of beams retrofitted with wire mesh at 45 degree which is 69.05mm as compared to those with wire mesh at zero degree, for which it is 56.82mm, and for 60 degree, for which it is 63.0 mm.

The load deflection curves were idealized as quadri-linear curves as explained in section 3.6. Using the idealized curves the ductility ratio i.e. ratio of deflection at ultimate load to yield load, and energy absorption i.e. area under the curve up to ultimate load are calculated and presented in Table 3.14. It is observed that the ductility ratio increases by 4.47, 0.40 and 0.82 percent and energy absorption increases by 76.27, 73.98, and 70.42 percent for Type-B, Type-C and Type-D beams respectively as compared to the control beams (Type-A).

The results indicate that the beams retrofitted with wire mesh at 45 degree as reinforcement in the ferrocement jacket is best among all the three with regards to enhanced maximum load carrying capacity followed by 60 degree and zero degree respectively. However, the ductility ratio and energy absorption capacity is highest in case of beams retrofitted wire mesh at zero degree followed by forty-five degrees and sixty degrees. The increase in ductility ratio and energy absorption of beams retrofitted using ferrocement jacket having welded wire mesh at different orientations, as reinforcement are makes the retrofitted beams suitable for dynamic load applications.

A detailed cost analysis to check the economic feasibility of different wire mesh orientations is presented in the succeeding section.

3.8.3 Cost Analysis

A comparative cost analysis for four types of beams is presented in Table 3.15.

It is noted that beams retrofitted with wire mesh oriented at zero degree are the most efficient of the three orientations as its cost to strength ratio is the lowest at 1.19 as compared to the other two orientations for which the value is 1.21 and 1.30 for wire mesh at 45 degrees and 60 degrees, respectively.

Thus, the beams retrofitted using ferrocement jackets having wire mesh orientation at zero degree are most efficient (lowest cost to strength ratio) as compared to other orientations.

Table 3.13: Load v/s. Deflection Data For Control Beam And Beams Retrofitted with Ferrocement Jacket having Welded Wire Mesh at Different Orientations

S. No	Control Beam (Type –A^{++})			Beam with Wire Mesh at 0^0 (Type –B^{++})			Beam with Wire Mesh at 45^0 (Type –C^{++})			Beam with Wire Mesh at 60^0 (Type – D^{++})		
	Load	Deflection (mm) at		Load	Deflection (mm) at		Load	Deflection (mm) at		Load	Deflection (mm) at	
	(kN)	L/2	L/4	(kN)	L/2	L/4	(kN)	L/2	L/4	(kN)	L/2	L/4
1	3	2.1	1.20	3	2.8	1.8	3	3.35	2.12	3	2.43	1.82
2	4	3.0	1.82	4	4.4	3.0	4	4.42	3.0	4	3.58	2.4
3	6	5.0	3.02	6	7.0	4.89	6	6.50	4.5	6	5.61	3.16
4	8	8.3	5.00	8	9.0	6.48	8	8.87	6.0	8	7.30	4.20
5	10	10.98	7.00	10	10.87	7.76	10	10.9	7.74	10	9.76	4.87
6	12	14.0	9.22	12	12.8	9.2	12	13.75	9.26	12	11.85	6.0
7	14	17.0	11.2	14	14.76	10.15	14	15.75	11.45	14	13.24	7.76
8	16	20.0	13.50	16	17.95	13.42	16	17.63	13.98	16	15.73	9.84
9	20	28.0	19.00	18	20.34	15.36	18	20.42	16.76	18	18.00	11.95
10	21.8	44.85	33.4	20	22.76	16.9	20	23.2	17.5	20	21.00	13.72
11	21	61.28		22	24.76	18.5	22	26.8	21.0	22	23.33	15.0
12	18	76.28		24	28.4	20.22	24	32.0	25.0	24	27.00	17.5
13				26	36.0	24.0	26	34.4	28.0	26	34.00	24.0
14				28	47.05	32.04	28	38.0	31.45	28	50.00	36.34
15				30	53.82	-	30	41.95	35	30	58.20	41.52
16				31.8	56.82		32	57.37	40.2	31.9	63.0	45.51
17				30	80.62		33.2	69.05	42.82	29	78	
18				25	100.62		26	99.05		25	102	

Table 3.14: Test Results of Beams Retrofitted Using Ferrocement Jacket having Welded Wire Mesh at Different Orientation

Sr. No	Beam type	P_{max} (kN)	M_{max} (kN-m)	Ductility Ratio*	Energy Absorption** (kN-m)	Increase in Energy Absorption (%)
1	Type-A++	21.8	14.99	2.46	1244.27	-
2	Type-B++	31.8	21.862	2.57	2193.22	76.27
3	Type-C++	33.2	22.825	2.46	2164.72	73.98
4	Type-D++	31.9	21.93	2.48	2120.45	70.42

* *Ductility ratio of the beams is defined as ratio of deflection at ultimate load to the yield load calculated from idealized quadri-linear load deflection curve*

** *Area under the load deflection curve upto ultimate load*

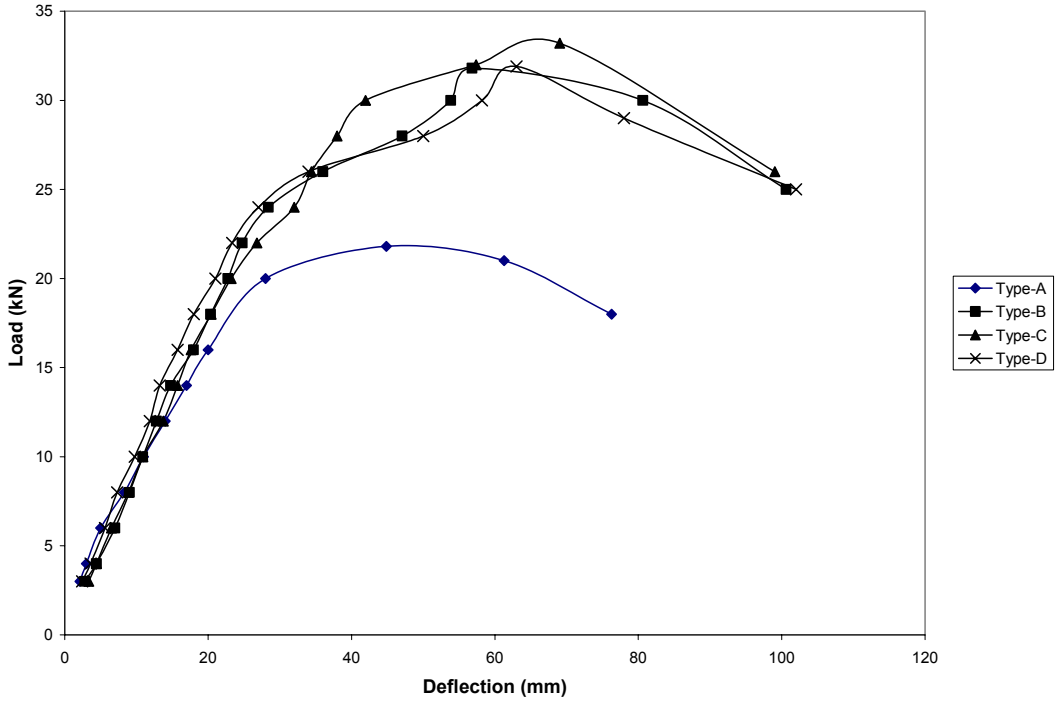

Figure 3.6: Load v/s. Deflection Curve at Mid Span for Control Beam and Beams Retrofitted with Wire mesh at Different Orientations

Table 3.15: Cost Analysis of Beams Retrofitted Using Ferrocement Jacket having Welded Wire Mesh at Different Orientations

Material	Rate(Rs.)	Cost (Rs.) of Beam type			
		A[++]	B[++]	C[++]	D[++]
Concrete Ingredients					
Cement (kg)	215	215	215	215	215
Rebars (kg)					
10mm	30.10	148.724	148.724	148.724	148.724
8mm	30.75	97.14	97.14	97.14	97.14
6mm	33.75	111.52	111.52	111.52	111.52
Coarse Aggregates (cft)	14.0	50.89	50.89	50.89	50.89
Fine aggregates (cft)	17.0	29.56	29.56	29.56	29.56
Labour for control beams	Lump Sum	200	200	200	200
Cost of Ingredients		*852.834*	*852.834*	*852.834*	*852.834*
Retrofitting Material					
Welded Wire mesh	Lump Sum	-	330	420[*]	480[*]
Additional material like cement, Fine aggregates, screws etc.	Lump Sum	-	107	107	107
Labour	Lump Sum	-	192	192	192
Cost of Retrofitting		-	*629*	*719*	*779*
Total Cost		**852.834**	**1481.834**	**1572.834**	**1631.834**
Cost ratio		1.0	1.74	1.84	1.91
Strength Ratio		1.0	1.46	1.52	1.46
Cost/Strength Ratio		1.0	1.19	1.21	1.30

[++] Beam Type A = Control unretrofitted beam
Beam Type B = Beam retrofitted with welded wire mesh oriented at zero degree
Beam Type C = Beam retrofitted with welded wire mesh oriented at 45 degree
Beam Type D = Beam retrofitted with welded wire mesh oriented at 60 degree

* The cost of the wire mesh at 45 degrees and 60 degrees orientation increases due to wastages at these angles

(a) 0^0 Orientation

(b) 45^0 Orientation

(c) 60^0 Orientation

Plate 3.5 Different Wire Mesh Orientations

3.9 EFFECT OF TYPE OF WIRE MESH ON STRENGTH OF BEAM RETROFITTED USING FERROCEMENT JACKETS

The third study was carried out to study the effect of type of wire mesh on strength of beam retrofitted using ferrocement jackets. Two types of wire mesh commonly available in market viz. welded wire mesh and woven wire mesh were adopted as reinforcement for the ferrocement jacket used for retrofitting of the beams.

In this study again, six prototype beams of size 127mm x 227mm x 4100mm reinforced with three bars of 12mm diameter in tension and two bars of 8mm diameter

in compression were cast using the proportioned mix. Out of these six beams, two beams which were used as control beams (Type- A) were tested to failure to find out the safe load carrying capacity corresponding to the allowable deflection as per *IS:456-2000* i.e. span /250. The other four beams were stressed to a predetermined stress level, 60 percent of the safe load obtained from the testing of control beams, and two each were then retrofitted with 25 mm thick ferrocement jacket using two layers of 40 mm x 40 mm square welded wire mesh and with 30 mm x 25 mm GI woven wire mesh, made with 1:2 cement sand mortar and a w/c ratio of 0.40.

The set of beams (two each) were divided into three categories depending upon the type of wire mesh used in the ferrocement jacket. The control beams were designated as type-A, whereas those having welded wire mesh as reinforcement were designated as type – B beams and those having woven wire mesh were designated as type – C beams.

3.9.1 Testing of Beams

All the six beams, controlled as well as retrofitted were tested as per arrangement explained in section 3.5. After testing the control specimens, the other four beams were stressed to 60 percent of safe load and were subsequently retrofitted using the procedure explained in section 3.4. A set of two beams each were retrofitted with each type of wire mesh using cement slurry as the bonding agent. After the application of the bonding agent, retrofitting of the beam was done by applying 25mm thick cement sand mortar on the soffit and two sides of the beam in U-shape as ferrocement jackets, having different types of wire mesh. The beams were cured for 7 days before testing. The retrofitted beams were again tested to obtain the values of load and corresponding deflections.

3.9.2 Results And Discussion

First, the two control beams were tested to failure. The maximum load corresponding to an allowable deflection of 15mm (span/250) was obtained from load deflection curve as 19.875 kN. The remaining four beams were then stressed to 60 percent of this average safe load i.e. 11.925 kN. Subsequently, the retrofitting of beams was carried out using different type of wire meshes as mentioned earlier. These retrofitted beams were then loaded to failure and the data was recorded in the form of loads and corresponding deflections. Table 3.16 presents the data pertaining to the load

deflection values for the control beams and beams retrofitted using welded and woven wire meshes. Fig 3.7 shows the load deflection behaviour at the mid span points of the beams.

It is observed from the Table 3.16 and curves of Fig. 3.7 that with an increase in the load there is a considerable increase in deflection for all the beams. It is also observed that corresponding to the serviceability requirement of 15 mm deflection the load increased from 19.875 kN for the control beam to 24.01 kN for the beams retrofitted using woven wire mesh, whereas, it decreased to 18.37 kN for beams retrofitted using welded wire mesh. Therefore, the safe load carrying capacity of the beams retrofitted using welded wire mesh decreased by 7.57 percent, whereas for the beams retrofitted with woven wire mesh it increased by 20.75 percent, as compared to the control beams. The maximum loads for beams retrofitted using welded wire mesh and woven wire mesh are 43.65 kN and 45.4 kN, respectively, relative to 38.7 kN for the control beam. This indicates that there is an increase in the maximum load carrying capacity by 12.8 percent and 17.31 percent, for beams retrofitted using welded and woven wire meshes, respectively.

The crack spacing in beams before and after the retrofitting was also noted, and it was observed that spacing of the cracks decreases in both the cases after retrofitting. Thus, as noted earlier as well, after retrofitting there is a better distribution of stresses in the beams.

The plotted load deflection curves are also idealized as quadri-linear curves as explained in section 3.6, and from the idealized curves the deflection ductility ratio i.e. ratio of deflection at ultimate load and yield load, and toughness i.e. area under the load deflection curves are determined and tabulated in Table 3.17. It is observed that the toughness of the beams in case of welded wire mesh increases by 7.08 percent, whereas it increases by 55.93 percent in case of woven wire mesh as compared to the control beams.

During the testing it was also noticed that the beams retrofitted using welded wire mesh failed suddenly due the breaking of the wire at the weld spots due to which there is a relatively less increase in the toughness as compared to the woven wire mesh. The decrease in the ductility ratio in welded wire mesh is also due to the sudden breakage of welded wire mesh from the points of weld. Therefore, the use of welded wire mesh is not recommended for retrofitting purposes, where the aim is to increase the ductility and energy absorption capacity of the beams so that they

behave better during earthquakes after retrofitting.

3.10 CONCLUSIONS FROM PILOT STUDIES

Based upon the discussion and analysis of test results of the pilot studies undertaken, the following conclusions were drawn:

1. All the three types of bonding agents viz. cement slurry, epoxy resin and shear connectors with cement slurry as bonding agent, are found useful in increasing the strength and ductility of the retrofitted beams. However, cement slurry is the most efficient of the three bonding agents as its cost to strength ratio is lowest as compared to the others. The maximum strength was the highest in case of the beams retrofitted with shear connectors. This procedure needs technical supervision and skilled labour during application and, therefore, has the higher cost.
2. The beams retrofitted using welded wire mesh at 45-degrees orientation had highest load carrying capacity compared to the other orientations. However, the wire mesh oriented at zero degree was the most efficient as it's cost to strength ratio was the lowest.
3. Beams retrofitted with a ferrocement jacket having woven wire mesh as reinforcement had the highest load carrying capacity, a significant increase in the ductility ratio and energy absorption as compared to the welded wire mesh reinforcement.

Thus, considering the overall economy and usefulness, the following combination of parameters was adopted for further detailed investigations and proposing a mathematical model.

- Woven wire mesh as reinforcement in the ferrocement jacket
- Zero degree orientation of mesh, and
- Cement slurry as the bonding agent.

Table 3.16: Load v/s. Deflection Data For Control Beam And Beams Retrofitted with Ferrocement Jacket Reinforced with Different Types of Wire Mesh

S.No.	Beam-1 Type-A#			Beam-2 Type-A#			Beam –1 Type –B#			Beam –2 Type –B#			Beam –1 Type –C#			Beam –2 Type –C#		
	Load (kN)	Deflection (mm) at		Load (kN)	Deflection (mm) at		Load (kN)	Deflection (mm) at		Load (kN)	Deflection (mm) at		Load (kN)	Deflection (mm) at		Load (kN)	Deflection (mm) at	
		L/2	L/4		L/2	L/4		L/2	L/4		L/2	L/4		L/2	L/4		L/2	L/4
1	0	0	0.00	0	0	0.00	0	0.00	0.00	0	0	0.00	0	0.00	0.00	0	0.00	0.00
2	2	0.91	0.65	2	1.72	1.30	2	3.25	1.91	2	3.05	1.66	2	1.14	0.82	2	1.16	0.81
3	4	1.82	1.29	4	3.44	2.60	4	4.72	2.94	4	4.70	2.72	4	2.17	1.53	4	2.07	1.47
4	6	2.81	1.98	6	5.16	3.90	6	6.46	4.11	6	6.25	3.78	6	3.01	2.12	6	3.36	2.35
5	8	4.18	2.94	8	6.88	5.20	8	7.63	4.90	8	7.84	4.87	8	4.01	2.86	8	4.49	3.15
6	10	5.55	3.89	10	8.58	6.43	10	8.97	5.81	10	9.44	5.97	10	5.35	3.74	10	5.89	4.13
7	12	7.16	4.82	12	10.25	7.60	12	10.23	6.69	12	10.94	7.06	12	6.79	4.75	12	7.17	5.03
8	14	8.83	5.75	14	11.94	8.81	14	11.49	7.59	14	12.43	8.12	14	7.82	5.45	14	8.40	5.90
9	16	10.51	6.67	16	13.64	10.05	16	12.74	8.54	16	13.93	9.11	16	9.36	6.56	16	9.61	6.75
10	18	11.94	7.75	18	15.34	11.27	18	14.07	9.37	18	15.43	10.12	18	10.66	7.44	18	11.05	7.76
11	20	13.33	8.83	20	17.07	12.53	20	15.48	10.09	20	16.93	11.14	20	11.84	8.24	20	12.53	8.81
12	22	14.73	9.83	22	18.82	13.83	22	16.85	10.98	22	18.41	12.19	22	13.74	9.56	22	13.75	9.65
13	24	16.22	10.90	24	20.67	15.14	24	18.20	11.99	24	19.88	13.25	24	14.92	10.38	24	15.05	10.60
14	26	17.77	12.02	26	22.52	16.46	26	19.54	13.08	26	21.67	14.40	26	16.33	11.36	26	16.82	11.87
15	28	19.29	13.12	28	24.36	17.78	28	20.90	14.30	28	23.51	15.56	28	17.54	12.28	28	18.18	12.83
16	30	21.09	14.35	30	26.09	18.99	30	22.25	15.51	30	25.62	16.89	30	19.23	13.40	30	19.48	13.73
17	32	23.05	15.65	32	27.79	20.17	32	23.83	16.57	32	27.80	18.27	32	21.21	14.77	32	21.15	14.87
18	34	25.02	16.95	34	30.36	21.65	34	25.41	17.63	34	29.90	19.61	34	22.70	15.82	34	22.90	16.02
19	36	26.98	18.26	36	33.09	23.19	36	27.04	18.74	36	31.97	20.95	36	24.53	16.89	36	24.76	17.31
20	38	29.73	20.20	37	38.66	26.36	38	28.73	19.91	38	34.35	22.47	38	26.80	18.19	38	26.26	18.25
21	40	36.91	25.77	33.5	50		40	30.85	21.81	40	36.89	24.09	40	28.58	19.37	40	27.59	19.15
22	40.4	38.35	26.89	30	58		41.3	32.33	23.21	42	40.27	26.24	42	30.49	21.15	42	29.41	20.48
23	37	50.0					39	40.24		44	45.09	29.13	44	32.50	22.53	44	32.36	22.59
24	32	62.0					35	50.38		46	50.27	35.29	44.9	46.59	30.73	45.9	42.98	27.94
25										44	59.64		37.5	76.59	38.44	38.5	66.08	36.85

71

Table 3.17: Test Results of Beams Retrofitted Using Ferrocement Jacket Different Types of Wire Meshes

Type of Beam	P_S (kN)	P_{max} (kN)	Ductility Ratio* (Δ_U/Δ_Y)	Energy Absorption** (kN-m)	Increase in Energy Absorption (%)
Control Beam **Type –A**#	19.875	38.70	1.81	1495.1	-
Beam Retrofitted with welded wire mesh **Type -B**#	18.37	43.65	1.50	1600.9	7.08
Beam Retrofitted with woven wire mesh **Type -C**#	24.01	45.4	1.87	2331.32	55.93

* *Ductility ratio of the beams is defined as ratio of deflection at ultimate load to the yield load calculated from idealized quadri-linear load deflection curve*

** *Area under the load deflection curve up to ultimate load*

P_s = Load corresponding to allowable deflection of L/250 i.e. 15 mm

Beam Type A = Control unretrofitted beam
Beam Type B = Beam retrofitted with welded wire mesh
Beam Type C = Beam retrofitted with woven wire mesh

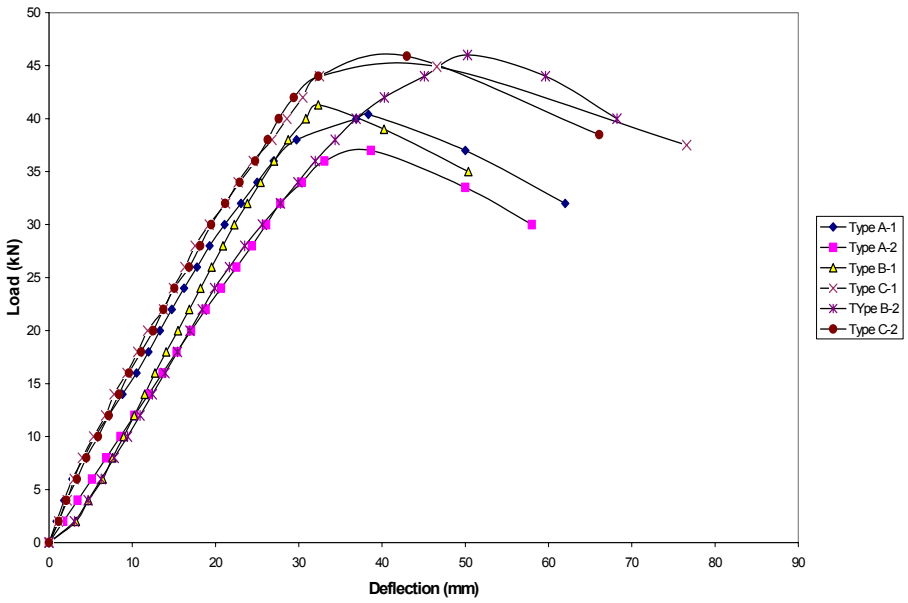

Figure 3.7: Load v/s. Deflection Curve at Mid Span for Control Beams and Beams Retrofitted with Different Type of Wire Mesh

71

CHAPTER –4
EXPERIMENTAL PROGRAM

4.1 GENERAL

The experimental program was designed to study the effect of various parameters on the strength of reinforced concrete beams initially stressed in flexure to pre-determined levels, and subsequently retrofitted with jackets. In total fifty two prototype beams of size 127 mm x 227 mm x 4100 mm were cast, twenty-four beams, two for each parameter, in addition to four control beams, were cast for a particular method of retrofitting.

For the purpose of investigations, of the two sets of beams, one set is retrofitted with ferrocement jacket wherein, the variation in parameters was finalized considering gaps in the available literature and on the basis of results of pilot testing carried out in the laboratory.

The other set of twenty-four beams, were retrofitted using Glass Fibre Reinforced Polymer (GFRP) jackets with fibres oriented at 0^0 and 45^0 to the longitudinal axis of the beam.

Figs 4.1 and 4.2 show the flow chart of the experimental program.

4.2 MATERIALS

Materials similar to ones used in the pilot study were used throughout the study for casting the beams. Relevant tests in accordance with Indian standard codes of practice were conducted to determine the physical properties of the materials used in the study. The details of the materials used for casting and retrofitting of the beams using ferrocement jackets along with their properties are presented in the previous chapter in Section 3.1. The properties of the GFRP fabric and resin used for the retrofitting of the beams using GFRP jackets are presented in the subsequent sections.

4.2.1 GFRP Fabric

Tyfo® SEH-51 composite of FYFE Co. make was used as the GFRP fabric. This is a custom weave, uni-directional and aramid hybrid fabric system. The glass material is orientated in the 0^0 direction with aramid fibres at 90^0. The Tyfo® S Epoxy was used as a bonding agent for fixing the jacket to the beam faces for retrofitting. This is a two-component epoxy matrix material for bonding applications. The typical

properties of the materials as provided by the manufacturer are listed in Tables 4.1 to 4.3.

Table 4.1: Dry Glass Fibre Properties

S. No.	Property	Typical Test Value
1	Tensile Strength (GPa)	3.24
2	Tensile Modulus (GPa)	72.4
3	Ultimate Elongation (%)	4.5
4	Weight (g/m^2)	915
5	Fibre Thickness (mm)	0.36

Table 4.2 Composite Gross Jacket Properties

S. No.	Property	Typical Test Value
1.	Ultimate tensile strength in primary fibre direction (MPa)	575
2.	Elongation at break (%)	2.2
3.	Tensile Modulus (GPa)	26.1
4.	Ultimate tensile strength 90 degree to primary fibre (MPa)	43
5.	Jacket Thickness (mm)	1.3

Table 4.3 Material Properties of Epoxy Resin

S. No.	Property	Typical Test Value
1.	Tensile strength (MPa)	72.4
2.	Tensile modulus (GPa)	3.18
3.	Elongation Percent (%)	5.0
4.	Flexural Strength (MPa)	123.4
5.	Flexural Modulus (GPa)	3.12

4.3 CASTING OF REINFORCED CONCRETE BEAMS

The prototype beams of size 127 mm x 227 mm x 4100 mm were cast as per the procedure explained in section 3.3 of previous chapter. The beams were cast corresponding to the parameters fixed based on the pilot programme to study the

effect of variations on the strength characteristics of the beams, as presented in Fig. 4.1.

4.4 PROCESS OF RETROFITTING

The retrofitting of the beams was done with two types of jackets, namely GFRP and ferrocement jackets. The method of retrofitting followed was as follows:

4.4.1 Retrofitting Using GFRP Jackets

For the purpose of investigation with GFRP jackets twenty-four prototype beams were cast. Half of these beams were designed as under reinforced sections and remaining were designed as balanced section, using limit state design theory. Four beams from each category were stressed to 60 percent, 75 percent and 90 percent of the safe load calculated from the maximum load achieved for the control beams. These beams were subsequently retrofitted using Tyfo® SEH-51 GFRP jacket to study its effect on the strength of the stressed beams. The beams were partially destressed (due to self weight only) by putting them upside down. The surface of these beams was then cleaned and dried, and cavities if any, were removed by repairing the surface with cement paste. Subsequently, the edges of the beams were rounded as shown in Plate 4.1. Tyfo® S epoxy was mixed in ratio of 100.0 parts of A to 42.0 parts of B by volume, and then applied on the prepared surface of the beams as well as on the GFRP sheet. The sheet is than wrapped on the three surfaces of the stressed beam in a U-shape with fibres at 0^0 and 45^0 to the longitudinal axis of the beam, respectively as shown in Plate 4.2.

4.4.2 Retrofitting Using Ferrocement Jacket

For the second part of the investigation twenty-four prototype beams were cast. Twelve beams were designed as under reinforced sections and the other twelve were designed as balanced sections using limit state design theory. Four beams from each category i.e. balanced and under reinforced were stressed to 60 percent, 75 percent and 90 percent of safe load calculated from the test results of the control beams. The beams were partially de-stressed (due to self weight only) by putting them upside down. The surface of the stressed beams was then chipped creating grooves on surfaces of the beams and cleaned with metallic brush using potable water. One coat of cement slurry was applied on the cleaned surface as a bonding agent before placing the wire mesh cage on it without repairing the initial cracks. The cage was properly

placed ensuring tight fit with the help of mild steel wire and 1:2 cement mortar with a water cement ratio of 0.4 was applied.

4.5 TESTING ARRANGEMENT

All the control as well as retrofitted beams, were tested as per arrangement explained in section 3.5.

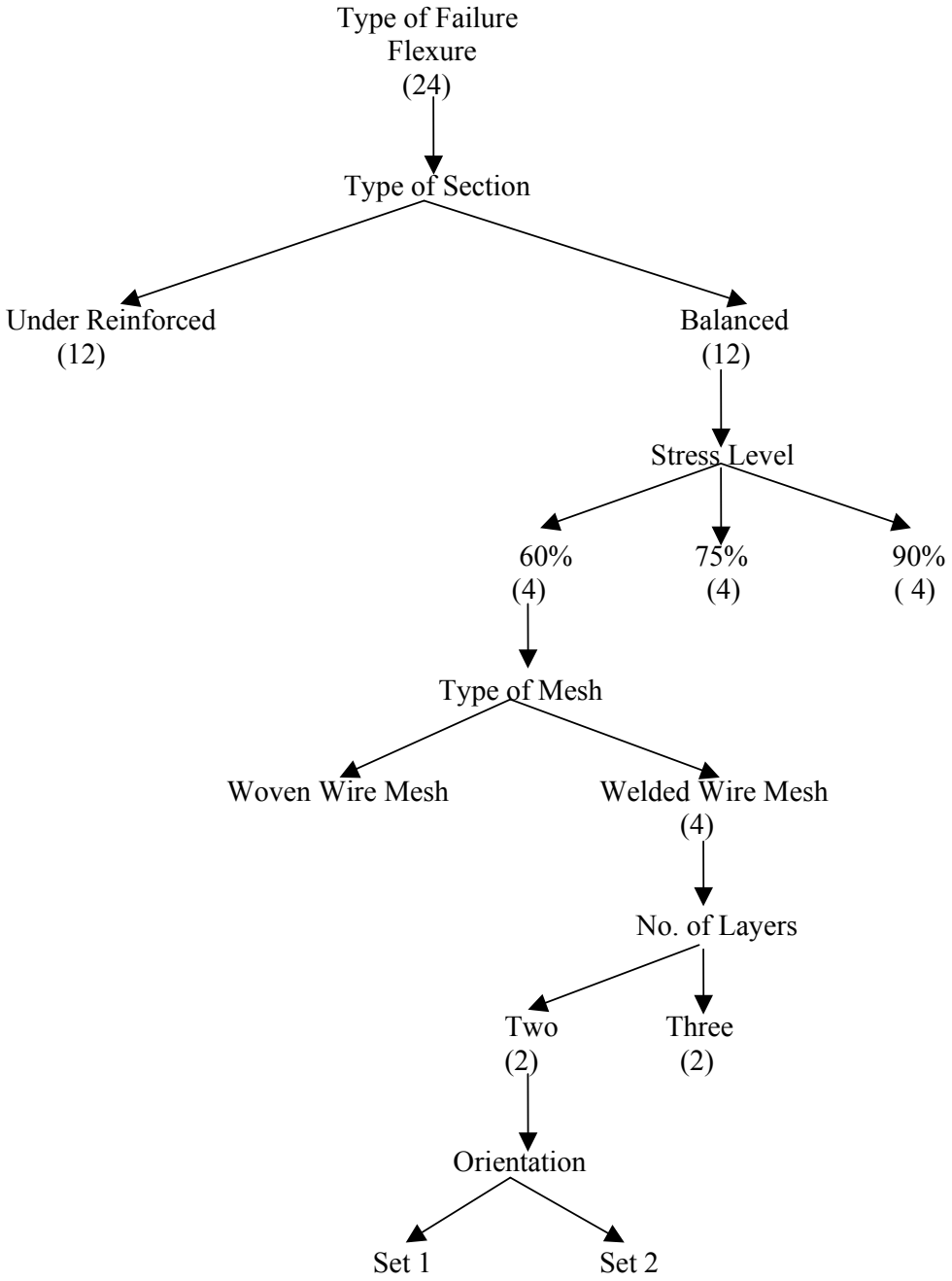

Fig. 4.1 Flow Diagram for Retrofitting using Ferrocement Jackets

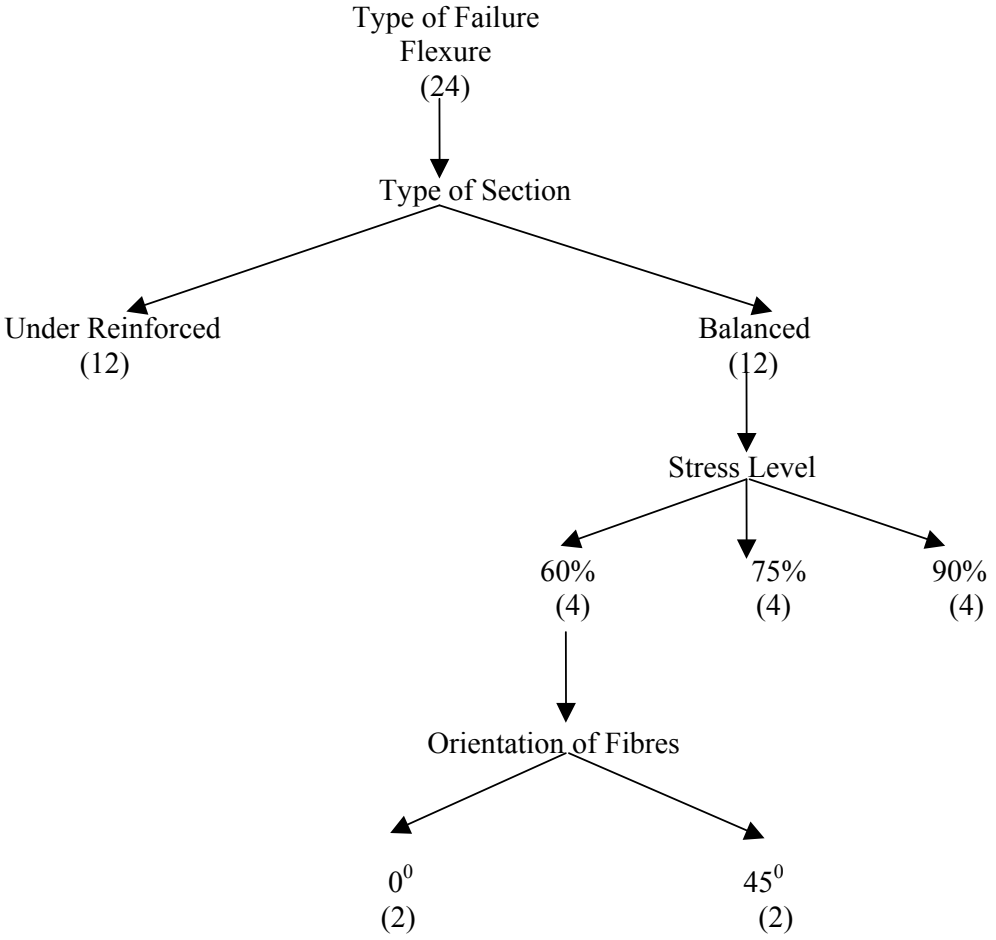

Fig. 4.2 Flow Diagram for Retrofitting Using GFRP Jackets

(a) Rounding of Edges of Beam-1

(b) Rounding of Edges of Beam-2

(c) Rounding of Edges of Beam-3

(d) Repaired Surface of the Beams

Plate 4.1 Surface Preparation for Retrofitting of Beams for GFRP Jacket

(a) Application of Epoxy Resin to Surface of Beam and GFRP Sheets

(b) Fixing GFRP sheets to the Beams

Plate 4.2 Application of GFRP Jacket

CHAPTER –5

RETROFITTING OF BEAMS USING FERROCEMENT JACKETS

5.1 GENERAL

In this chapter the data obtained from testing of retrofitted beams is presented, analyzed and discussed. The entire chapter is divided into three sections. In the first section test results of the beams retrofitted using ferrocement jackets and reinforced with two layers of woven wire mesh are discussed. The second section presents discussion of results of the beams retrofitted using ferrocement jackets reinforced with three layers of woven wire mesh, and the third section carries the comparative analysis.

The retrofitting of the beams using ferrocement jacketing is carried out in two phases. In the first phase the beams are stressed to a fixed percentage of the safe load i.e. load corresponding to allowable deflection of 15 mm (L/250), calculated from the test results of the control beams. As earlier enumerated, three levels of stressing viz. 60, 75, and 90 percent of the safe load were taken up for studying the effect of retrofitting. In the second phase, two or three layers of GI woven wire mesh are provided in U-shape as shown in Plate 3.2(d) and then a 25 mm thick layer of cement mortar is applied to the sides and soffit of the beam. The retrofitted beams are then cured for a period of 7 days and tested as per the procedure presented in Section 3.5.

Out of a total of the twenty four beams cast for the purpose, twelve were retrofitted with ferrocement jacketing having two layers of GI woven wire mesh as reinforcement and the remaining twelve with three layers of the same mesh. Out of the twelve beams, six were designed to be under-reinforced and the other six were designed as balanced sections.

The experimental load deflection results for the control beams and beams retrofitted using U-shaped ferrocement jackets reinforced with two and three layers of GI woven wire mesh, bonded to the surface of beams using cement slurry as bonding agent, are given in Tables 5.1 to 5.14. The load deflection curves for the data obtained from the experimental programme are plotted in Figs. 5.1 to 5.11. These curves were idealized as quadri-linear curves as explained in section 3.6 and various parameters such as maximum load carrying capacity, safe load carrying capacity, ductility ratio, and toughness are calculated and the same are tabulated in Table 5.15. The effect of the

different layers of GI woven wire mesh on the various parameters listed above is studied and the detailed discussion is presented in the succeeding section.

5.2 BEHAVIOUR OF RETROFITTED BEAMS

The maximum load, safe load, ductility and toughness of the retrofitted beams calculated from the test results are summarized in Table 5.15. The number of cracks, their spacing, and depth were also noted and are reported in Tables 5.16 and 5.17.

It is noted that both maximum and safe load carrying capacities of beams increased after retrofitting. This increase can be attributed to increase in the stiffness of sections after retrofitting. The highest increase in the maximum load carrying capacity is of the range of 50 percent and is observed in case of under reinforced beams retrofitted with three layers of GI woven wire mesh as reinforcement. Further, it is observed that the percentage increase in strength decreases as the initial stress level increases from 60 percent to 90 percent of safe load. This reduced increase in the load carrying capacity with initial stress level can be attributed to loss in stiffness of the beams due to initial stressing. It is also observed that with increase in the percentage of reinforcement in the ferrocement jackets the load carrying capacity of the beams increase. This trend is observed for both balanced as well as under-reinforced sections. However, with increase in percentage of main reinforcement in the beams, the percentage increase in strength decreases.

All retrofitted beams show a similar type of load deflection behaviour. However, due to the higher flexural stiffness, all the retrofitted beams exhibited reduced deflections as compared to the control beams.

The crack pattern for all the beams at various stages of loading was also noted and is shown in Plates 5.1 to 5.20. It was observed that cracks starts from the soffit of the beams in the flexural zone, and slowly propagate outwards and upwards. It is noted that with increase in load the number and depth of cracks increase, whereas the spacing of cracks decrease, thereby indicating a better distribution of stresses in the retrofitted beams.

5.3 BEAMS RETROFITTED WITH FERROCEMENT JACKETS REINFORCED WITH TWO LAYERS OF GI WOVEN WIRE MESH

The results of testing of individual beams in the form of loads and deflections at mid and quarter span points are presented in Tables 5.3 to 5.8. Figures 5.1, 5.2, and 5.3

show the load deflection plots of the beams retrofitted with ferrocement jackets having two layers of GI woven wire mesh. The Table 5.15 presents the values of parameters like ductility ratio, toughness etc., which have been derived from the quadri-linear curves which are superimposed on the load deflection curves to get the values of the elastic load ($P_{e)}$, yield load ($P_{Y)}$, maximum load ($P_{max)}$ and ultimate load (P_U). The ultimate load point is defined as that point where load drops to 85% of the maximum load and the ductility ratio is defined as the ratio of deflection at ultimate load to the yield load calculated corresponding to the above values. Toughness is defined as the total area under the fitted quadri-linear curve.

5.3.1 Effect on Strength of Beams

The average maximum load carrying capacity of the under reinforced beams as obtained from the experimental data is 22.4 kN for the control beams, where as, it is found to be 32.1 kN, 32.65 kN, and 30.5 kN for the retrofitted beams initially stressed to 60 percent, 75 percent and 90 percent of the safe load, respectively, indicating that after retrofitting, the maximum load carrying capacity increased by 33.75 percent, 36.04 percent, and 27.08.

Similarly, the value of safe load (load corresponding to an allowable deflection of L/250 which is equal to 15mm) as obtained from the experimental data is 11.99 kN, 16.02 kN, 15.90 kN, and 15.13 kN for the control beam and retrofitted beams initially stressed to 60 percent, 75 percent and 90 percent of the safe load, respectively. Thus for under reinforced beams, on the same line as the maximum load carrying capacity, the safe load carrying capacity of the initially stressed beams also increases by 33.55 percent, 32.55 percent, and 26.13 percent.

The average maximum load carrying capacity of the balanced beams as obtained from the experimental data is 38.7 kN for the control beam. Where as, it found to be 45.4 kN, 46.2 kN, and 46.15 kN for the beams stressed to 60 percent, 75 percent and 90 percent of the safe load and subsequently retrofitted using ferrocement jacketing. Thus it can be said that after retrofitting the maximum load carrying capacity increases by 17.30 percent, 19.38 percent, and 19.25 percent respectively, for the beams initially stressed to 60, 75, and 90 percent levels, respectively.

Similarly, the value of safe load (load corresponding to an allowable deflection of L/250 which is equal to 15mm) as obtained from the experimental data is 19.87 kN, 24.01 kN, 22.43 kN, and 22.31 kN for the control beam and retrofitted beams initially

stressed to 60 percent, 75 percent and 90 percent of the safe load respectively. Thus for balanced beams, on the same line as the maximum load carrying capacity, the safe load carrying capacity of the initially stressed beams also increases by 20.80 percent, 12.85 percent, and 12.25 percent.

So it can be concluded that in all cases when the beams are retrofitted with ferrocement jacketing reinforced with the two layer of GI woven wire mesh the maximum load carrying capacity as well as safe load carrying capacity of the beams increases appreciably. However the increase is more in case of under reinforced section as compared to the balanced section because after the retrofitting of both sections by the same type of jackets the percentage increase in stiffness of the balanced section will be comparatively less to that of under reinforced section, hence the increase in load carrying capacity. Thus with percentage increase in tension reinforcement in the original beams, the increase in load carrying capacity of the beams after retrofitting decreases.

5.3.2 Effect on Deflection Ductility Ratio and Toughness of Beams

The ductility ratio as calculated from fitted quadri-linear curves and reported in Table 5.15 for the under reinforced sections is found to be 2.27 for the control beam and it increases to, 2.28, 2.82, and 3.74, respectively, for the retrofitted beams initially stressed to 60 percent, 75 percent and 90 percent of the safe load indicating an increase of 0.44 percent, 24.22 percent, and 65.2 percent for the beams after retrofitting. In case of balanced sections the ductility ratio as calculated from the experimental results is found to be 1.81, 1.87, 1.87, and 2.05 for the control beam and retrofitted beams initially stressed to 60 percent, 75 percent and 90 percent of the safe load, respectively. Thus, in case of balanced section the ductility ratio increases by 3.3 percent, 3.3 percent and 13.25 percent for the 60, 75 and 90 stressed beams after retrofitting, respectively. It is also observed from the table that the ductility ratio is higher for under reinforced sections as compared to balanced sections at all levels.

The area under the idealized curve for control beams and retrofitted beams was calculated to find out the toughness of the section and is also presented in the Table 5.15. It is noted from the table that the toughness of the under reinforced section increases on an average by 77.63 percent after retrofitting, whereas the corresponding increase in case of the balanced section is of the order of 57.74 percent. The increase in ductility ratio and toughness can be attributed to increase in flexural stiffness of

beams after retrofitting. From the experimental results given in table 5.15 it can be noted that the toughness of the both the type of beams (under reinforced and balanced) increase with increase in the percentage of reinforcement in the ferrocement jackets. This increase in the energy absorption capacity can be attributed to the increase in the stiffness of the section. It can also be noted that the increase in ductility ratio and toughness is more in case of under reinforced sections as compared to the balanced sections. The increase in ductility ratio and toughness of the section clearly indicates that energy absorption capacity of the beams increases after retrofitting, thereby, improving their behaviour during the earthquakes.

Table 5.1: Load v/s. Deflection Data for Under Reinforced Control Beams

Sr. No.	Beam1				Beam 2			
	Load (kN)	Deflection (mm) at			Load (kN)	Deflection (mm) at		
		L/2	L/4	3L/4		L/2	L/4	3L/4
1	0	0	0	0	0	0	0	0
2	2	1.52	0.46	.48	2	2.37	0.99	0.89
3	4	3.0	1.82	1.81	4	4.74	1.98	1.78
4	6	5.0	3.02	3.04	6	7.23	3.69	3.56
5	8	8.3	5.0	5.02	8	9.78	5.88	5.92
6	10	10.98	7.0	7.05	10	12.85	7.86	8.13
7	12	14	9.22	9.25	12	16.1	9.78	10.23
8	14	17	11.2	11.28	14	19.1	11.89	12.23
9	16	20	13.5	13.52	16	22.26	14.07	14.33
10	20	28	16	16.04	18	26.18	16.7	16.87
11	21.8	44.85	33.4	33.45	20	31.63	20	20.17
12	21	61.28			22	38.9	24.05	23.01
13	18	76.28			23	48.3	28.6	27.09
					20	79.3		

Table 5.2: Load v/s. Deflection Data for Balanced Control Beams

Sr. No.	Beam1				Beam 2			
	Load (kN)	Deflection (mm) at			Load (kN)	Deflection (mm) at		
		L/2	L/4	3L/4		L/2	L/4	3L/4
1	0	0	0	0	0	0	0	0
2	2	0.91	0.65	0.65	2	1.72	1.2	1.4
3	4	1.82	1.29	1.29	4	3.44	2.39	2.8
4	6	2.81	1.98	1.98	6	5.16	3.59	4.21
5	8	4.18	2.95	2.93	8	6.88	4.78	5.61
6	10	5.55	3.91	3.87	10	8.58	5.98	6.88
7	12	7.16	4.97	4.67	12	10.25	7.17	8.03
8	14	8.83	6.06	5.43	14	11.94	8.4	9.22
9	16	10.51	7.14	6.19	16	13.64	9.64	10.45
10	18	11.94	8.26	7.24	18	15.34	10.88	11.65
11	20	13.33	9.34	8.32	20	17.07	12.18	12.88
12	22	14.73	10.33	9.33	22	18.82	13.52	14.13
13	24	16.22	11.38	10.41	24	20.67	14.83	15.45
14	26	17.77	12.48	11.55	26	22.52	16.14	16.78
15	28	19.29	13.56	12.67	28	24.36	17.45	18.1
16	30	21.09	14.79	13.91	30	26.09	18.65	19.32
17	32	23.05	16.17	15.12	32	27.79	19.82	20.52
18	34	25.02	17.56	16.34	34	30.36	21.35	21.95
19	36	26.98	18.95	17.56	36	33.09	22.94	23.43
20	38	29.73	20.95	19.45	37	38.66	26.78	25.93
21	40	36.91	26.39	25.15	33.5	50.0		
22	40.4	38.35	27.48	26.29	30	58.0		
23	37	50.0						
24	32	62.0						

Table 5.3: Load v/s. Deflection Data for 60 percent Stressed Under Reinforced Beams Retrofitted with Ferrocement Jacket Reinforced with Two Layers of Woven Wire Mesh

Sr. No.	Beam1				Beam 2			
	Load (kN)	Deflection (mm) at			Load (kN)	Deflection (mm) at		
		L/2	L/4	Under load		L/2	L/4	Under load
1	0	0.00	0.00	0.00	0	0.00	0.00	0.00
2	2	1.23	0.83	1.25	2	1.71	0.94	1.24
3	4	2.65	1.79	2.50	4	2.72	1.98	2.57
4	6	4.48	3.01	4.09	6	4.45	3.04	3.81
5	8	6.22	4.23	5.63	8	6.54	4.53	5.79
6	10	8.02	5.49	7.33	10	8.95	6.22	7.96
7	12	10.18	6.98	9.61	12	10.89	8.24	9.58
8	14	12.41	8.88	11.29	14	13.10	9.77	11.56
9	16	14.51	10.46	12.76	16	15.50	10.78	13.24
10	18	16.61	11.77	14.36	18	17.03	12.19	15.02
11	20	18.91	12.93	16.49	20	19.72	13.12	17.48
12	22	21.44	14.61	18.97	22	22.25	14.88	19.75
13	24	23.88	16.41	21.33	24	25.00	17.22	22.25
14	26	26.24	18.33	23.56	26	26.96	19.21	24.92
15	28	30.82	21.11	27.66	28	31.00	21.29	27.63
16	30	38.17	25.49	34.19	30	39.42	26.94	36.27
17	32	57.74	35.86	50.23	32	54.09	31.08	42.05
18	30	74.56			32.2	60.77	33.22	44.91
19	26	88.56			29	64.14	43.68	60.05
					26.5	90.73		

Table 5.4: Load v/s. Deflection Data for 75 percent Stressed Under Reinforced Beams Retrofitted with Ferrocement jacket Reinforced with Two Layers of Woven Wire Mesh

Sr. No.	Beam1				Beam 2			
	Load (kN)	Deflection (mm) at			Load (kN)	Deflection (mm) at		
		L/2	L/4	Under load		L/2	L/4	Under load
1	0	0.00	0.00	0.00	0	0.00	0.00	0.00
2	2	1.38	1.04	1.34	2	1.34	1.01	1.28
3	4	3.88	2.00	2.55	4	2.61	1.94	2.51
4	6	5.78	3.95	5.18	6	5.72	3.90	5.09
5	8	7.48	5.12	6.71	8	7.39	5.09	6.64
6	10	9.78	6.62	8.68	10	9.53	6.54	8.61
7	12	11.06	7.50	9.96	12	10.94	7.51	9.95
8	14	13.02	8.96	11.78	14	12.90	8.94	11.76
9	16	15.18	10.37	13.67	16	15.03	10.45	13.54
10	18	17.68	12.17	15.91	18	17.58	12.27	15.85
11	20	19.88	13.46	17.80	20	19.68	13.75	17.65
12	22	22.03	15.12	19.86	22	22.08	15.39	19.58
13	24	25.22	17.08	22.50	24	25.03	17.31	22.16
14	26	28.04	19.02	24.99	26	27.96	19.21	24.69
15	28	34.85	22.88	30.67	28	34.70	23.33	30.18
16	30	44.28	28.10	38.22	30	44.17	28.70	38.15
17	31	49.85	30.99	42.69	31	49.44	31.62	42.18
18	32	58.96	35.83	49.73	32	58.12	36.68	49.42
19	32.4	65.02	39.04	54.45	33.2	63.70	39.80	54.11
20	32.1	82.55	42.75	59.87	33.2	80.70	43.54	59.30
21	27	99.5			27	102.7		

Table 5.5: Load v/s. Deflection Data for 90 percent Stressed Under Reinforced Beams Retrofitted with Ferrocement Jacket Reinforced with Two Layers of Woven Wire Mesh

Sr. No.	Beam1				Beam 2			
	Load (kN)	Deflection (mm) at			Load (kN)	Deflection (mm) at		
		L/2	L/4	Under load		L/2	L/4	Under load
1	0	0.00	0.00	0.00	0	0.00	0.00	0.00
2	2	2.15	0.65	1.19	2	2.53	0.96	1.23
3	4	4.86	3.04	4.43	4	5.26	3.31	4.33
4	6	6.89	4.53	6.37	6	7.11	4.76	6.38
5	8	8.51	5.60	7.88	8	8.69	5.87	7.81
6	10	10.21	6.77	9.41	10	10.96	7.42	9.95
7	12	12.01	7.96	11.02	12	12.23	8.27	11.10
8	14	13.64	9.05	12.00	14	13.91	9.43	12.59
9	16	15.99	10.67	14.63	16	15.90	10.79	14.39
10	18	18.29	12.26	16.68	18	17.90	12.15	16.14
11	20	20.89	14.02	19.00	20	20.46	13.93	18.47
12	22	23.15	15.54	21.01	22	22.83	15.55	20.60
13	24	28.15	17.91	25.25	24	25.47	17.46	23.17
14	26	47.14	30.17	41.33	26	28.75	19.52	26.08
15	28	66.22	40.89	56.78	28	46.70	29.49	40.38
16	28.9	73.13	45.71	63.09	29	55.47	34.65	47.81
17	29.1	80.11	50.30	67.70	29.6	69.88	43.25	61.13
18	29.9	87.13	50.59		30	76.38	50.31	66.68
19	25	107.13			30.6	82.88		
					31.1	88.12		
					25	113.12		

Table 5.6: Load v/s. Deflection Data for 60 percent Stressed Balanced Beams Retrofitted with Ferrocement Jacket Reinforced with Two Layers of Woven Wire Mesh

Sr. No.	Beam1				Beam 2			
	Load (kN)	Deflection (mm) at			Load (kN)	Deflection (mm) at		
		L/2	L/4	Under load		L/2	L/4	Under load
1	0	0.00	0.00	0.00	0	0.00	0.00	0.00
2	2	1.14	0.82	1.04	2	1.16	0.81	1.10
3	4	2.17	1.53	1.96	4	2.07	1.47	1.98
4	6	3.01	2.12	2.74	6	3.36	2.35	3.16
5	8	4.01	2.86	3.73	8	4.49	3.15	4.20
6	10	5.35	3.74	4.88	10	5.89	4.13	5.43
7	12	6.79	4.75	6.20	12	7.17	5.03	6.57
8	14	7.82	5.45	7.12	14	8.40	5.90	7.70
9	16	9.36	6.56	8.54	16	9.61	6.75	8.87
10	18	10.66	7.44	9.24	18	11.05	7.76	10.19
11	20	11.84	8.24	10.79	20	12.53	8.81	11.61
12	22	13.74	9.56	12.51	22	13.75	9.65	12.68
13	24	14.92	10.38	13.60	24	15.05	10.60	14.14
14	26	16.33	11.36	14.88	26	16.82	11.87	15.45
15	28	17.54	12.28	16.08	28	18.18	12.83	16.68
16	30	19.23	13.40	17.53	30	19.48	13.73	17.82
17	32	21.21	14.77	19.31	32	21.15	14.87	19.28
18	34	22.70	15.82	20.60	34	22.90	16.02	20.81
19	36	24.53	16.89	22.01	36	24.76	17.31	22.21
20	38	26.80	18.19	24.05	38	26.26	18.25	23.51
21	40	28.58	19.37	25.65	40	27.59	19.15	24.77
22	42	30.49	21.15	27.36	42	29.41	20.48	26.44
23	44	32.50	22.53	29.23	44	32.36	22.59	29.43
24	44.9	46.59	30.73	42.20	45.9	42.98	27.94	37.39
25	37.5	76.59	38.44	51.37	38.5	66.08	36.85	47.72

Table 5.7: Load v/s. Deflection Data for 75 percent Stressed Balanced Beams Retrofitted with Ferrocement Jacket Reinforced with Two Layers of Woven Wire Mesh

Sr. No.	Beam1				Beam 2			
	Load (kN)	Deflection (mm) at			Load (kN)	Deflection (mm) at		
		L/2	L/4	Under load		L/2	L/4	Under load
1	0	0.00	0.00	0.00	0	0.00	0.00	0.00
2	2	1.09	0.69	0.98	2	0.89	0.68	0.84
3	4	2.45	1.64	2.22	4	2.24	1.62	2.05
4	6	3.75	2.77	3.28	6	3.81	2.78	3.45
5	8	5.05	3.83	4.25	8	5.14	4.20	4.75
6	10	6.54	5.00	5.57	10	6.62	4.80	5.68
7	12	8.10	6.16	7.04	12	7.94	5.78	7.42
8	14	9.15	7.03	8.14	14	9.18	7.00	8.54
9	16	10.53	8.02	9.44	16	10.87	8.07	10.33
10	18	12.19	9.25	10.99	18	12.29	8.86	11.39
11	20	13.50	10.23	12.24	20	13.52	9.82	12.53
12	22	14.54	11.38	13.70	22	14.62	10.97	14.02
13	24	16.52	12.60	15.22	24	16.48	12.28	15.76
14	26	17.82	13.76	16.71	26	17.92	13.14	16.89
15	28	19.56	14.72	17.94	28	19.75	14.09	18.09
16	30	20.81	15.61	18.88	30	21.12	15.07	19.34
17	32	22.63	16.87	20.58	32	23.09	16.97	21.08
18	34	24.41	18.27	22.47	34	25.08	18.29	22.89
19	36	25.78	19.24	23.77	36	26.87	19.57	24.50
20	38	27.13	20.24	25.06	38	28.38	20.59	25.36
21	40	29.09	21.64	26.94	40	30.16	21.83	27.48
22	42	30.46	22.61	28.25	42	33.00	23.70	29.48
23	44	31.82	23.60	29.53	44	39.91	27.76	35.33
24	46	36.96	26.72	34.38	44.3	48.54	33.36	42.74
25	47	44.82	30.47	40.52	40	60.98	39.03	50.45
26	48.1	53.66	35.88	47.93	36	67.92		
27	44	66.59	48.53	60.84				
28	40	74.68						

Table 5.8: Load v/s. Deflection Data for 90 percent Stressed Balanced Beams Retrofitted with Ferrocement Jacket Reinforced with Two Layers of Woven Wire Mesh

Sr. No.	Beam1				Beam 2			
	Load (kN)	Deflection (mm) at			Load (kN)	Deflection (mm at)		
		L/2	L/4	Under load		L/2	L/4	Under load
1	0	0.00	0.00	0.00	0	0.00	0.00	0.00
2	2	1.12	0.78	1.03	2	1.07	0.71	1.02
3	4	2.02	1.40	1.88	4	2.00	1.41	1.93
4	6	2.89	2.05	2.73	6	3.59	2.75	3.39
5	8	4.35	3.05	4.07	8	5.29	3.96	4.91
6	10	5.63	3.93	5.23	10	6.94	5.11	6.48
7	12	7.24	5.02	6.65	12	8.18	5.94	7.57
8	14	8.54	5.88	7.81	14	9.73	7.02	8.99
9	16	9.88	6.77	8.98	16	11.31	8.01	10.32
10	18	11.02	7.57	10.00	18	12.63	8.94	11.52
11	20	12.37	8.52	11.21	20	14.05	10.07	12.91
12	22	13.89	9.64	12.60	22	15.86	11.36	14.52
13	24	15.29	10.65	13.88	24	17.32	12.36	15.89
14	26	16.68	11.66	15.17	26	18.75	13.33	17.24
15	28	18.12	12.69	16.51	28	20.51	14.55	18.85
16	30	19.55	13.72	17.83	30	22.08	15.61	20.31
17	32	20.65	14.51	18.85	32	24.10	16.98	22.20
18	34	22.22	15.60	20.26	34	25.85	18.25	23.85
19	36	23.34	16.41	21.33	36	27.56	19.40	25.49
20	38	25.15	17.55	23.06	38	29.29	20.64	27.09
21	40	26.55	18.53	24.34	40	31.50	22.11	29.05
22	42	28.39	19.80	25.98	42	34.13	23.78	31.24
23	44	30.14	20.96	27.54	44	37.79	26.02	34.30
24	46	36.01	25.06	32.62	44.4	49.06	31.62	42.19
25	47.9	47.05	30.98	42.34	38	69.06	41.38	56.13
26	44	65.38	41.53	58.47				
27	40	75.38	47.05	65.76				

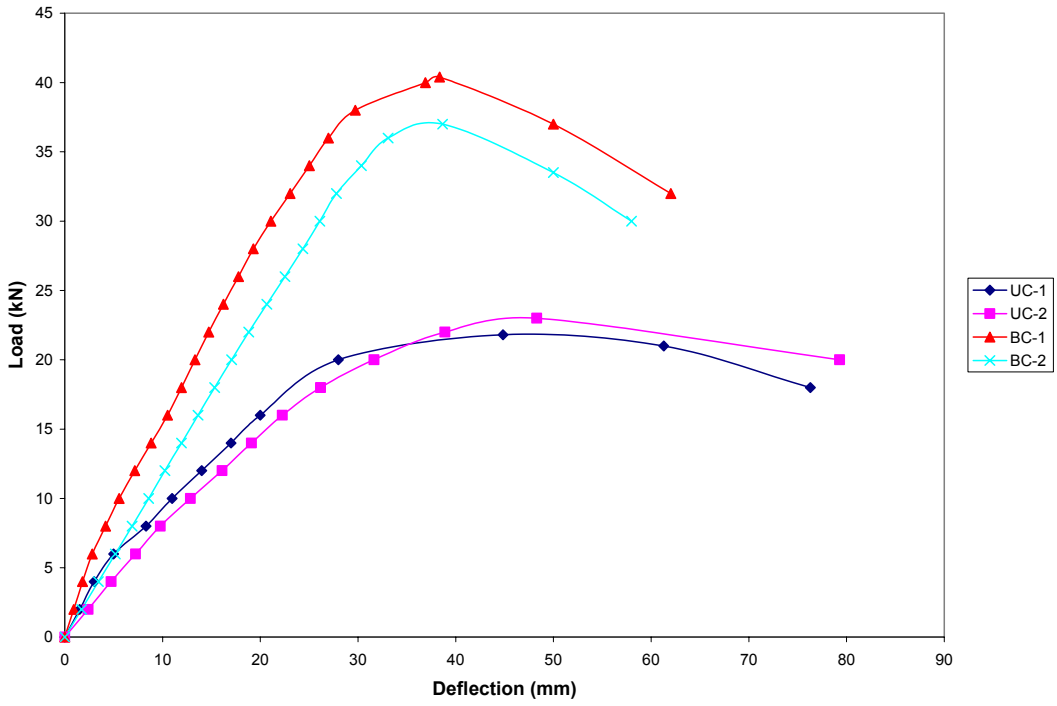

Fig. 5.1: Load v/s Deflection For Control Beams

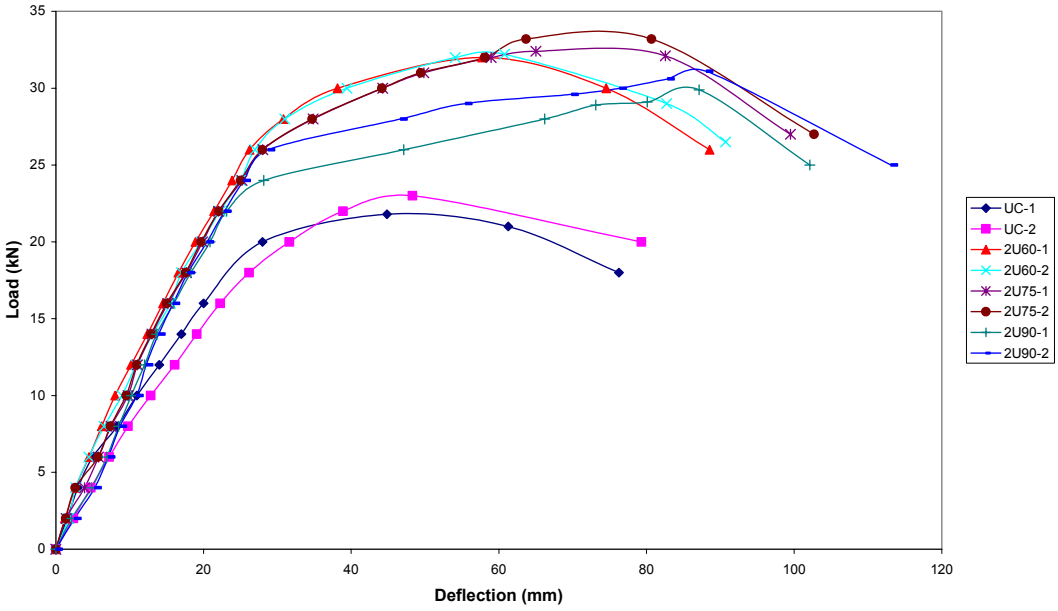

Fig. 5.2: Load v/s Mid- Span Deflection of Under Reinforced Beam Sections Retrofitted with Ferrocement Jacketing with Two Layers of Wire Mesh and Stressed to Different Levels.

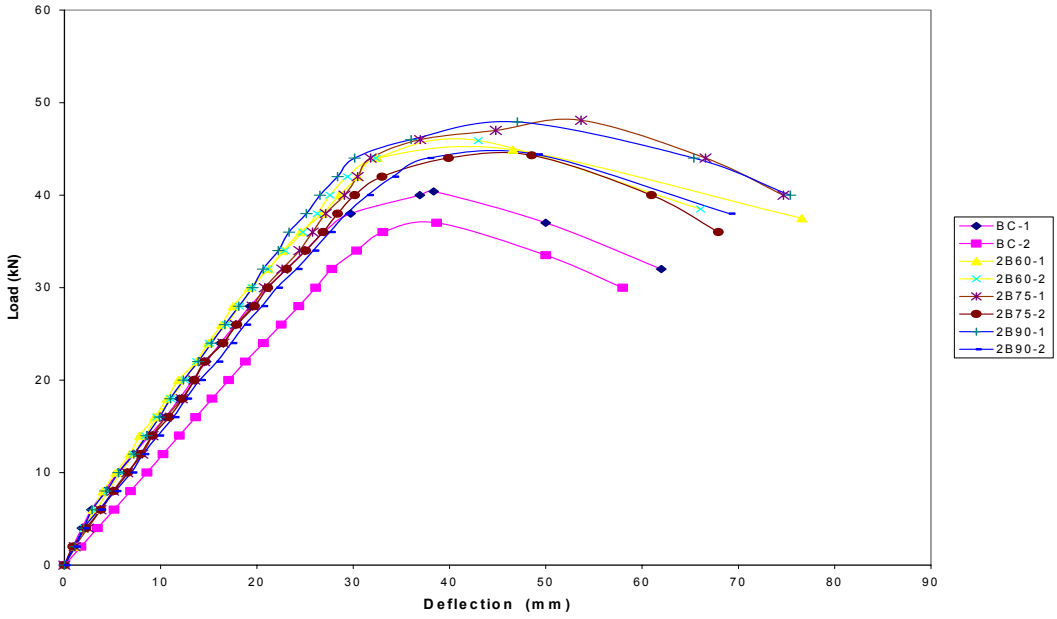

Fig. 5.3: Load v/s Mid- Span Deflection of Balanced Beam Sections Retrofitted with Ferrocement Jacketing with Two layers of Wire Mesh and Stressed to Different Levels

5.4 BEAMS RETROFITTED WITH FERROCEMENTS JACKETS REINFORCED WITH THREE LAYERS OF GI WOVEN WIRE MESH

The results of testing of individual beams in the form of loads and deflections at mid and quarter span points are presented in Tables 5.6 to 5.8 and 5.12 to 5.14. Figures 5.1, 5.4, and 5.5 show the load deflection plots of the beams retrofitted with ferrocement jackets having three layers of GI woven wire mesh. The Table 5.15 presents the values of parameters like ductility ratio, toughness etc., which have been derived from the quadri linear curves which are superimposed on the load deflection curves to get the values of the elastic load ($P_{e)}$, yield load ($P_{Y)}$, maximum load (P_{max}) and ultimate load (P_U). The ductility ratio is defined as that ratio of deflection at ultimate load and yield load calculated corresponding to the above values. Toughness is defined as the area under the fitted quadri linear curves up to ultimate load.

5.4.1 Effect on Strength of Beams

The average maximum load carrying capacity of the under reinforced beams as obtained from the experimental data is 22.4 kN for the control beam, where as, it is found to be 36.05 kN, 36.45 kN, and 35.6 kN for the retrofitted beams initially

stressed to 60 percent, 75 percent and 90 percent of the safe load, respectively, indicating that after retrofitting, the maximum load carrying capacity increases by 50.2 percent, 51.87 percent, and 48.33 percent.

Similarly, the value of safe load (load corresponding to an allowable deflection of L/250 which is equal to 15mm) as obtained from the experimental data is 11.99 kN, 21.20 kN, 21.30 kN, and 20.2 kN for the control beam and retrofitted beams initially stressed to 60 percent, 75 percent and 90 percent of the safe load, respectively. Thus for under reinforced beams, on the same line as the maximum load carrying capacity, the safe load carrying capacity of the initially stressed beams, also increases by 76.74 percent, 77.57 percent, and 68.40 percent.

The average maximum load carrying capacity of the balanced beams as obtained from the experimental data is 38.7 kN for the control beam. Where as, it found to be 52 kN, 51 kN, and 50.2 kN for the beams stressed to 60 percent, 75 percent and 90 percent of the safe load and subsequently retrofitted using ferrocement jacketing. Thus it can be said that after retrofitting the maximum load carrying capacity increases by 34.37 percent, 31.78 percent, and 29.71 percent respectively, for the beams initially stressed to 60, 75, and 90 percent levels, respectively.

Similarly, the value of safe load (load corresponding to an allowable deflection of L/250 which is equal to 15mm) as obtained from the experimental data is 19.87 kN, 26.01 kN, 26.02 kN, and 24.5 kN for the control beam and retrofitted beams initially stressed to 60 percent, 75 percent and 90 percent of the safe load respectively. Thus for balanced sections, on the same line as the maximum load carrying capacity, the safe load carrying capacity of the initially stressed beams also increases by 30.86 percent, 30.91 percent, and 23.27 percent.

So it can be observed that in all cases when the beams are retrofitted with ferrocement jacketing reinforced with the three layer of GI woven wire mesh the maximum load carrying capacity as well as safe load carrying capacity of the beams increases appreciably. However the increase is more in case of under reinforced section as compared to the balanced section because after the retrofitting of both sections by the same type of jackets the percentage increase in stiffness of the balanced section will be comparatively less to that of under reinforced section, hence the increase in load carrying capacity. Thus with percentage increase in tension reinforcement in the original beams, the increase in load carrying capacity of the beams after retrofitting decreases.

5.4.2 Effect on Deflection Ductility Ratio and Toughness of Beams

The ductility ratio as calculated from fitted quadri-linear curves and reported in Table 5.15 for the under reinforced sections is found to be 2.27 for the control beam and it increases to 2.4, 2.45, and 2.87, respectively, for the retrofitted beams initially stressed to 60 percent, 75 percent and 90 percent of the safe load indicating an increase of 5.72 percent, 7.92 percent, and 26.43 percent for the beams after retrofitting. In case of balanced sections the ductility ratio as calculated from the experimental results is found to be 1.81, 2.21, 1.89, and 1.99 for the control beam and retrofitted beams initially stressed to 60 percent, 75 percent and 90 percent of the safe load, respectively. Thus, in case of balanced section the ductility ratio increases by 22.1 percent, 4.42 percent and 9.94 percent for the 60, 75 and 90 stressed beams after retrofitting, respectively. It is also observed from the table that the ductility ratio is higher for under reinforced sections as compared to balanced sections at all levels.

The area under the curve for control beams and retrofitted beams is calculated to find out the toughness of the section and is also presented in the Table 5.15. It is noted from the table that the toughness of the under reinforced section on average increases by 118.45 percent after retrofitting, whereas the corresponding increase in case of the balanced section is of the order of 89.46 percent.

From the experimental results given in table 5.15 it can be noted that the toughness of the both the type of beams (under reinforced and balanced) increase with increase in the percentage of reinforcement in the ferrocement jackets. This increase in the energy absorption capacity can be attributed to the increase in the stiffness of the section. It can also be noted that the increase in ductility ratio and toughness is more in case of under reinforced sections as compared to the balanced sections. The increase in ductility ratio and toughness of the section clearly indicates that energy absorption capacity of the beams increases after retrofitting, thereby, improving their behaviour during the earthquakes.

Table 5.9: Load v/s. Deflection Data for 60 percent Stressed Under Reinforced Beams Retrofitted with Ferrocement Jacket Reinforced with Three Layers of Woven Wire Mesh

Sr. No.	Beam1				Beam 2			
	Load (kN)	Deflection (mm) at			Load (kN)	Deflection (mm) at		
		L/2	L/4	Under load		L/2	L/4	Under load
1	0	0.00	0.00	0.00	0	0.00	0.00	0.00
2	2	1.04	0.80	1.01	2	1.04	0.53	0.91
3	4	1.69	1.25	1.60	4	1.66	1.16	1.53
4	6	3.26	2.33	2.97	6	3.20	2.26	2.99
5	8	4.87	3.42	4.42	8	4.76	3.55	4.32
6	10	6.07	4.23	5.44	10	5.98	4.21	5.35
7	12	7.23	5.02	6.50	12	7.25	5.03	6.45
8	14	8.77	6.02	7.84	14	8.65	5.98	7.76
9	16	10.26	7.04	9.13	16	10.32	7.15	9.22
10	18	12.15	8.38	10.81	18	12.09	8.30	10.83
11	20	13.77	9.50	12.28	20	13.65	9.48	12.32
12	22	15.95	11.52	14.22	22	15.92	11.35	14.02
13	24	18.01	12.90	16.07	24	18.15	12.86	16.01
14	26	20.47	14.55	18.28	26	20.66	14.54	18.15
15	28	23.33	15.98	20.86	28	23.39	16.15	20.85
16	30	27.87	18.80	24.78	30	27.20	18.15	24.30
17	32	35.60	23.43	31.36	32	32.22	21.84	27.73
18	34.8	45.70	31.25	43.20	34	43.27	28.01	36.44
19	35	61.99	41.94	57.52	35.2	50.01	33.05	43.27
20	35.4	73.99	45.76	62.24	36.2	53.64	39.58	56.13
21	30	104.99			36.5	69.55		63.03
22					36.7	85.55		
					30	114.55		

Table 5.10: Load v/s. Deflection Data for 75 percent Stressed Under Reinforced Beams Retrofitted with Ferrocement Jacket Reinforced with Three Layers of Woven Wire Mesh

Sr. No.	Beam1				Beam 2			
	Load (kN)	Deflection (mm) at			Load (kN)	Deflection (mm) at		
		L/2	L/4	Under load		L/2	L/4	Under load
1	0	0.00	0.00	0.00	0	0.00	0.00	0.00
2	2	1.15	0.89	0.96	2	1.08	0.84	0.96
3	4	2.04	1.62	1.75	4	1.91	1.45	1.75
4	6	2.93	2.39	2.64	6	2.89	2.27	2.64
5	8	4.63	3.62	4.06	8	4.43	3.31	4.06
6	10	6.02	4.55	5.20	10	5.80	4.15	5.20
7	12	7.45	5.45	6.59	12	7.35	5.23	6.59
8	14	9.06	6.38	8.04	14	8.91	6.28	8.04
9	16	10.45	7.45	9.27	16	10.23	7.24	9.27
10	18	12.01	8.56	10.65	18	11.89	8.36	10.65
11	20	13.85	9.83	12.25	20	13.61	9.61	12.25
12	22	15.65	11.05	13.86	22	15.43	10.87	13.86
13	24	17.39	12.25	15.54	24	17.26	12.18	15.54
14	26	21.65	15.60	19.35	26	19.25	13.60	17.35
15	28	23.95	17.12	21.29	28	21.46	15.12	19.29
16	30	26.25	18.97	23.84	30	23.99	16.79	21.48
17	32	32.62	22.37	28.44	32	29.03	19.73	25.44
18	34	43.48	30.12	38.02	34	39.51	25.48	33.65
19	35	55.23	41.56	48.72	34.3	44.12	28.05	37.27
20	35.4	73.98	52.86	66.96	35.8	57.25	35.68	48.00
21	30	100.98			36.8	69.31	44.46	58.27
22					37.5	79.31		
23					35	91.31		
24					30	109.31		

Table 5.11: Load v/s. Deflection Data for 90 percent Stressed Under Reinforced Beams Retrofitted with Ferrocement Jacket Reinforced with Three Layers of Woven Wire Mesh

Sr. No.	Beam1				Beam 2			
	Load (kN)	Deflection (mm) at			Load (kN)	Deflection (mm) at		
		L/2	L/4	Under load		L/2	L/4	Under load
1	0	0.00	0.00	0.00	0	0.00	0.00	0.00
2	2	1.06	0.71	0.91	2	0.96	0.69	0.88
3	4	2.16	1.44	1.86	4	2.28	1.62	2.07
4	6	3.66	2.52	3.25	6	3.61	2.60	3.17
5	8	5.11	3.52	4.54	8	5.17	3.71	4.59
6	10	6.31	4.38	5.68	10	6.80	4.87	6.13
7	12	7.69	5.39	6.94	12	8.32	5.98	7.51
8	14	9.13	6.41	8.27	14	10.18	7.24	9.20
9	16	10.41	7.31	9.44	16	12.13	8.64	10.97
10	18	12.11	8.47	10.96	18	13.65	9.71	13.40
11	20	13.92	9.69	12.57	20	15.93	11.32	15.33
12	22	15.68	10.91	14.16	22	17.89	12.62	17.14
13	24	17.60	12.22	15.87	24	19.93	14.04	18.75
14	26	19.58	13.54	17.62	26	22.73	15.87	21.09
15	28	21.68	14.94	19.50	28	25.46	17.69	23.33
16	30	24.58	16.80	22.12	30	28.03	19.36	27.16
17	32	31.28	20.61	26.96	32	34.75	23.26	33.81
18	32.9	43.39	27.67	37.32	32.9	45.12	28.72	41.64
19	34	52.24	32.93	45.41	34	53.78	34.09	53.13
20	35.4	62.42	38.55	59.05	35.6	68.06	47.57	59.04
21	35.6	66.54	43.28	66.44	36	98.06		
22	33.7	80.54						
23	30	98.54						

Table 5.12: Load v/s. Deflection Data for 60 percent Stressed Balanced Beams Retrofitted with Ferrocement Jacket Reinforced with Three Layers of Woven Wire Mesh

Sr. No.	Beam1				Beam 2			
	Load (kN)	Deflection (mm) at			Load (kN)	Deflection (mm) at		
		L/2	L/4	Under load		L/2	L/4	Under load
1	0	0.00	0.00	0.00	0	0.00	0.00	0.00
2	2	0.73	0.49	0.66	2	0.64	0.45	0.57
3	4	1.84	1.24	1.68	4	1.27	0.87	1.14
4	6	2.92	1.93	2.63	6	1.97	1.33	1.74
5	8	3.94	3.07	3.56	8	3.27	2.24	2.93
6	10	4.97	3.68	4.44	10	5.60	3.93	5.02
7	12	5.97	4.38	5.42	12	6.76	4.73	6.04
8	14	6.98	5.08	6.37	14	7.66	5.33	6.88
9	16	8.07	5.86	7.36	16	8.75	6.09	7.88
10	18	9.21	6.69	8.44	18	10.42	7.25	9.38
11	20	10.42	7.54	9.49	20	11.42	8.98	10.31
12	22	11.75	8.32	10.76	22	13.05	9.09	11.77
13	24	13.21	9.56	12.11	24	14.34	9.99	12.92
14	26	14.36	10.41	13.16	26	15.60	10.86	14.05
15	28	15.68	11.40	14.35	28	17.32	12.03	15.60
16	30	16.89	12.29	15.47	30	18.64	13.43	16.78
17	32	18.56	13.50	16.95	32	20.10	14.47	18.11
18	34	20.31	14.82	18.52	34	21.75	15.60	19.58
19	36	21.56	15.70	19.67	36	23.59	16.81	21.27
20	38	23.05	16.74	21.02	38	25.15	17.94	22.53
21	40	24.35	17.63	22.18	40	26.90	19.08	24.11
22	42	25.55	18.66	23.28	42	28.50	20.23	25.54
23	44	27.29	19.75	24.84	44	30.32	21.79	27.17
24	46	28.91	20.90	26.30	46	33.36	24.04	29.88
25	48	30.53	22.01	27.75	48	37.19	27.12	33.15
26	50	32.40	23.26	29.45	49	43.42	31.07	38.78
27	52	34.44	24.57	31.24	50	51.21	35.77	44.71
28	53.5	46.33	31.90	41.19	50.5	61.22	39.54	53.02
29	50	61.11	40.55	54.36	49.5	64.71		57.24
30	48	68.35	45.75	60.84	43.5	81.71		
31	44.5	77.35	53.94	62.34				

Table 5.13: Load v/s. Deflection Data for 75 percent Stressed Balanced Beams Retrofitted with Ferrocement Jacket Reinforced with Three Layers of Woven Wire Mesh

Sr. No.	Beam1				Beam 2			
	Load (kN)	Deflection (mm) at			Load (kN)	Deflection (mm) at		
		L/2	L/4	Under load		L/2	L/4	Under load
1	0	0.00	0.00	0.00	0	0.00	0.00	0.00
2	2	1.00	0.72	0.92	2	0.87	0.68	0.80
3	4	2.05	1.47	1.87	4	1.99	1.49	1.81
4	6	3.33	2.37	3.05	6	2.83	2.28	2.58
5	8	4.60	3.28	4.21	8	3.65	3.20	3.80
6	10	5.61	4.01	5.14	10	4.85	3.94	4.88
7	12	6.85	4.91	6.29	12	6.03	4.74	5.95
8	14	8.04	5.73	7.34	14	7.24	5.54	7.03
9	16	9.00	6.39	8.21	16	8.46	6.35	8.12
10	18	10.26	7.30	9.34	18	9.85	7.28	9.36
11	20	11.21	7.97	10.20	20	11.33	8.25	10.67
12	22	12.61	8.96	11.44	22	12.62	9.13	11.93
13	24	13.66	9.68	12.41	24	14.03	10.11	13.20
14	26	14.71	10.41	13.39	26	15.24	10.95	14.31
15	28	15.99	11.31	14.54	28	16.77	11.99	15.67
16	30	17.26	12.22	15.71	30	18.29	13.00	17.12
17	32	18.63	13.18	16.97	32	20.11	14.25	18.78
18	34	19.85	14.62	18.14	34	21.80	15.43	20.34
19	36	21.08	15.28	19.31	36	23.53	16.63	21.90
20	38	22.22	15.87	20.24	38	24.94	17.56	23.17
21	40	23.79	16.95	21.68	40	26.60	18.62	24.61
22	42	25.40	17.98	23.02	42	28.62	20.00	26.47
23	44	27.06	19.17	24.58	44	30.82	21.43	28.41
24	46	28.95	20.42	26.24	46	33.25	23.05	30.54
25	48	31.39	21.92	28.33	48	37.33	25.63	33.72
26	50	36.44	24.98	32.63	50	42.47	28.37	38.09
27	50.7	44.21	29.21	38.66	51.3	49.96	33.62	44.20
28	48.5	58.83			50	59.95		
29	42.5	71.83			43	79.95		

Table 5.14: Load v/s. Deflection Data for 90 percent Stressed Balanced Beams Retrofitted with Ferrocement Jacket Reinforced with Three Layers of Woven Wire Mesh

Sr. No.	Beam1				Beam 2			
	Load (kN)	Deflection (mm) at			Load (kN)	Deflection (mm) at		
		L/2	L/4	Under load		L/2	L/4	Under load
1	0	0.00	0.00	0.00	0	0.00	0.00	0.00
2	2	1.28	0.96	1.22	2	1.15	0.65	1.04
3	4	2.18	1.60	2.06	4	2.11	1.32	1.91
4	6	3.18	2.33	3.00	6	3.07	1.96	2.72
5	8	4.60	3.33	4.31	8	4.43	2.84	3.93
6	10	5.63	4.04	5.25	10	5.92	3.96	5.64
7	12	6.84	4.89	6.33	12	7.10	4.78	6.30
8	14	7.91	5.62	7.29	14	8.34	5.67	7.45
9	16	9.41	6.65	8.65	16	9.63	6.54	8.59
10	18	10.53	7.42	9.67	18	11.14	7.62	9.89
11	20	11.45	8.15	10.60	20	12.66	8.66	11.31
12	22	12.93	9.12	11.83	22	13.99	9.34	12.53
13	24	14.10	9.95	12.88	24	15.32	10.02	13.75
14	26	15.31	10.81	14.00	26	16.78	11.06	15.06
15	28	16.56	11.70	15.14	28	18.34	12.12	16.47
16	30	17.84	12.60	16.30	30	20.00	13.28	17.99
17	32	19.61	13.83	17.86	32	21.49	14.27	19.30
18	34	20.87	14.68	19.02	34	23.07	15.39	20.74
19	36	22.21	15.60	20.28	36	24.71	16.34	22.23
20	38	24.02	16.63	21.75	38	26.12	17.26	23.49
21	40	25.61	17.73	23.18	40	27.71	18.36	24.94
22	42	27.33	18.91	24.68	42	29.20	19.39	26.25
23	44	29.17	20.21	26.40	44	31.42	20.88	28.20
24	46	31.02	21.44	28.08	46	33.62	22.33	30.15
25	48	33.28	22.95	30.07	48	36.75	24.30	32.99
26	50	36.29	24.84	32.65	49.4	47.41	30.03	41.10
27	50.7	46.01	30.22	40.66	45	65.03	38.81	53.13
28	49	55.85	35.90	53.77	42	71.38	42.39	58.17
29	44	70.60	43.95	56.26				

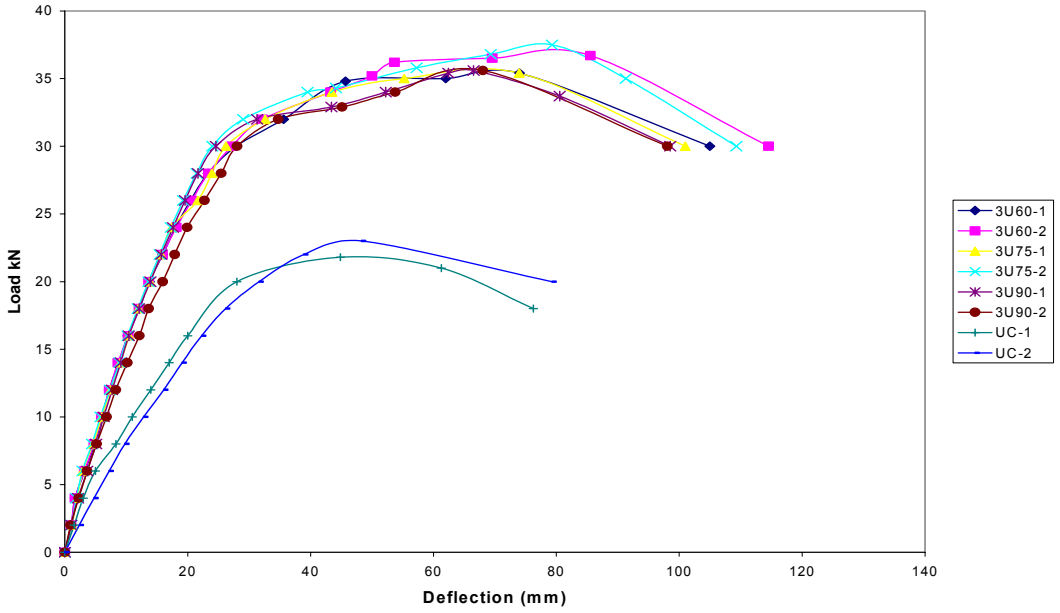

Fig. 5.4: Load v/s Mid- Span Deflection of Under Reinforced Beam Sections Retrofitted with Ferrocement Jacketing with Three Layers of Wire Mesh and Stressed to Different Levels

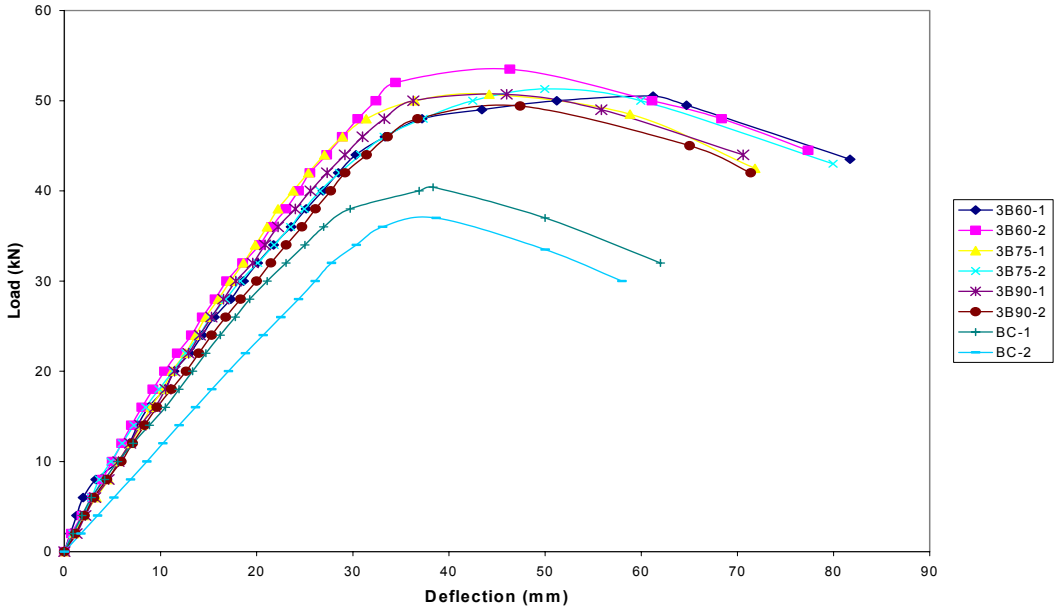

Fig. 5.5: Load v/s Mid- Span Deflection of Balanced Beam Sections Retrofitted with Ferrocement Jacketing with Three Layers of Wire Mesh and Stressed to Different Levels.

5.5 COMPARATIVE ANALYSIS

A comparative analysis of the effect of different layers of woven wire mesh used for retrofitting of initially stressed beams on the various parameters maximum load carrying capacity, safe load carrying capacity, deflection ductility ratio and toughness is presented in this section. It is found from the discussion in the preceding section that all these parameters increase considerably irrespective of the stress level, type of section, and number of layers of wire mesh.

However, on comparative analysis, it is observed that effect of change in initial stress level on all the observed parameters is almost negligible, but with change in type of section from under reinforced to balanced percentage increase in almost all the properties decrease. This can be attributed to the fact that during retrofitting, as extra steel is provided in the tension zone in the form of wire mesh, the balanced section acts as an over reinforced section, which results in its failure by crushing of concrete rather than by yielding of the reinforcement. A similar behaviour was also observed during the testing as well, wherein the balanced section after retrofitting failed in compression and the under reinforced sections failed by yielding of reinforcement.

The increase in the number of layers of wire mesh in the ferrocement jacket also affects the observed properties. It is observed that with increase in number of layers from two to three the average percentage increase in maximum load carrying capacity of the beams after retrofitting increases from 32 to 50 percent in case of under reinforced section while it increases from 18 to 32 percent for balanced sections. Similarly, the average percentage increase in safe load carrying capacity after retrofitting increases from 30 to 75 for the under reinforced section, where as it increases from 15 to 30 in case of balanced sections.

With increase in number of layers from two to three, average percentage increase of toughness of beam after retrofitting on an average increases by 52.58 percent in case of under reinforced section, whereas the increase is of order of and 54.93 percent for the balanced sections.

Thus, with increase in percentage of the reinforcement in ferrocement jackets all the observed properties increases due to increase in the stiffness of the jacket.

During the testing of the beams it was observed that after the retrofitting of the beams, the cracks in the beams originate from the soffit of the jacket and it propagate with the increase of load as shown in plate 5.3. In general no horizontal cracks were observed

at the interface of the original beam and jacket, indicating that there is no interfacial bond failure. However, at the maximum load the spalling of the ferrocement cover was observed. The crack spacing at maximum load for both retrofitted as well as un-retrofitted beams was also noted and it is observed that in all cases crack spacing in retrofitted beams decreases to 40-50 mm from original spacing of 80-120mmin case of control beams, indicating better distribution of stresses in case of beams retrofitted using ferrocement jacketing.

Table 5.15: Deflection Ductility and Toughness for Control Beams and Beams Retrofitted Using Ferrocement Jacketing

Type of Beam	P_S	P_e	P_Y	P_U	Ductility Ratio (Δ_U/Δ_Y)	Toughness (KN-mm)	Increase in Toughness (percent)
UC	11.995	16.5	21.5	22.4	2.27	1336.41	-
2U60	16.02	24	30	32.1	2.28	2112.27	58.05
2U75	15.90	26	32	32.65	2.83	2477.11	85.36
2U90	15.13	25	27	30.5	3.74	2532.51	89.50
3U60	21.2	29	35.6	36.05	2.4	3121.26	133.56
3U75	21.3	30	34	36.45	2.45	2979.86	122.82
3U90	20.2	29	32	35.6	2.87	2659.27	98.99
BC	19.875	33	37	38.7	1.81	1495.1	-
2B60	24.01	42	45	45.4	1.87	2331.33	55.93
2B75	22.43	40	44.5	46.2	1.87	2331.32	54.73
2B90	22.31	42	44	46.15	2.05	2430.21	62.55
3B60	26.01	48	50	52	2.21	3067.24	105.16
3B75	26.02	45	50	51	1.89	2798.7	87.19
3B90	24.5	46.5	49	50.2	1.99	2631.75	76.03

2U60 Under Reinforced section stressed to 60 percent of safe load and retrofitted using ferrocement jacketing reinforced with two layers of wire mesh.

2U75 Under Reinforced section stressed to 75 percent of safe load and retrofitted using ferrocement jacketing reinforced with two layers of wire mesh.

2U90 Under Reinforced section stressed to 90 percent of safe load and retrofitted using ferrocement jacketing reinforced with two layers of wire mesh.

3U60 Under Reinforced section stressed to 60 percent of safe load and retrofitted using ferrocement jacketing reinforced with two layers of wire mesh.

3U75 Under Reinforced section stressed to 75 percent of safe load and retrofitted using ferrocement jacketing reinforced with two layers of wire mesh.

3U90 Under Reinforced section stressed to 90 percent of safe load and retrofitted using ferrocement jacketing reinforced with two layers of wire mesh.

2B60 Balanced section stressed to 60 percent of safe load and retrofitted using ferrocement jacketing reinforced with two layers of wire mesh.

2B75 Balanced section stressed to 75 percent of safe load and retrofitted using ferrocement jacketing reinforced with two layers of wire mesh.

2B90 Balanced section stressed to 90 percent of safe load and retrofitted using ferrocement jacket having two layers of wire mesh.

3B60 Balanced section stressed to 60 percent of safe load and retrofitted using ferrocement jacketing reinforced with two layers of wire mesh.

3B75 Balanced section stressed to 75 percent of safe load and retrofitted using ferrocement jacketing reinforced with two layers of wire mesh.

3B90 Balanced section stressed to 90 percent of safe load and retrofitted using ferrocement jacketing reinforced with two layers of wire mesh.

Table 5.16 Number of Cracks at Different Stress Level

Type of Beam	No. of Cracks at First Crack Level	No. of cracks at 18 kN load	No. of Cracks at 30 kN load	No. of Cracks at Failure
2B60(1)	4	10	15	22
2B60(2)	4	14	17	21
2B75(1)	4	12	14	16
2B75(2)	9	12	14	22
2B90(1)	3	7	17	24
2B90(2)	5	11	22	29
3B60(1)	9	17	22	30
3B60(2)	10	19	23	29
3B75(1)	7	16	23	29
3B75(2)	7	17	22	30
3B90(1)	9	16	21	25
3B90(2)	7	15	21	29
2U60(1)	11	14	-	24
2U60(2)	9	12	-	23
2U75(1)	6	9	-	26
2U75(2)	7	9	-	28
2U90(1)	11	18	-	27
2U90(2)	9	17	-	26
3U60(1)	5	15	-	28
3U60(2)	6	15	-	27
3U75(1)	4	14	-	20
3U75(2)	4	19	-	29
3U90(1)	6	20	-	26
3U90(2)	6	21	-	28

Table 5.17 Spacing and Depth of Cracks in Control and Retrofitted Beams at Failure

S.No.	Type of Beam	Minimum Spacing of Cracks (mm)	Maximum Spacing of Cracks (mm)	Depth of Crack (mm)
1.	UC-1	45	140	170
2.	UC-2	44	110	172
3.	2U60-1	31	126	196
4.	2U60-2	29	150	250
5.	2U75-1	21	212	220
6.	2U75-2	25	180	215
7.	2U90-1	20	181	201
8.	2U90-2	22	165	222
9.	3U60-1	29	174	203
10.	3U60-2	30	184	210
11.	3U75-1	29	194	196
12.	3U75-2	20	155	213
13.	3U90-1	28	175	196
14.	3U90-2	18	174	165
15.	BC-1	75	150	136
16.	BC-2	72	162	125
17.	2B60-1	25	152	210
18.	2B60-2	18	144	207
19.	2B75-1	40	151	201
20.	2B75-2	30	190	191
21.	2B90-1	20	100	250
22.	2B90-2	40	160	250
23.	3B60-1	19	160	190
24.	3B60-2	21	140	178
25.	3B75-1	28	161	186
26.	3B75-2	28	150	186
27.	3B90-1	37	177	215
28.	3B90-2	25	130	161

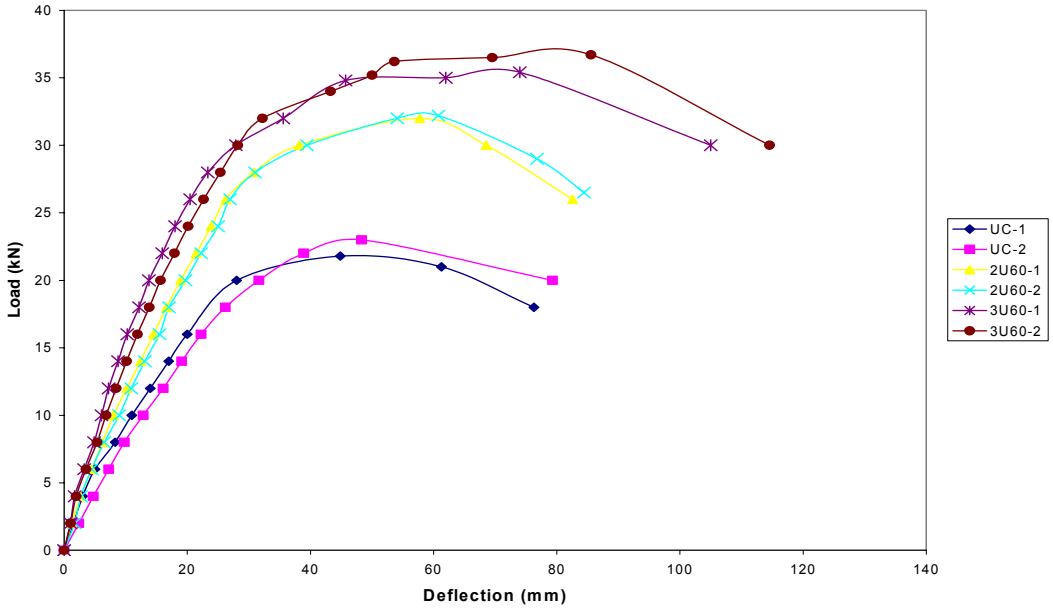

Fig 5.6: Load v/s Mid- Span Deflection of Under Reinforced Beam Sections Retrofitted with Ferrocement Jacketing with Different Layers of Wire Mesh and Stressed to 60 percent Stress Level

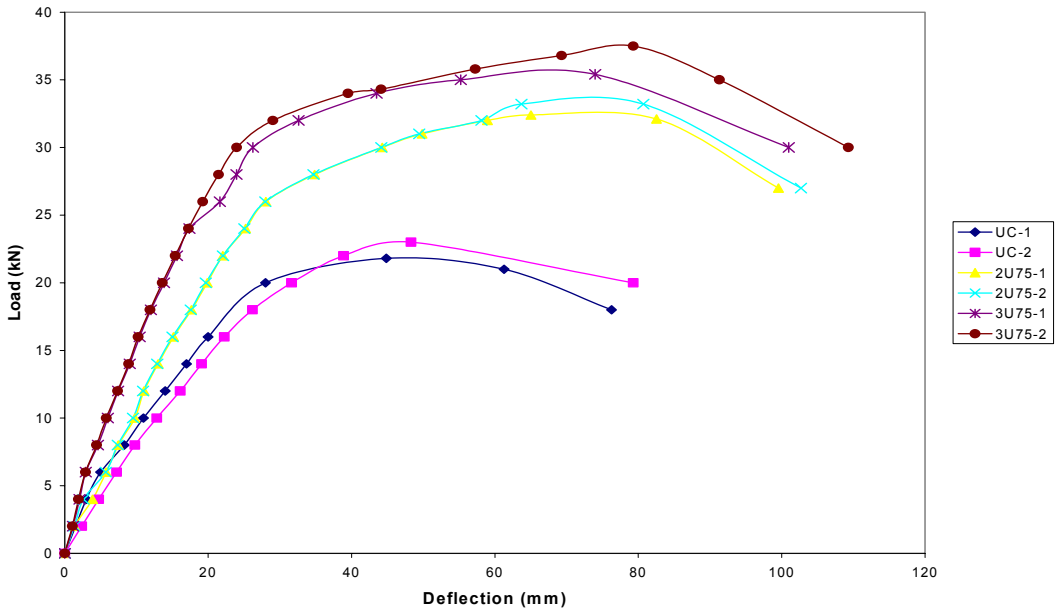

Fig. 5.7: Load v/s Mid- Span Deflection of Under Reinforced Beam Sections Retrofitted with Ferrocement Jacketing with Different Layers of Wire Mesh and Stressed to 75 percent Stress Level

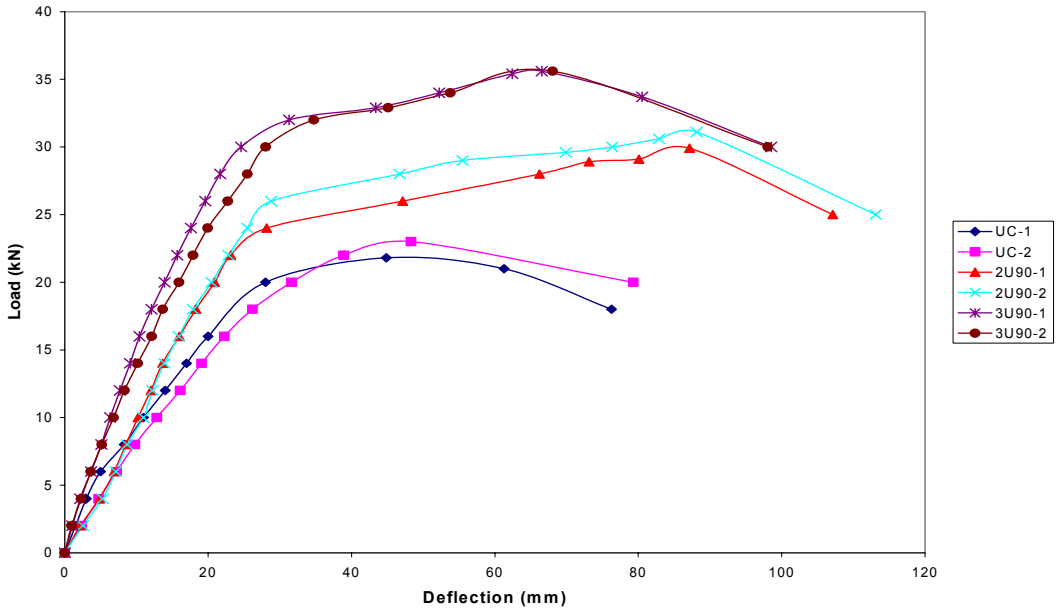

Fig. 5.8: Load v/s Mid- Span Deflection of Under Reinforced Beam Sections Retrofitted with Ferrocement Jacketing with Different Layers of Wire Mesh and Stressed to 90 percent Stress Level

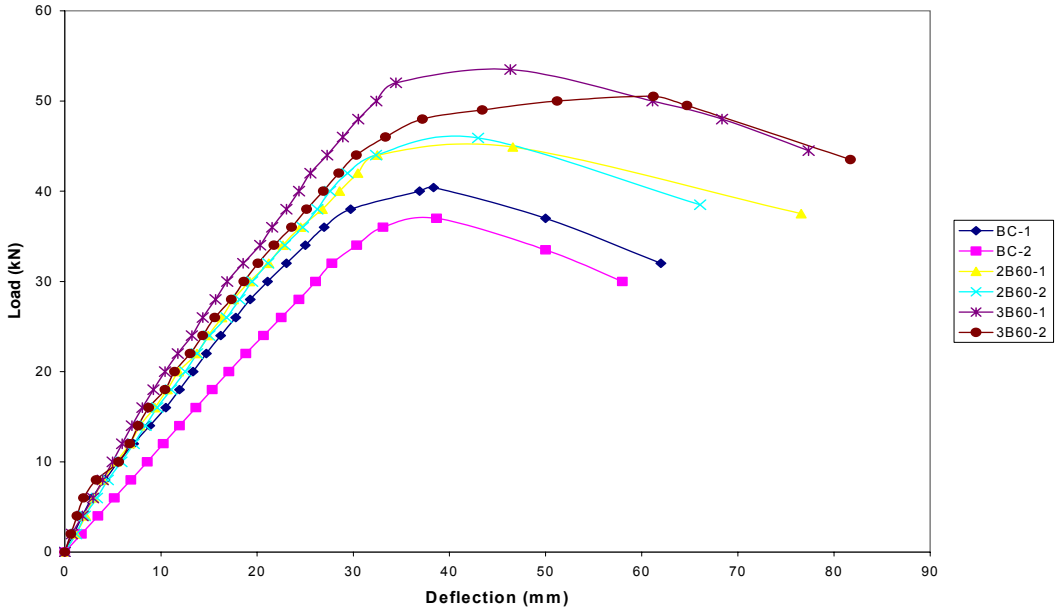

Fig. 5.9: Load v/s Mid- Span Deflection of Balanced Beam Sections Retrofitted with Ferrocement Jacketing with Different Layers of Wire Mesh and Stressed to 60 percent Stress Level

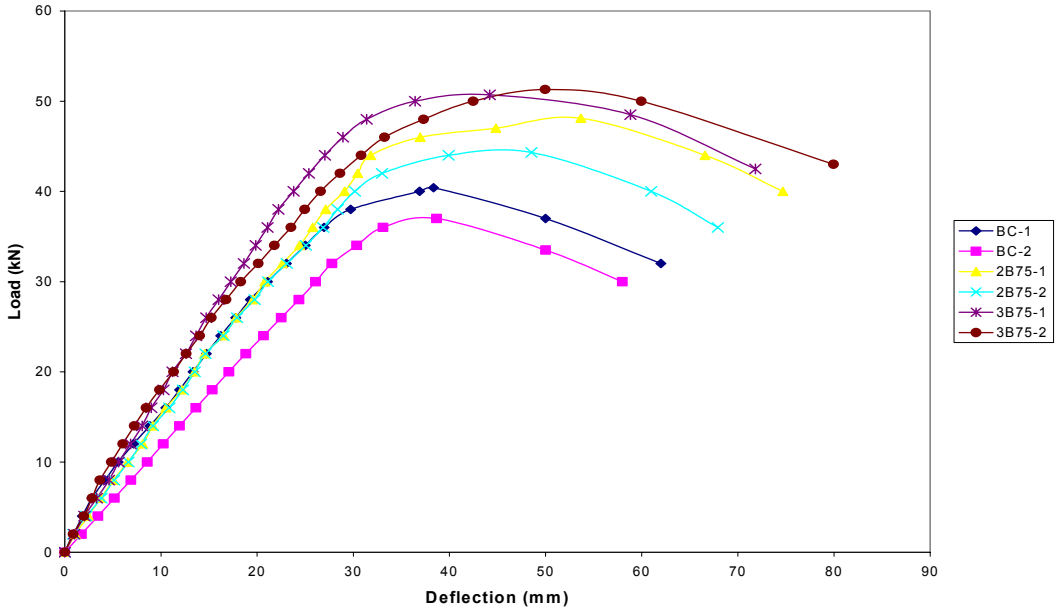

Fig. 5.10: Load v/s Mid- Span Deflection of Balanced Beam Sections Retrofitted with Ferrocement Jacketing with Different Layers of Wire Mesh and Stressed to 75 percent Stress Level

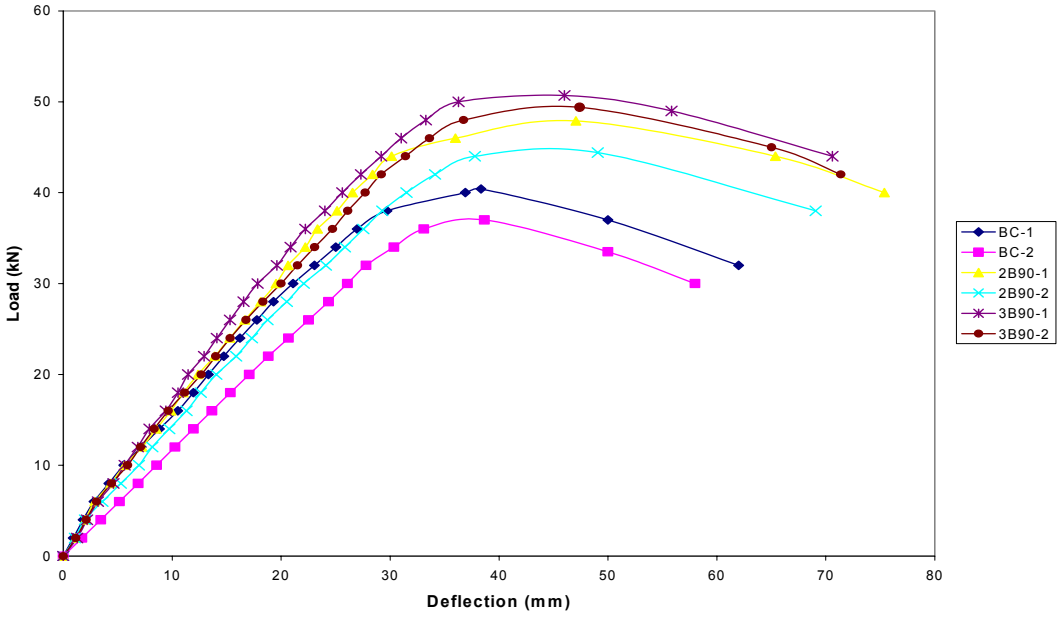

Fig. 5.11: Load v/s Mid- Span Deflection of Balanced Beam Sections Retrofitted with Ferrocement Jacketing with Different Layers of Wire Mesh and Stressed to 90 percent Stress Level

2B60(1)- at 10 kN Load

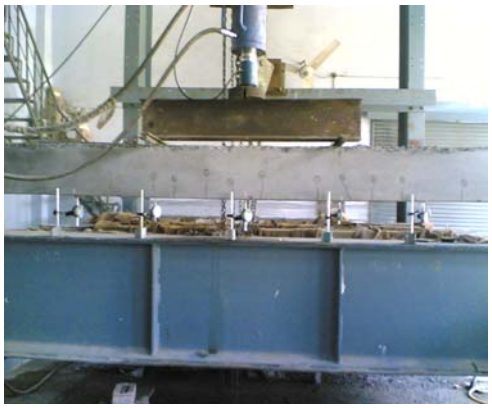

2B60(1) – at 18 kN Load

2B60(1) – at 30 kN Load

2B60(1)- Failure 1 (Spalling of Cover)

2B60(1)- Failure 2 (Crushing of Concrete)

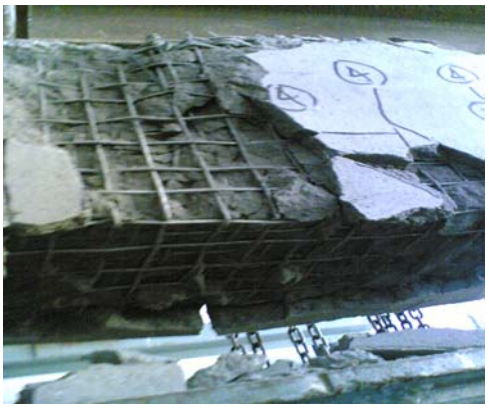

2B60(1)- Failure 3 (After removing cover)

Plate 5.1 Crack Patterns in Balanced Beams Retrofitted with Ferrocement Jackets Reinforced with Two Layers of GI Woven Wire Mesh and Stressed to 60% Level

2B60(2)- at 10 kN Load

2B60(2)- at 18 kN Load

2B60(2)- at 30 kN Load

2B60(2) – at Failure

Plate 5.2 Crack Patterns in Balanced Beams Retrofitted with Ferrocement Jackets Reinforced with Two Layers of GI Woven Wire Mesh and Stressed to 60% Level

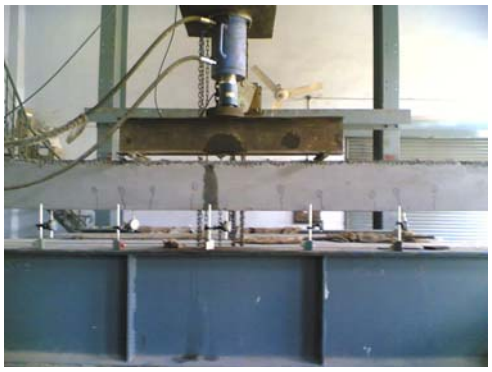

3B60(1)- at 10 kN Load

3B60(1)- at 18 kN Load

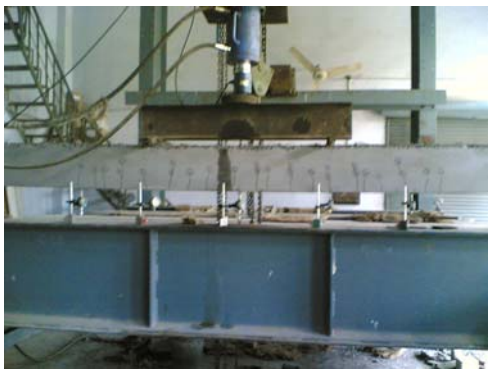

3B60(1) – at 30 kN Load

3B60(1) – at Failure 1

3B60(1) – at Failure 2

Plate 5.3 Crack Patterns in Balanced Beams Retrofitted with Ferrocement Jackets Reinforced with Three Layers of GI Woven Wire Mesh and Stressed to 60% Level

3B60(2)- at 10 kN Load

3B60(2) – at 18 kN Load

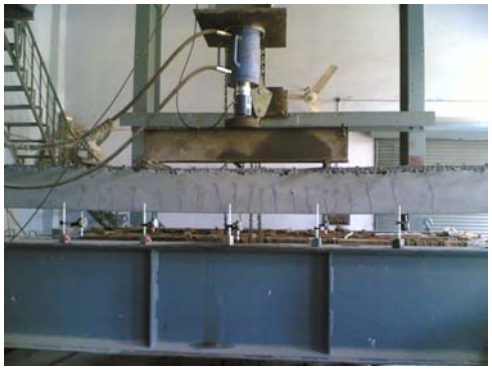

3B60(2) – at 30 kN Load

3B60(2) – at Failure 1

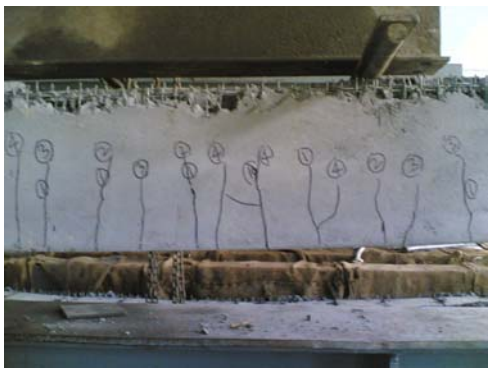

3B60(2)- at Failure 2

3B60(2) – at Failure 3

Plate 5.4 Crack Patterns in Balanced Beams Retrofitted with Ferrocement Jackets Reinforced with Three Layers of GI Woven Wire Mesh and Stressed to 60% Level

2B75(1) – at 10 kN Load

2B75(1) – at 18 kN load

2B75(1) – at 30 kN Load

2B75(1)- at Failure

Plate 5.5 Crack Patterns in Balanced Beams Retrofitted with Ferrocement Jackets Reinforced with Two Layers of GI Woven Wire Mesh and Stressed to 75% Level

2B75(2) – at 10 kN Load

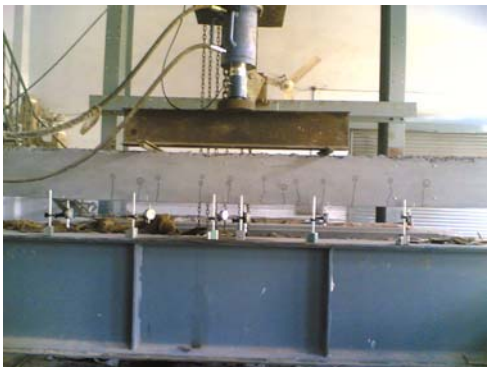

2B75(2) – at 18kN Load

2B75(2) – at 30 kN Load

2B75(2) – at Failure

Plate 5.6 Crack Patterns in Balanced Beams Retrofitted with Ferrocement Jackets Reinforced with Two Layers of GI Woven Wire Mesh and Stressed to 75% Level

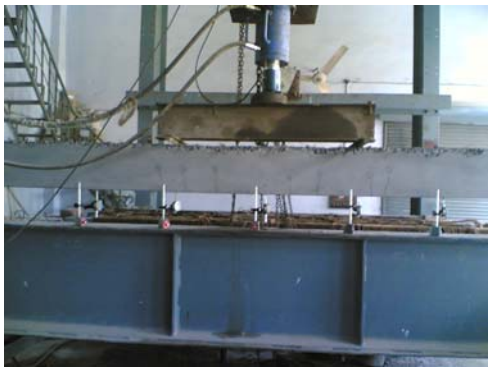

3B75(1) – at 10 kN Load

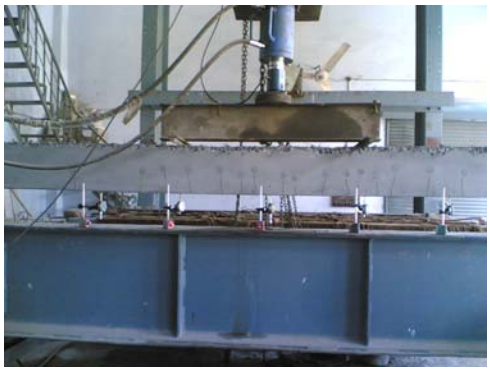

3B75(1) – at 18 kN Load

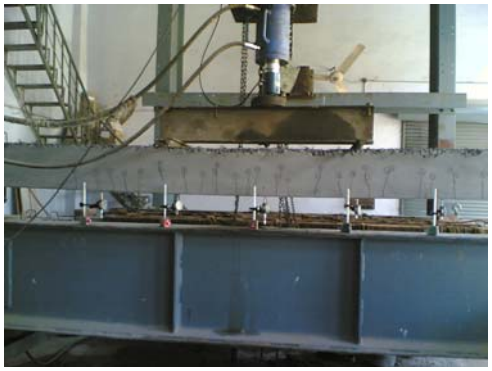

3B75(1) – at 30 kN Load

3B75(1) – at Failure 1

3B75(1) – at Failure 2

Plate 5.7 Crack Patterns in Balanced Beams Retrofitted with Ferrocement Jackets Reinforced with Three Layers of GI Woven Wire Mesh and Stressed to 75% Level

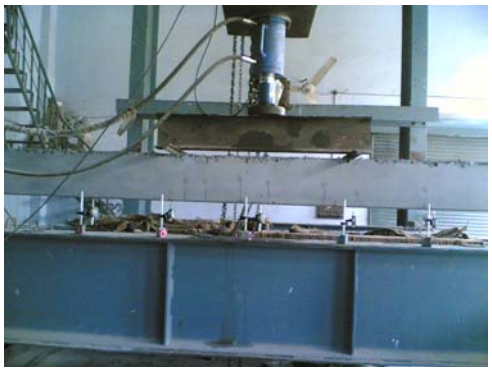

3B75(2) – at 10 kN Load

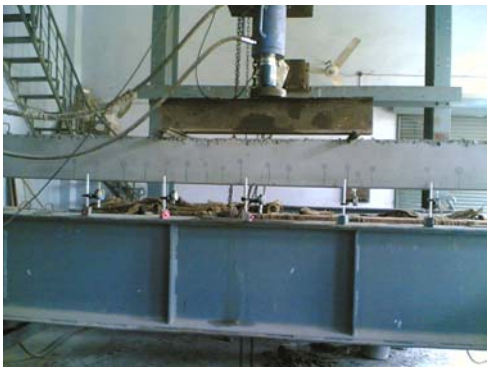

3B75(2) – at 18 kN Load

3B75(2) – at 30 kN Load

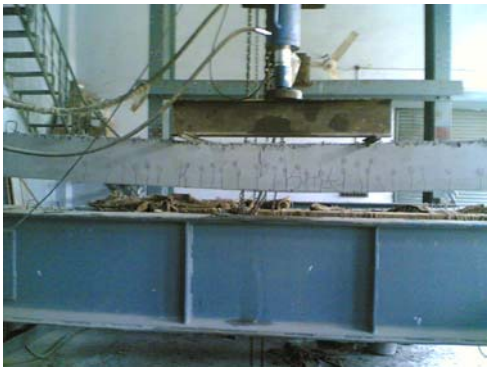

3B75(2) – at Failure 1

3B75(2) – at Failure 2

Plate 5.8 Crack Patterns in Balanced Beams Retrofitted with Ferrocement Jackets Reinforced with Three Layers of GI Woven Wire Mesh and Stressed to 75% Level

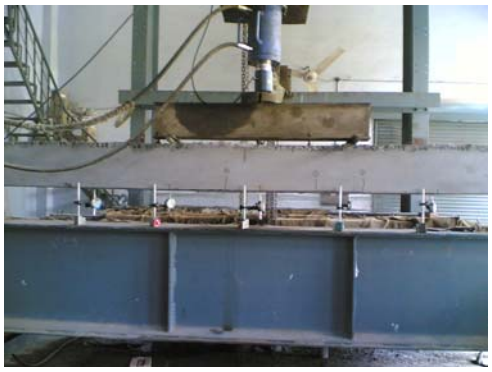

2B90(1) – at 10 kN

2B90(1) – at 18 kN Load

2B90(1) – at 36 kN Load

2B90(1) – at Failure 1

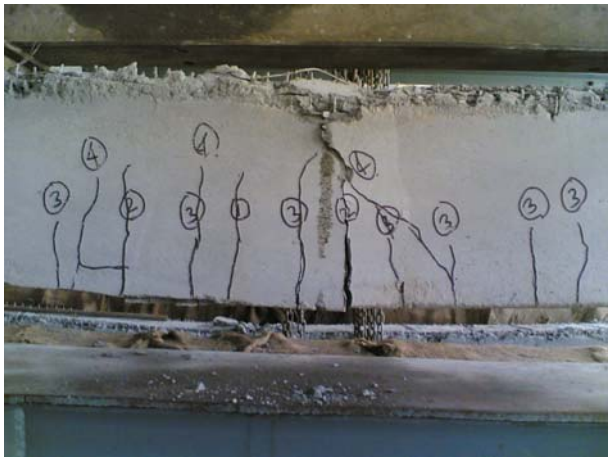

2B90(1) – at Failure 2

Plate 5.9 Crack Patterns in Balanced Beams Retrofitted with Ferrocement Jackets Reinforced with Two Layers of GI Woven Wire Mesh and Stressed to 90% Level

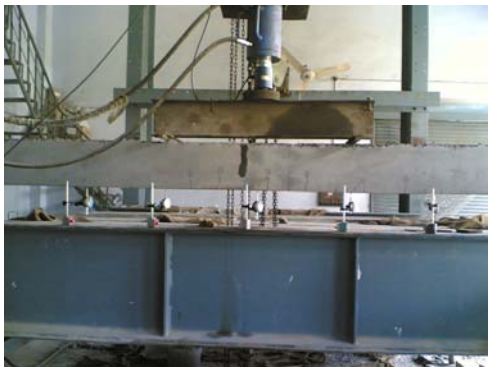

2B90(2) – at 10 kN Load

2B90(2) – at 18 kN Load

2B90(2) – at 30 kN Load

2B90(2) – at Failure

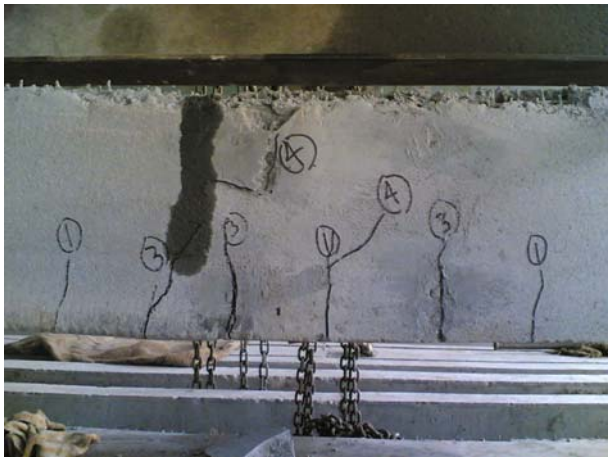

2B90(2) – at Failure

Plate 5.10 Crack Patterns in Balanced Beams Retrofitted with Ferrocement Jackets Reinforced with Two Layers of GI Woven Wire Mesh and Stressed to 90% Level

3B90(1) – at 10 kN Load

3B90(1) – at 18 kN Load

3B90(1) – at 30 kN Load

3B90(1) – at Failure 1

3B90(1) – at Failure 2

Plate 5.11 Crack Patterns in Balanced Beams Retrofitted with Ferrocement Jackets Reinforced with Three Layers of GI Woven Wire Mesh and Stressed to 90% Level

3B90(2) – at 10 kN

3B90(2) – at 18 kN Load

3B90(2) – at 30 kN Load

3B90(2) –at Failure 1

3B90(2) – at Failure 2

3B90(2) – at Failure 3

Plate 5.12 Crack Patterns in Balanced Beams Retrofitted with Ferrocement Jackets Reinforced with Three Layers of GI Woven Wire Mesh and Stressed to 90% Level

2U60(1) – at 8 kN Load

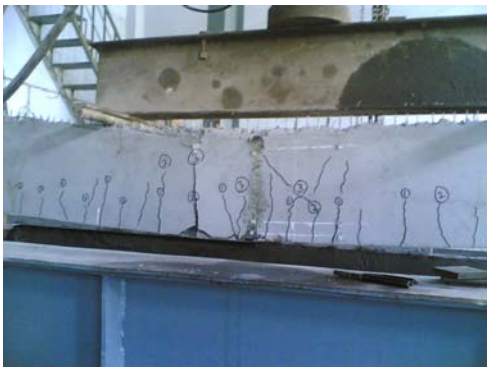

2U60(1) – at Failure

2U60(2) – at 8 kN Load

2U60(2) – at 18 kN Load

2U60(2) – at Failure 1

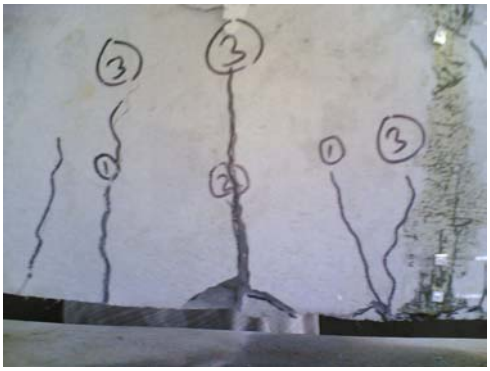

2U60(2) –at Failure 2

Plate 5.13 Crack Patterns in Under Reinforced Beams Retrofitted with Ferrocement Jackets Reinforced with Two Layers of GI Woven Wire Mesh and Stressed to 60% Level

3U60(1) – at 8 kN Load

3U60(1) – at 18 kN Load

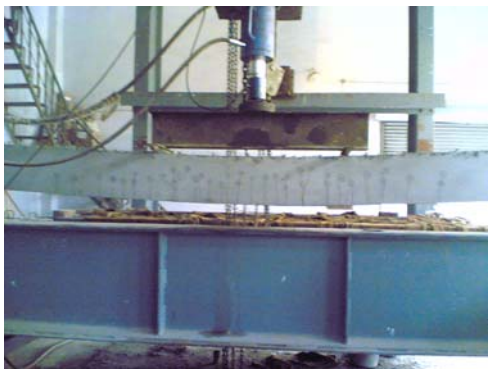

3U60(1) – at Failure

3U60(2) – at 8 kN Load

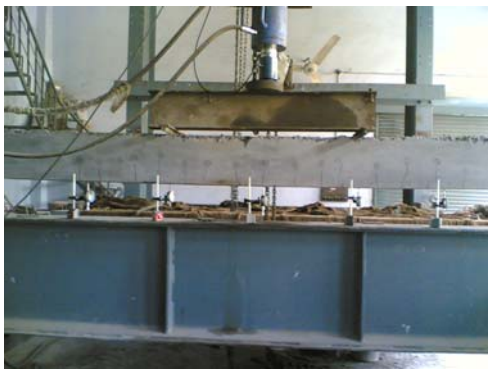

3U60(2) – at 18 kN Load

3U60(2) – at Failure

Plate 5.14 Crack Patterns in Under Reinforced Beams Retrofitted with Ferrocement Jackets Reinforced with Three Layers of GI Woven Wire Mesh and Stressed to 60% Level

2U75 – at 8kN Load

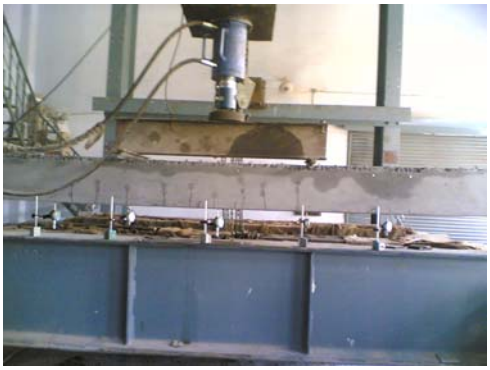

2U75 – at 18 kN Load

2U75 – at Failure 1

2U75 – at Failure 2

Plate 5.15 Crack Patterns in Under Reinforced Beams Retrofitted with Ferrocement Jackets Reinforced with Two Layers of GI Woven Wire Mesh and Stressed to 75% Level

3U75(1) – at 8 kN Load

3U75(1) – at 18 kN Load

3U75(1) – at Failure

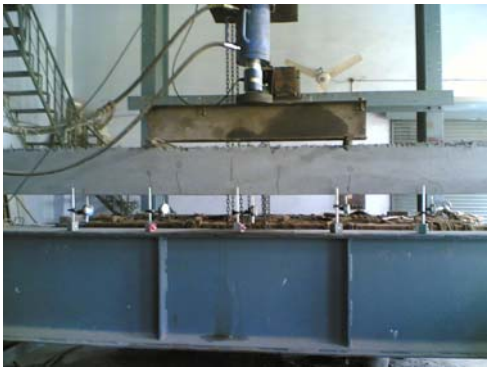

3U75(2) – at 8 kN Load

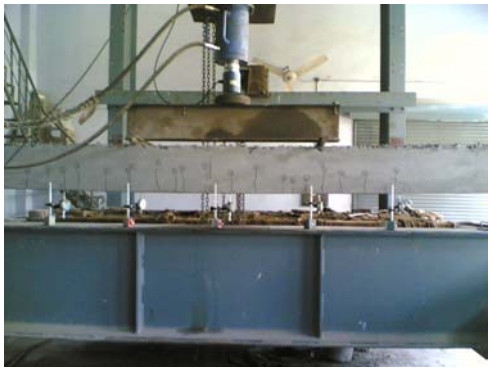

3U75(2) – at 18 kN Load

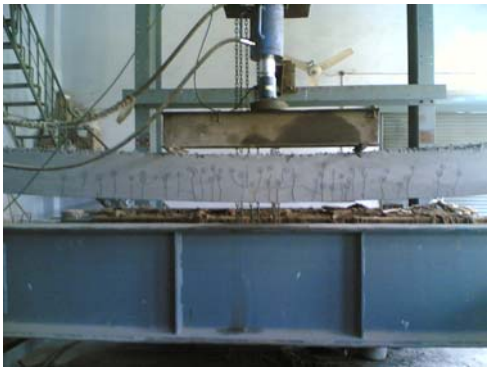

3U75(2) – at Failure

Plate 5.16 Crack Patterns in Under Reinforced Beams Retrofitted with Ferrocement Jackets Reinforced with Three Layers of GI Woven Wire Mesh and Stressed to 75% Level

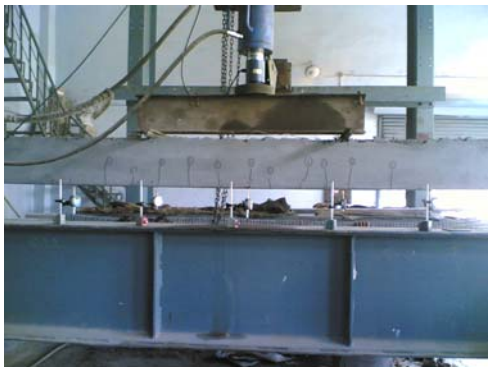

2U90(1) – at 8 kN Load

2U90(1) – at 18 kN Load

2U90(1) – at Failure

2U90(2) – at 8 kN Load

2U90(2) – at 18 kN Load

2U90(2) – at Failure

Plate 5.17 Crack Patterns in Under Reinforced Beams Retrofitted with Ferrocement Jackets Reinforced with Two Layers of GI Woven Wire Mesh and Stressed to 90% Level

3U90(1) – at 8 kN Load

3U90(1) –at 18 kN Load

3U90(1)- at Failure

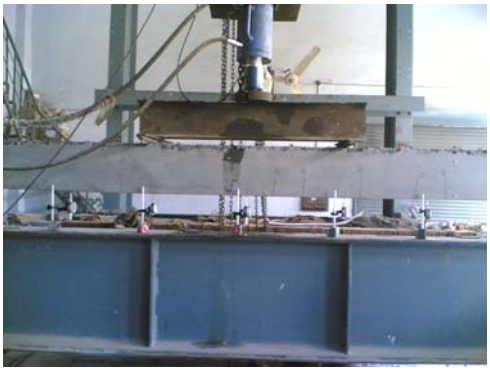

3U90(2) – at 8 kN Load

3U90(2) – at 18 kN Laod

3U90(2) – at Failure

Plate 5.18 Crack Patterns in Under Reinforced Beams Retrofitted with Ferrocement Jackets Reinforced with Three Layers of GI Woven Wire Mesh and Stressed to 90% Level

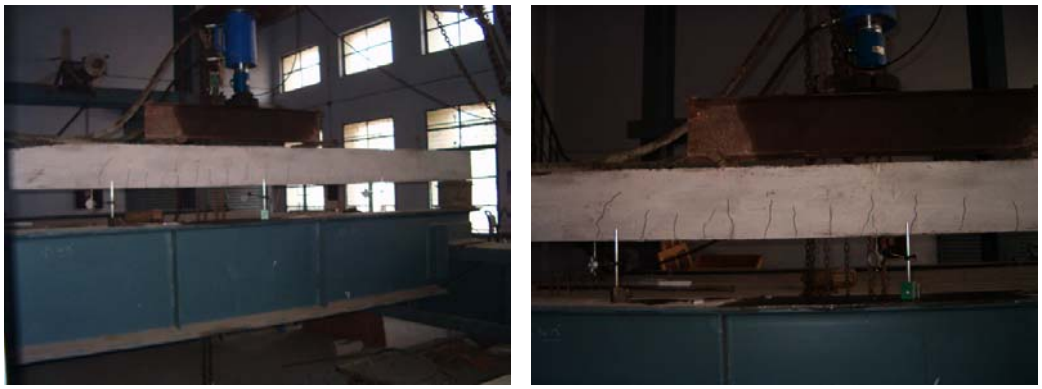

Plate 5.19 Crack Patterns in Balanced Control Beams

Plate 5.20 Crack Patterns in Under Reinforced Control Beams

CHAPTER –6

RETROFITTING OF BEAMS USING GFRP JACKETS

6.1 GENERAL

This chapter presents the experimental results of testing of control beams and beams retrofitted using GFRP jacketing with fibres orientated at 0^0 and 45^0 to the longitudinal axis of the beams. The data obtained from testing is analyzed and discussed. The entire chapter is divided into three sections, in the first sections the beams retrofitted using GFRP jackets and fibres orientated at 0^0 to the longitudinal axis of the beam are discussed, In the second section the beams retrofitted using GFRP jackets and fibres orientated at 45^0 to the longitudinal axis of the beam are discussed, and finally the third presents the comparative details of the effect of fibre orientation i.e. 0^0 or 45^0 to the longitudinal axis of the beam on the strength of retrofitted beams, and when the beams are stressed to different stress levels.

The results for the control beams and beams retrofitted using U-shaped jackets with 0^0 and 45^0 orientation of fibres are given in Tables 6.1 to 6.14. The load deflection curves for the data obtained from the experimental results are plotted in Fig 6.1 to 6.11 and fitted through quadri-linear curves as explained in section 3.6, and various parameters such as maximum load carrying capacity, safe load carrying capacity, ductility ratio, toughness are calculated and tabulated in Table 6.15. The effect of various parameters studied is as under:

6.2 BEHAVIOUR OF RETROFITTED BEAMS

All the retrofitted as well control beams are tested under two point loading system, as explained in the Section 3.5 of the Chapter 3. Figs. 6.1 to 6.11 show the load deflection plots of the retrofitted and the control beams. The maximum load, safe load, ductility and toughness of the retrofitted beams calculated from the test results are summarized in Table 6.15.

It was observed during testing that the under reinforced retrofitted beams failed in tension due to rupture of the glass fibres, whereas the balanced beams failed by crushing of concrete followed by the rupture of glass fibres as shown in Plates 6.1 to 6.4. The modes of failures are same as per the model predicted by *Chen et al (2002)*. In some of the specimens, debonding of the GFRP jackets was also observed near the

sharp edges at top of the beam. This debonding took place due to formation of air pockets near the sharp edges of the beam.

It was further observed that after the retrofitting of the beams there is no appreciable increase in the safe and maximum load carrying capacities of the beams. This may be attributed to loss in stiffness of the section due to initial stressing of the beams. However, the load carrying capacities of the beams increased when the fibres are oriented at 45 degrees to the longitudinal axis of the beams. This increase in the load carrying capacity of the retrofitted beams can be attributed to the confinement provided by the fibres in the compression zone, due to which the compressive component of the internal moment couple provided by the concrete increases, leading to an increased load carrying capacity.

All the retrofitted beams underwent large deflections as compared to the control beams, hence the ductility ratio and toughness of the beams increased after retrofitting. This increase was again higher in the beams retrofitted with fibres at 45 degrees, due higher in the load carrying capacity of the beams, as compared to those with fibres at zero degrees.

6.3 BEAMS RETROFITTED USING GFRP JACKETS WITH FIBRES AT ZERO DEGREE TO THE LONGITUDINAL AXIS OF BEAM

Out of a total twenty-four beams cast, twelve were retrofitted using GFRP jackets with fibres oriented at zero degree to the longitudinal axis of the beam. Six of these were designed as under reinforced sections and remaining six were designed as balanced sections. Two beams from each type i.e. balanced and under reinforced were stressed to 60 percent, 75 percent and 90 percent respectively of safe load obtained from the testing of the control beams. The load deflection data obtained from the testing of the beams is plotted and presented for each beam separately in the curves shown in Fig. 6.1 to 6.11

6.3.1 Effect on Strength of Beams

Fig. 6.1 shows the load deflection curve for the control beams tested as per procedure laid down in section 3.5. It is observed from the test results that the under reinforced beams underwent large deflections as compared to balanced sections. The average maximum load carrying capacity was 22.4 kN for under reinforced control beams as compared to 38.7 kN for balanced control beams.

The other beams, which were subsequently stressed to 60, 75 and 90 percent of the safe load respectively for the respective section, and retrofitted with GFRP having fibres at zero degree to the longitudinal axis. They were tested again to obtain their load carrying capacity.

For under reinforced section the average maximum load carrying capacity obtained experimentally was 24.2 kN, 22.3 kN, and 19.7 kN respectively, for retrofitted beams stressed to 60, 75 and 90 percent stress levels. So, the maximum load capacity of under reinforced retrofitted beams increased by 8.03 percent for 60 percent stressed beam whereas it decreased by 0.45 and 12.05 percent for 75 and 90 percent level.

The average safe load carrying capacity as obtained experimentally (at deflection of span/250) after the retrofitting decreased by 7.32, 8.68 and 22.2 percent as compared to the control beams, at stress levels of 60, 75 and 90 percent respectively

For the balanced retrofitted beams the average maximum load obtained experimentally was 42.75 kN, 41.75 kN and 40.45 kN, respectively for the retrofitted beams stressed to 60, 75 and 90 percent stress level, indicating an increase of 10.4, 7.88 and 4.52 percent for stress level 60, 75 and 90 percent respectively. The safe load carrying capacity increased by 7.17 and 0.63 percent with stress level 60 and 75 percent, however it decreased by 9.28 percent as compared to control beam, at a stress level of 90 percent.

Thus, it can be concluded that there is no appreciable increase in the strength (both maximum and safe) after the retrofitting of the beams with GFRP jackets with fibres at zero degree to the longitudinal axis of the beams, except in the case of balanced sections where both maximum and safe load carrying capacity increases by approximately 5-10 percent after retrofitting, which is also not very appreciable. The strength of the section decreases with an increase in the stress level, which is due to a decrease in the stiffness of section due to higher initial stress level.

It was also observed that the under reinforced beams failed by the rupture of the fibres and balanced sections failed by the crushing of concrete as shown in Plates 6.3 and 6.6. This indicates that the balanced section starts behaving as an over reinforced section after retrofitting due to the extra reinforcement provided in the tension zone in the form of GFRP wrapping. Moreover, no surface cracks were observed due to the GFRP wrapping which makes the structure more durable

6.3.2 Effect on Ductility Ratio and Toughness

The deflection ductility ratio defined as the ratio of the deflection at ultimate load and yield load is calculated using quadri-linear curves and is shown in Table 6.15. The ductility ratio of under reinforced sections increases by 5.79 percent, 15.75 percent and 10.85 percent respectively, for the beams stressed to 60, 75 and 90 percent stress level. In case of balanced sections the percentage increase in the ductility ratio is 10.77 percent, 16.8 percent and 11.05 percent respectively, for beams stressed to 60, 75 and 90 percent stress level

The area under the quadri-linear curves, idealized as explained in section 3.6, is calculated to find the toughness of the section before and after retrofitting, and is shown in Table 6.15. The toughness of the under reinforced and balanced beams increased by 22.54, 11.08, and 6.44 percent and 50.53, 38.33 and 31.29 percent respectively for the beams stressed to 60, 75 and 90 percent stress level.

So, both deflection ductility ratio and toughness of the beams retrofitted using GFRP jackets with fibres at an orientation of zero degree to the longitudinal axis of beams increases considerably.

Table 6.1: Load v/s. Deflection Data for Under Reinforced Control Beams

Sr. No.	Beam1				Beam 2			
	Load (kN)	Deflection (mm) at			Load (kN)	Deflection (mm) at		
		L/2	L/4	3L/4		L/2	L/4	3L/4
1	1	0	0	0	0	0	0	0
2	2	2	1.52	0.46	.48	2	2.37	0.99
3	3	4	3.0	1.82	1.81	4	4.74	1.98
4	4	6	5.0	3.02	3.04	6	7.23	3.69
5	5	8	8.3	5.0	5.02	8	9.78	5.88
6	6	10	10.98	7.0	7.05	10	12.85	7.86
7	7	12	14	9.22	9.25	12	16.1	9.78
8	8	14	17	11.2	11.28	14	19.1	11.89
9	9	16	20	13.5	13.52	16	22.26	14.07
10	10	20	28	16	16.04	18	26.18	16.7
11	11	21.8	44.85	33.4	33.45	20	31.63	20
12	12	21	61.28			22	38.9	24.05
13	13	18	76.28			23	48.3	28.6
						20	79.3	

Table 6.2: Load v/s. Deflection Data for Balanced Control Beams

Sr. No.	Beam1				Beam 2			
	Load (kN)	Deflection (mm) at			Load (kN)	Deflection (mm) at		
		L/2	L/4	3L/4		L/2	L/4	3L/4
1	0	0	0	0	0	0	0	0
2	2	0.91	0.65	0.65	2	1.72	1.2	1.4
3	4	1.82	1.29	1.29	4	3.44	2.39	2.8
4	6	2.81	1.98	1.98	6	5.16	3.59	4.21
5	8	4.18	2.95	2.93	8	6.88	4.78	5.61
6	10	5.55	3.91	3.87	10	8.58	5.98	6.88
7	12	7.16	4.97	4.67	12	10.25	7.17	8.03
8	14	8.83	6.06	5.43	14	11.94	8.4	9.22
9	16	10.51	7.14	6.19	16	13.64	9.64	10.45
10	18	11.94	8.26	7.24	18	15.34	10.88	11.65
11	20	13.33	9.34	8.32	20	17.07	12.18	12.88
12	22	14.73	10.33	9.33	22	18.82	13.52	14.13
13	24	16.22	11.38	10.41	24	20.67	14.83	15.45
14	26	17.77	12.48	11.55	26	22.52	16.14	16.78
15	28	19.29	13.56	12.67	28	24.36	17.45	18.1
16	30	21.09	14.79	13.91	30	26.09	18.65	19.32
17	32	23.05	16.17	15.12	32	27.79	19.82	20.52
18	34	25.02	17.56	16.34	34	30.36	21.35	21.95
19	36	26.98	18.95	17.56	36	33.09	22.94	23.43
20	38	29.73	20.95	19.45	37	38.66	26.78	25.93
21	40	36.91	26.39	25.15	33.5	50.0		
22	40.4	38.35	27.48	26.29	30	58.0		
23	37	50.0						
24	62.0							

Table 6.3: Load v/s. Deflection Data for 60 percent Stressed Under Reinforced Beams Retrofitted with GFRP Jacket with Fibres at 0^0 to the Longitudinal axis of the Beam

Sr. No.	Beam1				Beam 2			
	Load (kN)	Deflection (mm) at			Load (kN)	Deflection (mm) at		
		L/2	L/4	3L/4		L/2	L/4	3L/4
1	0	0	0	0	0	0	0	0
2	2	2.58	1.58	1.37	2	2.8	1.72	1.42
3	4	5.16	4.24	4.2	4	5.26	4.56	4.36
4	6	7.42	5.86	5.89	6	7.56	6.08	6.06
5	8	9.74	7.48	7.75	8	9.72	7.96	7.96
6	10	12.15	9.17	9.62	10	12.48	9.78	9.84
7	12	14.6	11.08	11.67	12	14.4	11.72	12.02
8	14	17.55	12.92	13.62	14	17.68	13.62	13.92
9	16	20.63	15.1	15.9	16	21.05	15.98	16.26
10	18	23.4	17.27	18.07	18	24.2	18.04	18.48
11	20	28.72	21.71	22.33	20	28.92	22.38	22.63
12	22	36.86	25.41	26.67	22	37.56	25.98	27.56
13	23.4	47.41	33.16	34.05	24	49.2	35.78	35.48
14	23.9	65.69	42.54	44.8	24.5	67.24	44.06	46.18
15	22	80.69			22	84.24		
16	20	90.69			20	93.24		

Table 6.4: Load v/s. Deflection Data for 75 percent Stressed Under Reinforced Beams Retrofitted with GFRP Jacket with Fibres at 0^0 to the Longitudinal axis of the Beam

Sr. No.	Beam1				Beam 2			
	Load (kN)	Deflection (mm) at			Load (kN)	Deflection (mm) at		
		L/2	L/4	3L/4		L/2	L/4	3L/4
1	0	0	0	0	0	0	0	0
2	2	2.06	1.49	1.57	2	1.98	1.42	1.49
3	4	4.16	3.01	3.17	4	3.86	3.06	3.27
4	6	6.44	4.64	4.85	6	6.12	4.88	4.62
5	8	9.15	6.42	6.75	8	9.02	6.58	6.86
6	10	11.75	8.19	8.61	10	11.72	7.98	8.78
7	12	14.84	10.44	10.78	12	14.82	10.76	11.12
8	14	18.39	12.98	13.53	14	18.42	13.06	13.96
9	16	21.96	15.41	16.3	16	22.0	15.56	16.78
10	18	28.15	19.66	20.76	18	27.96	19.56	21.26
11	20	37.4	25.46	26.78	20	37.2	25.86	27.22
12	22	48.85	33	33.38	22.6	49.24	34.24	34.76
13	21	68.24			22	67.68		
14	18	89.24			18	90.68		

Table 6.5: Load v/s. Deflection Data for 90 percent Stressed Under Reinforced Beams Retrofitted with GFRP Jacket with Fibres at 0^0 to the Longitudinal axis of the Beam

Sr. No.	Beam1				Beam 2			
	Load (kN)	Deflection (mm) at			Load (kN)	Deflection (mm) at		
		L/2	L/4	3L/4		L/2	L/4	3L/4
1	0	0	0	0	0	0	0	0
2	2	3.2	2.16	2.06	2	3.85	2.74	3.06
3	4	5.77	3.66	3.79	4	5.85	4.75	5.21
4	6	8.34	5.26	5.58	6	8.3	7.11	7.62
5	8	11.12	7.18	7.55	8	11.21	9.74	10.33
6	10	14.25	9.4	9.74	10	14.77	12.16	12.92
7	12	17.5	11.78	11.95	12	17.92	14.8	15.64
8	14	20.81	14.26	14.23	14	21.92	17.93	18.61
9	16	24.38	17.53	17.3	16	28.33	21.44	21.78
10	18	37.06	25.16	24.74	18	37.95	27.55	27.39
11	18.4	44.55	29.3	28.45	19	45.12	30.4	30.18
12	19.4	70.73	43.95	45.25	19.9	57.1	37.4	38.8
13	17	86.73			20	68.9	46.27	50.72
14					19	80.9		
					17	90.9		

Table 6.6: Load v/s. Deflection Data for 60 percent Stressed Balanced Beams Retrofitted with GFRP Jacket with Fibres at 0^0 to the Longitudinal axis of the Beam

Sr. No.	Beam1				Beam 2			
	Load (kN)	Deflection (mm) at			Load (kN)	Deflection (mm) at		
		L/2	L/4	3L/4		L/2	L/4	3L/4
1	0	0	0	0	0	0	0	0
2	2	1.79	1.3	0.88	2	1.76	1.16	1.48
3	4	3.01	2.11	1.64	4	3.13	2.1	2.54
4	6	4.27	2.96	2.37	6	4.39	2.96	3.43
5	8	5.6	3.86	3.11	8	5.66	3.81	4.3
6	10	6.91	4.78	4.02	10	6.97	4.7	5.18
7	12	8.18	5.61	4.95	12	8.34	5.65	6.1
8	14	9.5	6.48	5.94	14	9.76	6.66	7.1
9	16	11	7.49	7.07	16	11.18	7.67	8.08
10	18	12.4	8.46	8.15	18	12.6	8.69	9
11	20	13.91	9.46	9.29	20	14.08	9.72	9.91
12	22	15.45	10.47	10.45	22	15.58	10.74	10.82
13	24	17.05	11.51	11.64	24	17.07	11.8	11.88
14	26	18.64	12.55	12.82	26	18.56	12.86	12.99
15	28	20.45	20.45	20.45	28	19.99	13.89	14.12
16	30	22.25	22.25	22.25	30	21.4	14.92	15.25
17	32	22.88	15.43	15.92	32	22.75	15.96	16.4
18	34	23.65	17.08	17.67	34	24	17.05	17.58
19	36	24.7	18.41	19.14	36	25.27	18.14	18.77
20	38	26.66	19.95	20.77	38	27.14	19.43	20.09
21	40	29.55	21.7	22.55	40	30.48	21.54	22.18
22	42	35.39	25.13	25.46	42	39.97	26.74	27.99
23	43	51.32	34.09	37.5	42.5	42.38	28.02	29.53
24	38	64.58			42.5	51.36	33.77	36.58
25	35	71.35			38	67.56		
26					35	73.35		

Table 6.7: Load v/s. Deflection Data for 75 percent Stressed Balanced Beams Retrofitted with GFRP Jacket with Fibres at 0^0 to the Longitudinal axis of the Beam

Sr. No.	Beam1				Beam 2			
	Load (kN)	Deflection (mm) at			Load (kN)	Deflection (mm) at		
		L/2	L/4	3L/4		L/2	L/4	3L/4
1	0	0	0	0	0	0	0	0
2	2	2.11	1.66	0.72	2	2.29	1.15	1.19
3	4	3.54	2.8	1.53	4	3.84	2.24	2.25
4	6	4.76	3.77	2.4	6	5.19	3.22	3.18
5	8	6.13	4.76	3.38	8	6.52	4.19	4.15
6	10	7.58	5.79	4.46	10	7.84	5.16	5.15
7	12	9.1	6.85	5.62	12	9.26	6.18	6.18
8	14	10.48	7.81	6.73	14	10.67	7.24	7.26
9	16	11.96	8.84	7.83	16	12.05	8.3	8.33
10	18	13.52	9.92	8.96	18	13.38	9.27	9.3
11	20	15.16	11.03	10.13	20	14.86	10.29	10.34
12	22	16.71	12.13	11.26	22	16.42	11.35	11.4
13	24	18.24	13.22	12.4	24	18.06	12.45	12.49
14	26	19.86	14.37	13.57	26	19.51	13.44	13.46
15	28	21.47	15.52	14.75	28	21.03	14.53	14.48
16	30	22.96	16.63	15.91	30	22.64	15.76	15.57
17	32	24.62	17.79	17.16	32	24.08	16.92	16.64
18	34	26.52	19.08	18.56	34	25.34	18.02	17.68
19	36	28.42	20.35	19.95	36	26.88	19.2	18.83
20	38	30.25	21.45	21.28	38	28.58	20.44	20.04
21	40	34.1	23.55	24.08	40	31.28	22.3	21.85
22	41.2	45.13	30.25	33.8	41	38.27	26.42	26.42
23	38	56.42			42.3	49.53	32.95	34.24
24	35	62.98			38	60.68		
25					35	70.24		

Table 6.8: Load v/s. Deflection Data for 90 percent Stressed Balanced Beams Retrofitted with GFRP Jacket with Fibres at 0^0 to the Longitudinal axis of the Beam

Sr. No.	Beam1				Beam 2			
	Load (kN)	Deflection (mm) at			Load (kN)	Deflection (mm) at		
		L/2	L/4	3L/4		L/2	L/4	3L/4
1	0	0	0	0	0	0	0	0
2	2	2.6	1.69	1.52	2	2.17	1.39	1
3	4	5.2	3.38	3.05	4	3.56	2.4	1.88
4	6	6.81	4.46	4.14	6	4.89	3.35	2.76
5	8	8.35	5.49	5.53	8	6.35	4.31	3.69
6	10	9.82	6.48	7.24	10	7.8	5.25	4.65
7	12	11.74	7.76	7.74	12	9.18	6.21	5.63
8	14	13.56	8.99	8.75	14	10.55	7.15	6.68
9	16	15.35	10.2	16	16	11.9	8.1	7.72
10	18	16.95	11.28	11.57	18	13.25	9.05	8.75
11	20	18.98	12.5	13.18	20	14.66	10.07	9.78
12	22	21.11	13.8	14.53	22	16.09	11.09	10.81
13	24	22.23	14.88	15.27	24	17.71	12.17	11.96
14	26	23.35	15.96	16	26	19.52	19.52	19.52
15	28	26.04	17.72	17.92	28	21.07	14.36	14.43
16	30	28.78	19.35	19.71	30	22.46	15.47	15.67
17	32	31.55	20.85	21.37	32	23.45	16.68	17.02
18	34	34.9	22.88	23.35	34	24.25	17.98	18.46
19	36	38.83	25.43	25.66	36	26.24	19.79	20.56
20	38	42.13	27.82	28.07	38	32.01	23.36	24.52
21	40	47.57	30.72	31.43	38.9	37.29	37.29	37.29
22	42	55.14	34.12	35.74	38.9	48.19		
23	36	66.5	39.32	42.67	35	60.24		

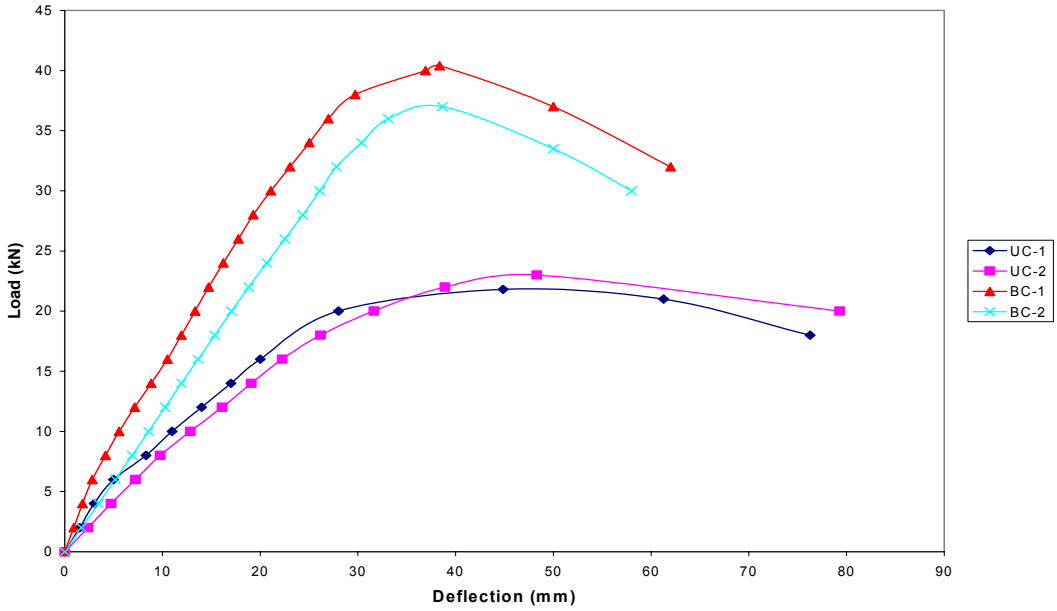

Fig. 6.1: Load v/s Deflection For Control Beams

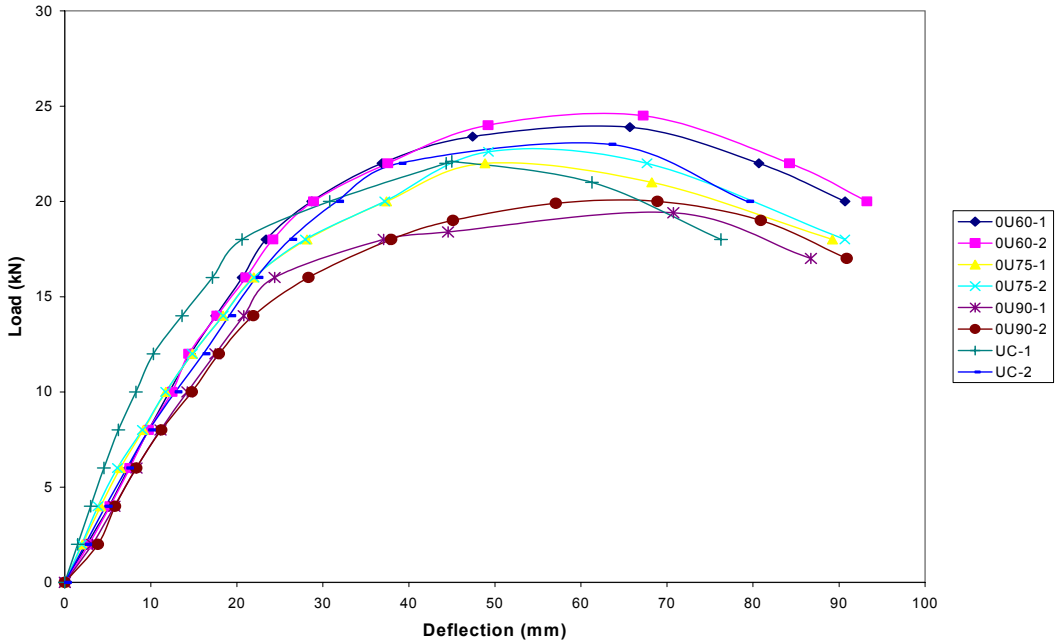

Fig. 6.2: Load v/s Mid Span Deflection of Under Reinforced Beams Retrofitted with GFRP Jacketing with fibres at 0^0 to the Longitudinal Axis of the Beam

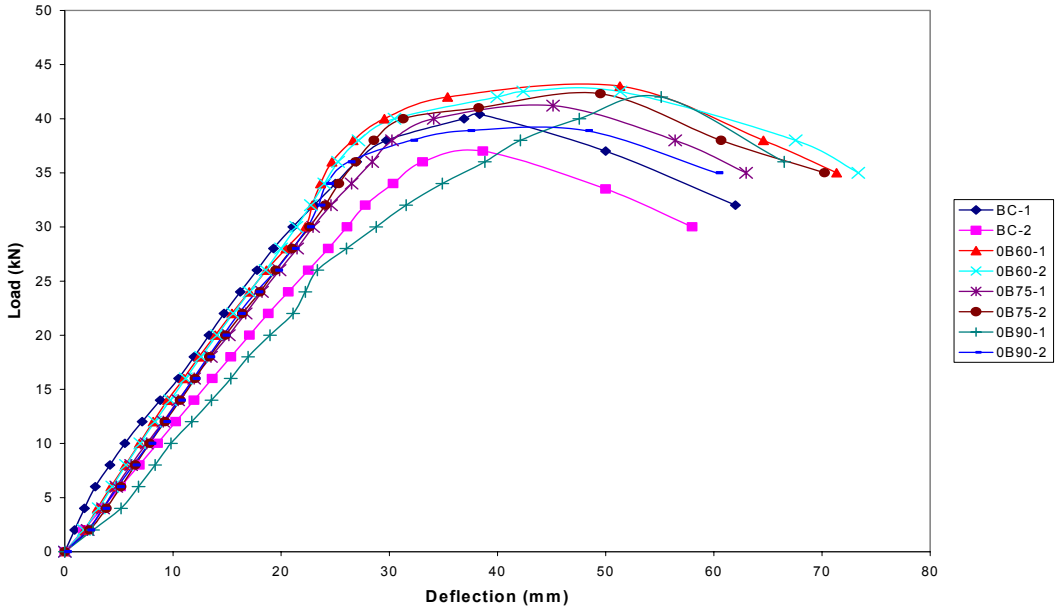

Fig. 6.3: Load v/s Mid Span Deflection of Balanced Beams Retrofitted with GFRP Jacketing with fibres at 0^0 to the Longitudinal Axis of the Beam

6.4 BEAMS RETROFITTED USING GFRP JACKETS WITH FIBRES AT FORTY FIVE DEGREES TO THE LONGITUDINAL AXIS OF BEAM

The other twelve beams were retrofitted using GFRP jacket with fibres at an orientation of 45 degrees to the longitudinal axis of the beams. The experimental results obtained are presented for each of the beams separately in the Tables 6.1 to 6.14 and the load deflection curves plotted using experimental results are shown in Figs. 6.1 to 6.11

6.4.1 Effect on Strength of Beams

Fig. 6.1 shows the load deflection curve for the control beams tested as per procedure laid down in section 3.5. It is observed from the test results that under reinforced beams underwent large deflections as compared to balanced sections, as expected. The average maximum load carrying capacity is found to be 22.4 kN for under reinforced sections as compared to 38.7 kN for balanced sections.

The other beams which were subsequently stressed to 60, 75 and 90 of the safe load for the respective section, were retrofitted with GFRP having fibres at forty five degrees to the longitudinal axis, were tested to compute their load carrying capacity

It is observed from the Figures 6.3 and 6.5 that for the under reinforced beams maximum load carrying capacity of the beams obtained experimentally was 29.3 kN,

29.35 kN and 24.4 kN, respectively for the beams stressed to 60, 75 and 90 percent stress level, indicating an increase of 30.8, 31.03, and 4.86 percent, respectively. Whereas, in the case of balanced sections the corresponding value of the maximum load was 45.0 kN, 44.35 kN and 44.0 kN, indicating an increase of 16.28, 14.6 and 13.69 percent for stress levels 60, 75 and 90 percent, respectively

The safe load of the under reinforced beams decreased by 4.52, 5.58 and 4.71 percent as compared to control beams at stress levels 60, 75 and 90 percent respectively. In the case of balanced reinforced beams retrofitted with GFRP jackets, with fibres at forty-five degrees, the safe load decreased by 0.63, 4.6 and 22.06 percent as compared to the control beams, at stress levels 60, 75 and 90 percent respectively.

Thus, it can be concluded that the maximum load carrying capacity of the under reinforced beams increased by approximately 30 percent except in the case of beams stressed to 90 percent stress level, whereas in case of balanced sections the percentage increase was only about 13-17 percent. But in both cases the safe load decreased from 0.63 percent to 22.06 percent.

6.4.2 Effect on Ductility Ratio and Toughness

The deflection ductility ratio of the under reinforced sections increased by 12.9, 4.39, and 37.33 percent respectively for beams stressed to 60, 75 and 90 percent stress level. Whereas in the case of balanced sections the percentage increase was 14.32, 9.23, and 20.88 percent respectively.

The toughness of under reinforced beams increases by 60.08, 57.05, and 23.78 percent respectively for beams stressed to 60, 75 and 90 percent stress level. Whereas in case of balanced section the percentage increase is 97.04, 83.49, and 97.71 percent respectively.

Thus, after retrofitting of the beams with GFRP jackets, with fibres at 45 degrees to the longitudinal axis of the beam, both the deflection ductility ratio as well as the toughness of the section increases considerably.

Table 6.9: Load v/s. Deflection Data for 60 percent Stressed Under Reinforced Beams Retrofitted with GFRP Jacket with Fibres at 45^0 to the Longitudinal axis of the Beam

Sr. No.	Beam1				Beam 2			
	Load (kN)	Deflection (mm) at			Load (kN)	Deflection (mm) at		
		L/2	L/4	3L/4		L/2	L/4	3L/4
1	0	0	0	0	0	0	0	0
2	2	2.18	1.55	1.08	2	2.57	1.57	1.08
3	4	4.51	3.25	2.78	4	4.84	3.21	2.58
4	6	7.03	5.11	4.63	6	7.44	5.08	4.26
5	8	9.32	6.86	6.37	8	9.61	6.94	5.93
6	10	11.85	8.82	8.31	10	11.75	9.24	7.82
7	12	14.68	11	10.48	12	13.64	10.64	9.2
8	14	17.38	12.9	12.45	14	16.21	12.31	10.92
9	16	19.73	14.77	14.38	16	18.87	13.99	13.13
10	18	21.68	16.98	16.69	18	21.76	15.99	15.11
11	20	24.75	19.45	19.34	20	25.25	18.35	17.1
12	22	29.15	22.08	22.32	22	28.37	20.75	19.23
13	24	36.29	25.54	25.74	24	32.85	23.78	22.4
14	26	46.23	32.08	32.38	26	40.87	28.66	27.98
15	28	60.56	41.82	42.21	28	51.05	34.81	34.88
16	28.6	65.15	45.02	45.42	30	64.88	43.55	43.54
17	27.5	78.38			31	72.7	48.53	48
18	25	90.38			28.5	88.7		
19					25	100.2		

Table 6.10: Load v/s. Deflection Data for 75 percent Stressed Under Reinforced Beams Retrofitted with GFRP Jacket with Fibres at 45^0 to the Longitudinal axis of the Beam

Sr. No.	Beam1				Beam 2			
	Load (kN)	Deflection (mm) at			Load (kN)	Deflection (mm) at		
		L/2	L/4	3L/4		L/2	L/4	3L/4
1	0	0	0	0	0	0	0	0
2	2	2.53	1.74	2.24	2	2.36	1.66	1.88
3	4	4.76	3.26	4.16	4	4.42	3.16	3.75
4	6	7.29	4.93	6.14	6	7.09	4.72	5.45
5	8	9.92	6.66	8.17	8	9.72	6.76	7.26
6	10	12.13	8.11	10.2	10	11.98	8.08	9.5
7	12	14.55	9.8	12.37	12	14.42	9.72	10.26
8	14	17.51	11.55	14.49	14	17.62	11.66	12.57
9	16	19.77	13.26	16.57	16	19.62	13.36	14.08
10	18	20.88	14.88	14.88	18	21.04	15.06	16.10
11	20	23.6	16.64	21.56	20	23.96	16.98	18.24
12	22	27.43	18.95	24.48	22	27.56	19.36	20.12
13	24	35.25	23.09	30.08	24	32.48	23.45	24.76
14	26	42.92	27.29	35.51	26	43.36	27.86	28.42
15	28	48.21	36.22	47.13	28	48.02	36.49	37.14
16	29.5	67.97	45.46	54.18	29.2	65.56	47.02	48.34
17	28	83.97			27.5	78.56		
	25	95.97			25	90.56		

Table 6.11: Load v/s. Deflection Data for 90 percent Stressed Under Reinforced Beams Retrofitted with GFRP Jacket with Fibres at 45^0 to the Longitudinal axis of the Beam

Sr. No.	Beam1				Beam 2			
	Load (kN)	Deflection (mm) at			Load (kN)	Deflection (mm) at		
		L/2	L/4	3L/4		L/2	L/4	3L/4
1	0	0	0	0	0	0	0	0
2	2	2.11	1.26	1.42	2	1.51	1.19	1.69
3	4	4.97	2.78	2.72	4	4.28	3.07	3.82
4	6	6.19	4.42	4.22	6	6.75	4.78	5.65
5	8	8.61	6.08	5.93	8	9.17	6.42	7.32
6	10	11.1	7.76	7.69	10	12.23	8.55	9.63
7	12	13.48	9.38	9.35	12	14.66	10.56	11.64
8	14	16.25	11.15	11.2	14	17.33	12.44	13.55
9	16	19.03	12.93	13.08	16	20.53	14.28	16.08
10	18	21.48	19.45	20.09	18	22.7	16.4	18.68
11	20	35.01	26.15	26.54	20	29.85	20.95	22.92
12	22	53.12	37.19	39.28	22	41.7	28.47	32.25
13	24	65.18	49.9	50	24	57.2	38.19	42.65
14	22.5	80.18			24.8	63.55	45.13	46.4
15	20	90.18			23	82.55		
16					20	92.55		

Table 6.12: Load v/s. Deflection Data for 60 percent Stressed Balanced Beams Retrofitted with GFRP Jacket with Fibres at 45^0 to the Longitudinal axis of the Beam

Sr. No.	Beam1				Beam 2			
	Load (kN)	Deflection (mm) at			Load (kN)	Deflection (mm) at		
		L/2	L/4	3L/4		L/2	L/4	3L/4
1	0	0	0	0	0	0	0	0
2	2	2.16	1.16	1.3	2	2.29	1.48	1.7
3	4	4.02	2.07	2.2	4	4.39	2.51	2.8
4	6	5.34	3	3.08	6	5.73	3.4	3.75
5	8	6.29	3.98	4.02	8	6.99	4.3	4.68
6	10	7.5	4.79	4.82	10	8.52	5.22	5.5
7	12	8.78	5.6	5.64	12	9.88	6.29	6.67
8	14	10.15	6.49	6.58	14	11.21	7.39	7.78
9	16	11.65	7.53	7.71	16	12.57	8.47	8.87
10	18	13.2	8.61	8.89	18	14.03	9.49	9.95
11	20	14.83	9.78	10.19	20	15.49	10.49	11.02
12	22	16.34	10.89	11.36	22	16.96	11.47	12.08
13	24	17.83	11.98	12.51	24	18.43	12.45	13.14
14	26	19.43	13.13	13.63	26	18.97	13.43	14.24
15	28	21.03	14.27	14.72	28	19.41	14.4	15.34
16	30	22.56	15.34	15.67	30	21.83	15.48	16.54
17	32	24.07	16.39	16.77	32	24.24	16.57	17.73
18	34	25.62	17.45	18.03	34	25.68	17.65	18.85
19	36	28.01	19.43	19.71	36	31.29	19.03	20.33
20	38	32.12	21.61	21.96	38	38.1	20.86	22.39
21	40	41.22	25.39	26.56	40	43.31	23.7	25.97
22	42	51.68	30.88	33.38	42	51.75	28.76	32.31
23	44	57.78	37..38	39.22	44	59.98	35.7	39.96
24	45.5	65.82	45.14	47.64	44.5	68.56	42.34	48.32
25	42	79.82			42	82.56		
26	36	90.82			36	92.56		

Table 6.13: Load v/s. Deflection Data for 75 percent Stressed Balanced Beams Retrofitted with GFRP Jacket with Fibres at 45^0 to the Longitudinal axis of the Beam

Sr. No.	Beam1				Beam 2			
	Load (kN)	Deflection (mm) at			Load (kN)	Deflection (mm) at		
		L/2	L/4	3L/4		L/2	L/4	3L/4
1	0	0	0	0	0	0	0	0
2	2	2.07	1.61	1.48	2	2.75	1.58	1.71
3	4	3.62	2.81	2.55	4	4.7	2.86	2.9
4	6	4.93	3.81	3.45	6	6.41	4.17	3.98
5	8	6.28	4.81	4.41	8	8.15	8.15	8.15
6	10	7.6	5.75	5.34	10	9.57	6.55	5.99
7	12	8.86	6.64	6.25	12	11.05	7.57	7.06
8	14	10.16	7.56	7.2	14	12.57	8.59	8.2
9	16	11.51	8.52	8.2	16	14.15	9.64	9.36
10	18	12.92	9.5	9.2	18	15.81	10.76	10.58
11	20	14.35	10.49	10.22	20	17.41	11.87	11.76
12	22	15.83	11.54	11.28	22	18.82	12.87	12.82
13	24	17.3	12.58	12.31	24	20.23	13.86	13.87
14	26	18.76	13.62	13.31	26	21.5	14.91	14.97
15	28	20.21	14.65	14.29	28	22.65	16.02	16.1
16	30	21.64	15.67	15.18	30	23.92	17.13	17.25
17	32	22.97	16.7	16.08	32	25.49	18.23	18.43
18	34	23.91	17.78	16.98	34	31.32	19.65	19.81
19	36	25.61	19.03	18.11	36	37.62	21.11	21.21
20	38	27.63	20.35	19.34	38	40.66	22.91	22.94
21	40	30.7	22.35	21.26	40	45.01	25.53	25.37
22	42	38.84	27.91	26.18	42	51.91	29.89	29.34
23	44	47.41	35.62	31.73	43.2	57.95	34.17	33.23
24	45.5	64.79	48.14	46.52	41	68.24		
25	42	79.79			36	79.24		
26	36	91.79						

Table 6.14: Load v/s. Deflection Data for 90 percent Stressed Balanced Beams Retrofitted with GFRP Jacket with Fibres at 45^0 to the Longitudinal axis of the Beam

Sr. No.	Beam1				Beam 2			
	Load (kN)	Deflection (mm) at			Load (kN)	Deflection (mm) at		
		L/2	L/4	3L/4		L/2	L/4	3L/4
1	0	0	0	0	0	0	0	0
2	2	2.72	1.7	2.02	2	2.6	1.62	1.82
3	4	4.81	3.16	3.66	4	4.92	3.26	3.36
4	6	6.69	4.48	5.08	6	6.78	4.78	4.88
5	8	8.59	5.8	6.5	8	8.58	5.98	6.3
6	10	10.26	6.98	7.78	10	10.16	6.78	7.72
7	12	11.88	8.07	8.95	12	12.02	8.38	8.84
8	14	13.62	10.09	10.26	14	13.65	10.16	10.36
9	16	15.44	11.16	11.47	16	15.48	11.45	11.42
10	18	17.27	11.85	12.63	18	17.48	12	13.0
11	20	18.94	13	13.57	20	19.26	13.25	14.12
12	22	20.49	14.25	14.56	22	21.02	14.52	15.02
13	24	21.9	15.54	15.73	24	22.14	15.94	16.12
14	26	23.28	16.82	16.92	26	23.34	17.26	17.24
15	28	24.59	18.11	18.2	28	24.98	18.38	18.78
16	30	26.12	19.32	19.41	30	26.72	19.64	19.84
17	32	27.86	20.49	20.6	32	28.26	21.04	21.03
18	34	29.69	21.66	21.81	34	30.02	22.15	22.36
19	36	31.29	22.77	22.93	36	31.78	23.16	23.76
20	38	33.03	23.91	24.17	38	33.65	24.34	24.96
21	40	35.13	25.15	25.65	40	36.0	25.95	26.12
22	42	39.3	27.66	28.23	42	44.12	35.46	34.62
23	44	49.78	33.97	34.3	43.8	70.16	45.12	44.98
24	44.2	73.98	44.65	44.43	42	82.16		
25	40	80.98			36	92.16		
26	36	90.98						

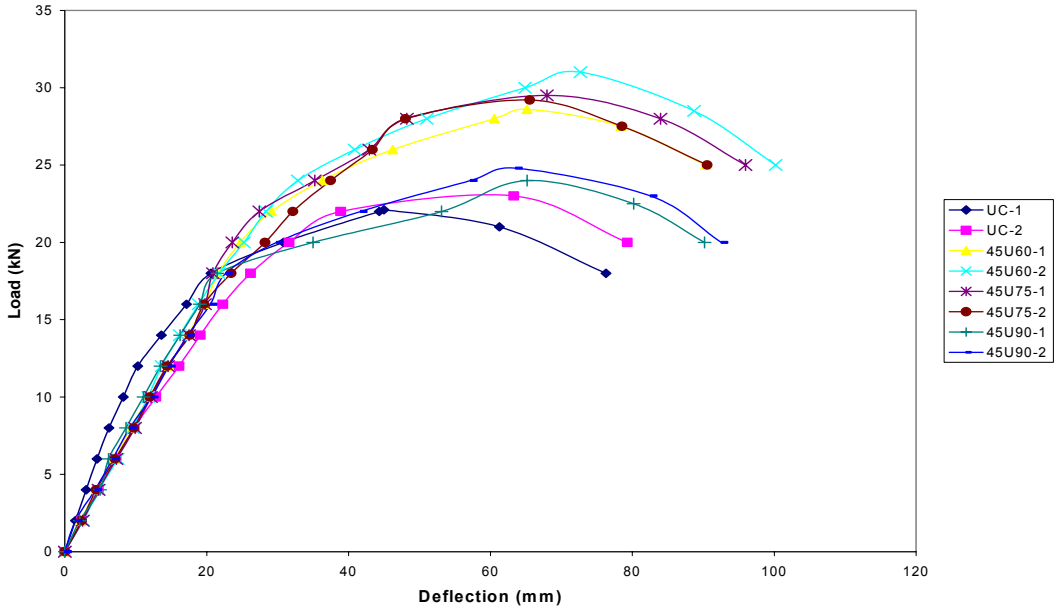

Fig. 6.4: Load v/s Mid Span Deflection of Under Reinforced Beams Retrofitted with GFRP Jacketing with fibres at 45^0 to the Longitudinal Axis of the Beam

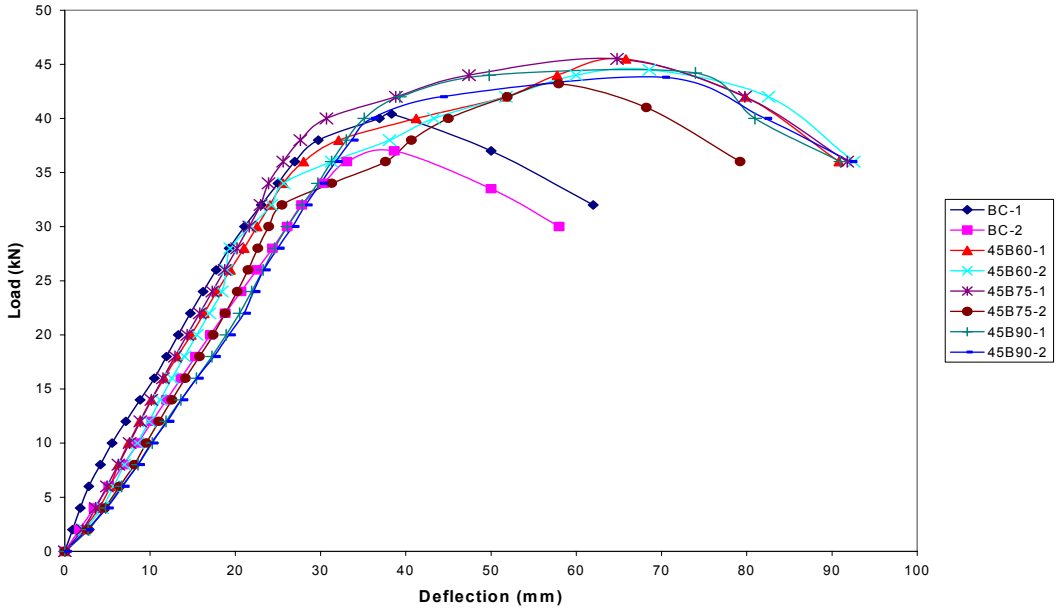

Fig. 6.5: Load v/s Mid Span Deflection of Balanced Beams Retrofitted with GFRP Jacketing with fibres at 45^0 to the Longitudinal Axis of the Beam

6.5 COMPARATIVE ANALYSIS

It can be observed from the experimental results that the beams retrofitted using GFRP jackets with fibres at forty five degrees to the longitudinal axis, yield a higher increase in the maximum load carrying capacity i.e. approximately 30-35 percent in case of under reinforced sections and 13-17 percent in case of balanced sections as compared to beams retrofitted using fibres at zero degrees to the longitudinal axis. It is also observed that after the retrofitting of the beams the increase in the maximum load carrying capacity decreases with an increase in the stress level and increases with a change in the orientation of fibres from zero degree to forty-five degrees.

The maximum load carrying capacity of retrofitted beams is calculated using the existing model as given by *Teng and Chen et al. (2002)*. These values work out to 27.71 kN and 47.73 kN for under reinforced and balanced beams, respectively. These are higher than the values obtained experimentally. The difference in the predicted and observed values is due to the reason that the said model does not consider the initial stress level while calculating the maximum load. So, there is a need of considering initial stress level for calculation of the maximum load carrying capacity of retrofitted beams.

The safe load carrying capacity for all the stressed beams decreases after the retrofitting. From the load deflection curves it can be seen that in almost all the cases the load deflection curve of the retrofitted beams is under the curve for the control beams in the initial phase and then the shift decreases. The shift also decreases with a decrease in the stress level. The reason for the same may be due to the amount of plastic deformation that has occurred in the materials during the initial stressing, and once that initial stress level is crossed the shift starts decreasing. The plastic deformation in the materials also decreases with a decrease in the stress level, hence the shift.

No cracks were observed in the beams after the retrofitting of the beams with GFRP jackets. However, it is observed that the beams fail by crushing of concrete first and followed by the fibre rupture in case of balanced sections, whereas it fails by fibre rupture in the case of under reinforced sections. Once the fibre ruptures the beam stops taking any further load.

There is lesser increases ductility ratio for the balanced sections as compared to under reinforced sections. The lower percentage increase in the ductility ratio for balanced

beams is due to the fact that retrofitting the beam leads to an over reinforced section which fails by crushing of concrete rather than yielding of steel.

The toughness of the under reinforced beams increased on an average by 30.16 percent, and for the balanced beams the toughness increased on an average by 66.4 percent. This clearly indicates that after the retrofitting, the beams can absorb much higher energy making them more suitable in earthquake prone areas.

Table 6.15: Deflection Ductility and Toughness for Retrofitted and Un-Retrofitted Beams Retrofitted Using GFRP Jackets

Type of Beam	P_{max}	Ductility Ratio (Δ_U/Δ_Y)	Increase in Ductility Ratio (Percent)	Toughness (KN-mm)	Increase in Toughness (Percent)
UC	22.40	2.27	-	1336.41	-
GFRP0-U60	24.20	2.40	5.79	1637.61	22.54
GFRP0-U75	22.30	2.63	15.75	1484.44	11.08
GFRP0-U90	19.70	2.52	10.85	1422.49	10.44
GFRP45-U60	29.30	2.56	12.9	2139.33	60.08
GFRP45-U75	29.35	2.37	4.39	2098.85	57.05
GFRP45-U90	24.40	3.12	37.3	1654.23	23.78
BC	38.30	1.81	-	1495.10	-
GFRP0-B60	42.75	2.0	10.77	2050.59	50.53
GFRP0-B75	41.75	2.11	16.8	2068.23	38.33
GFRP0-B90	40.45	2.01	11.05	1962.33	31.29
GFRP45-B60	45.00	2.07	14.32	2945.98	97.04
GFRP45-B75	44.35	1.98	9.23	2743.30	83.49
GFRP45-B90	44.00	2.19	20.88	2955.97	97.71

UC Under Reinforced Control Beam
BC Balanced Control Beam
GFRP0-U60 Under Reinforced Beams stressed to 60 percent of safe load and retrofitted using GFRP Jackets with Fibres Oriented at 0 degree to the Longitudinal Axis.
GFRP0-U75 Under Reinforced Beams stressed to 75 percent of safe load and retrofitted using GFRP Jackets with Fibres Oriented at 0 degree to the Longitudinal Axis
GFRP0-U90 Under Reinforced Beams stressed to 90 percent of safe load and retrofitted using GFRP Jackets with Fibres Oriented at 0 degree to the Longitudinal Axis.
GFRP45-U60 Under Reinforced Beams stressed to 60 percent of safe load and retrofitted using GFRP Jackets with Fibres Oriented at 45 degrees to the Longitudinal Axis.
GFRP45-U75 Under Reinforced Beams stressed to 75 percent of safe load and retrofitted using GFRP Jackets with Fibres Oriented at 45 degrees to the Longitudinal Axis
GFRP45-U90 Under Reinforced Beams stressed to 90 percent of safe load and retrofitted using GFRP Jackets with Fibres Oriented at 45 degrees to the Longitudinal Axis.
GFRP0-B60 Balanced Beams stressed to 60 percent of safe load and retrofitted using GFRP Jackets with Fibres Oriented at 0 degree to the Longitudinal Axis.
GFRP0-B75 Balanced Beams stressed to 75 percent of safe load and retrofitted using GFRP Jackets with Fibres Oriented at 0 degree to the Longitudinal Axis
GFRP0-B90 Balanced Beams stressed to 90 percent of safe load and retrofitted using GFRP Jackets with Fibres Oriented at 0 degree to the Longitudinal Axis.
GFRP45-B60 Balanced Beams stressed to 60 percent of safe load and retrofitted using GFRP Jackets with Fibres Oriented at 45 degrees to the Longitudinal Axis.
GFRP45-B75 Balanced Beams stressed to 75 percent of safe load and retrofitted using GFRP Jackets with Fibres Oriented at 45 degrees to the Longitudinal Axis
GFRP45-B90 Balanced Beams stressed to 90 percent of safe load and retrofitted using GFRP Jackets with Fibres Oriented at 45 degrees to the Longitudinal Axis.

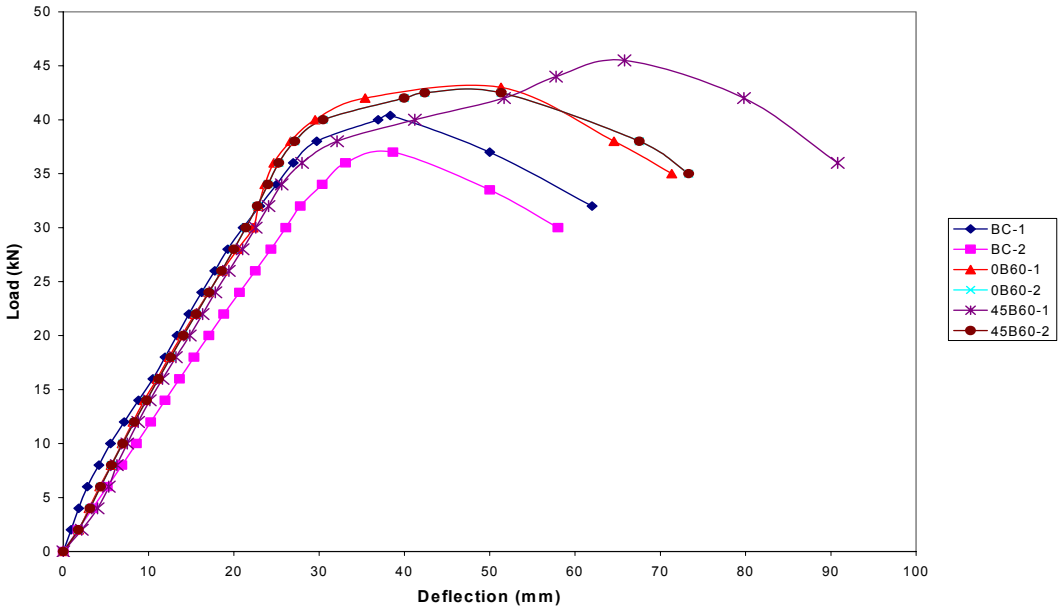

Fig. 6.6: Load v/s Mid Span Deflection of Balanced Beams Retrofitted with GFRP Jacketing and Stressed to 60 percent Stress Level

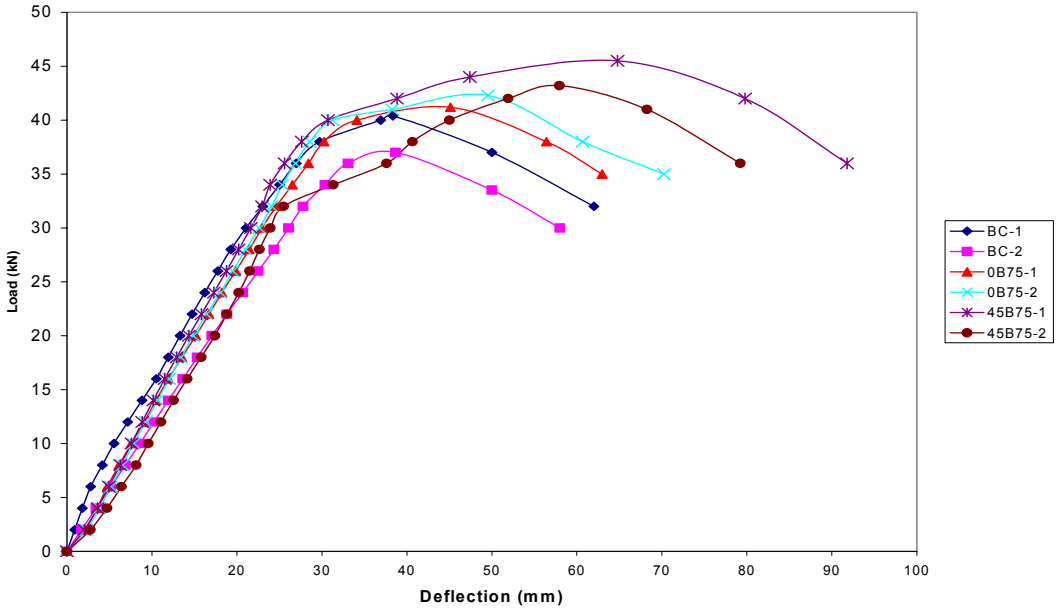

Fig. 6.7: Load v/s Mid Span Deflection of Balanced Beams Retrofitted with GFRP Jacketing and Stressed to 75 percent Stress Level

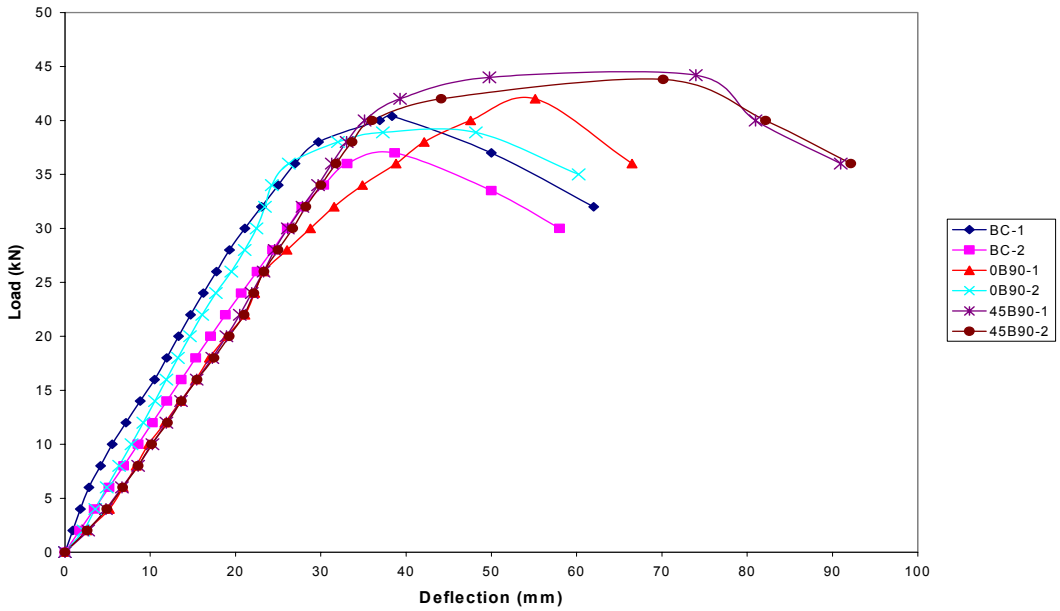

Fig. 6.8: Load v/s Mid Span Deflection of Balanced Beams Retrofitted with GFRP Jacketing and Stressed to 90 percent Stress Level

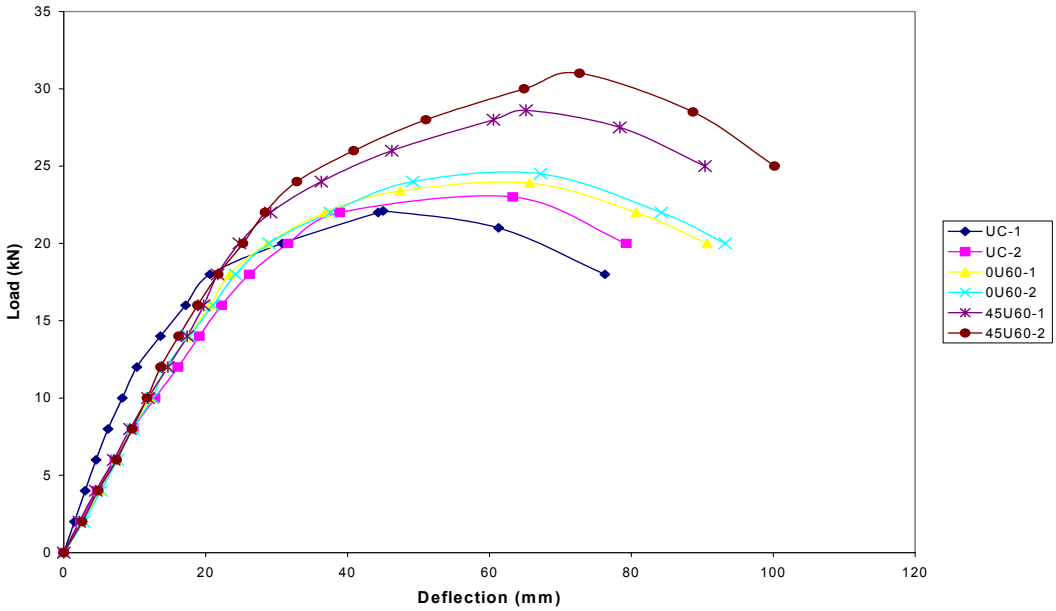

Fig. 6.9: Load v/s Mid Span Deflection of Under Reinforced Beams Retrofitted with GFRP Jacketing and Stressed to 60 percent Stress Level

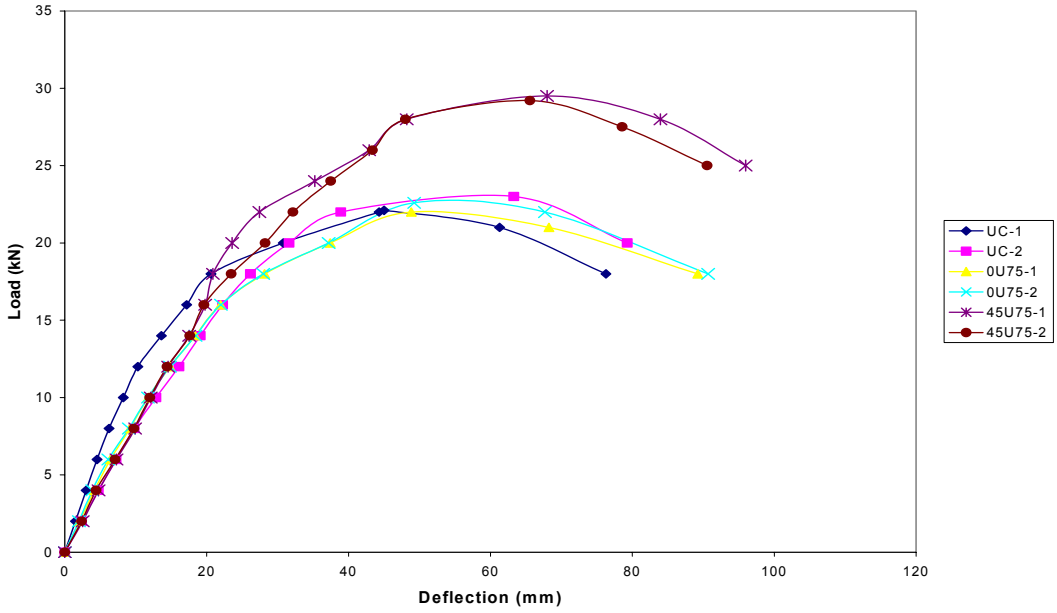

Fig. 6.10: Load v/s Mid Span Deflection of Under Reinforced Beams Retrofitted with GFRP Jacketing and Stressed to 75 percent Stress Level

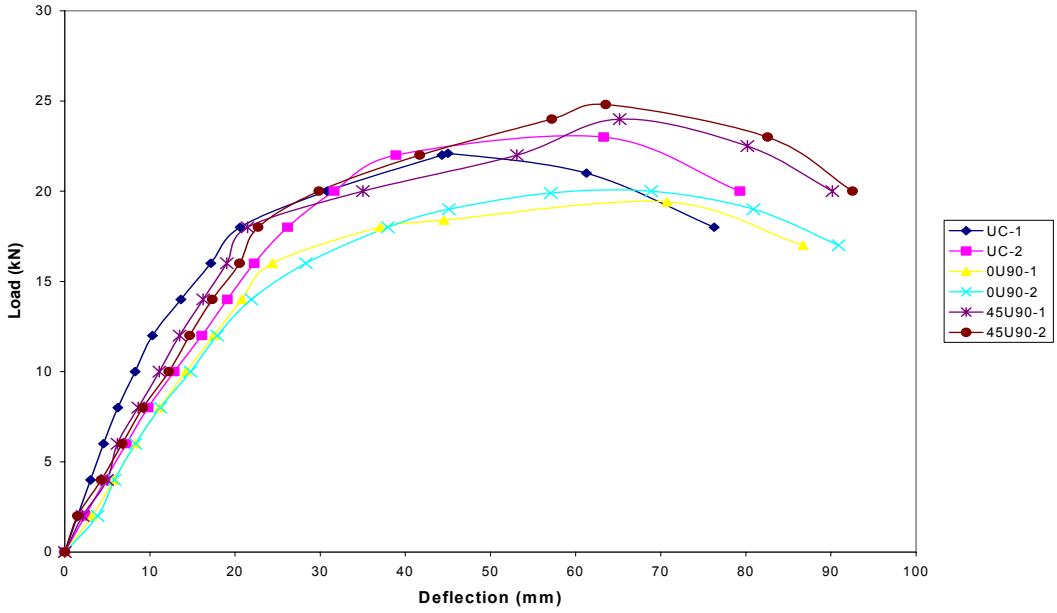

Fig. 6.11: Load v/s Mid Span Deflection of Under Reinforced Beams Retrofitted with GFRP Jacketing and Stressed to 90 percent Stress Level

Plate 6.1 Failure of Beam Retrofitted with GFRP Jacket with Fibres at zero Degree to The Longitudinal Axis of Beam

Plate 6.2 Failure of Beam Retrofitted with GFRP Jacket with Fibres at 45 Degree to The Longitudinal Axis of Beam

Plate 6.3 Crushing of Concrete in Balanced Beam Retrofitted with GFRP Jacketing

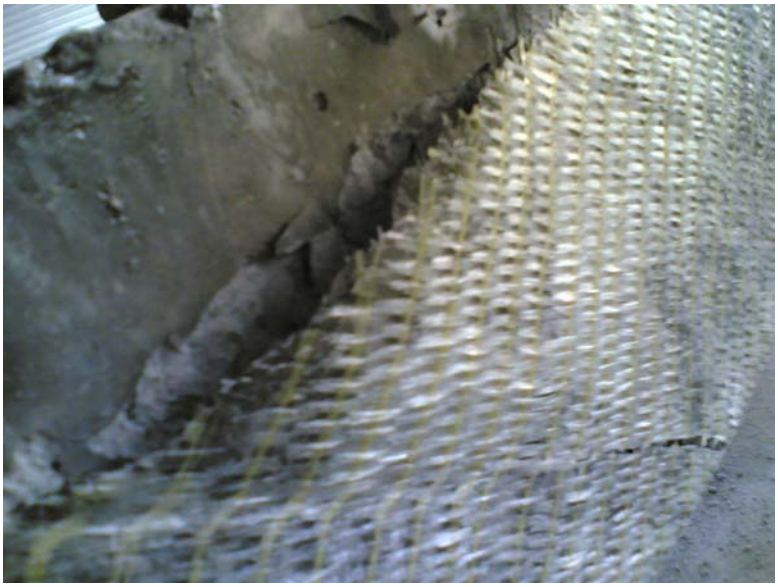

Plate 6.4 Debonding of GFRP Jacketing with Fibres at 45 Degree to the Longitudinal Axis of Beam

CHAPTER –7

MODELLING OF BEHAVIOUR AND VALIDATION

In this chapter a mathematical model using limit state theory is proposed to find the maximum and safe load carrying capacities for the beams retrofitted using ferrocement jacketing. The entire chapter is divided into two sections, wherein, in the first section a mathematical model is proposed for calculating the maximum and safe load carrying capacities of the retrofitted beams, and in the second section verification of the proposed models is done using data obtained from the results of tests carried out in the current study as well as for the test results quoted by other researchers.

7.1 MATHEMATICAL MODELING

In the present section, with an aim to develop a design methodology for retrofitting of stressed beams using ferrocement jackets, a mathematical model is developed. The succeeding section deals with the validation of the proposed mathematical model for the experimentally obtained results. The mathematical model is developed using limit state design procedure.

7.1.1 Maximum Load Carrying Capacity

The theoretical maximum load carrying capacity of the beams retrofitted using ferrocement jackets is calculated assuming composite behavior and linear strain distribution in the beam as shown in Fig. 7.1. Based on the flexural theory, the assumptions for the development of a mathematical model for the design of retrofitted beams for limit state of collapse in bending are modified and are specified as below.

1. Plane section normal to the axis remains plane after bending
2. The maximum strain in concrete at the outermost fibre is taken as 0.35% in bending regardless of the strength of concrete and ferrocement jacket,
3. As at the maximum load concrete and mortar cracks in tension, thus tensile strength of concrete and ferrocement jacket is ignored, and the entire tensile stresses are taken by steel in tension i.e. tensile reinforcement of the beam and wire mesh reinforcement in the ferrocement jacket.

4. The compressive force is resisted by concrete and mortar as well as by wire mesh in compression above the neutral axis
5. The relationship between stress-strain distribution in concrete and mortar is assumed to be parabolic as shown in Fig. 7.1. The maximum compressive stress is equal to $0.67f_{ck}$ (for calculation purposes, the partial factor of safety is assumed to be one).

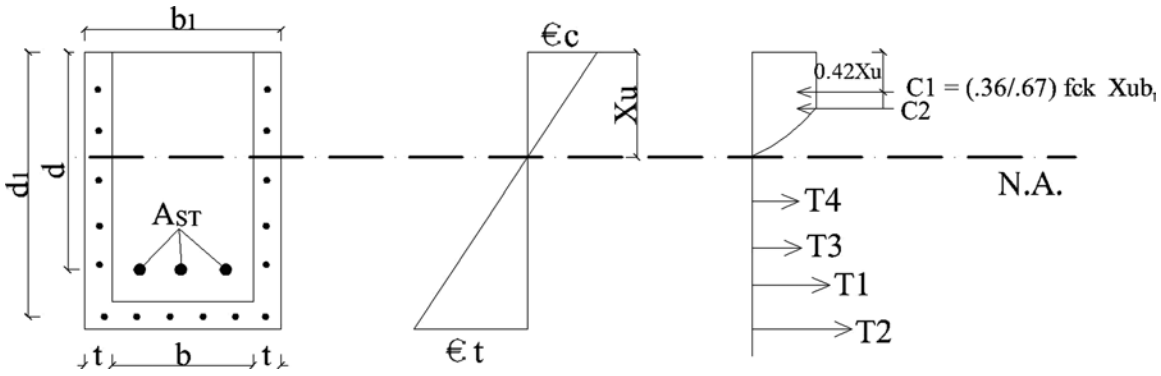

Fig. 7.1: Stress and Strain Variation in the Retrofitted Beam

Thus to find out the position of the neutral axis the compressive and tensile forces are equated.

$$\Sigma C = \Sigma T \qquad (7.1)$$

Where 'ΣC' is sum of the compressive force in the composite section and ΣT is the sum of the tensile forces T_1, T_2……..T_n where T_1, is the tensile force in tension reinforcement of beam and T_2, T_3……..T_n are the tensile forces in the wire mesh reinforcement of the ferrocement jacket.

The compressive force 'C' can be calculated from the area of rectangular-parabolic stress block using the expression given in *IS: 456-2000* and assuming a partial factor of safety one. So

$$C = \frac{0.36}{0.67} b_1 f_{ck} x_u = 0.542 b_1 f_{ck} x_u \qquad (7.2)$$

Where b_1 is the width of section after retrofitting and is given by

$$b_1 = b + 2t \qquad (7.3)$$

Where '*t*' is the thickness of the ferrocement jacket,

f_{ck} is the 28 days characteristic strength of concrete compression.

and x_u is the depth of neutral axis of the composite section

Tensile forces T_1, T_2 …..T_n can be calculated by multiplying yield strength of the main reinforcement and the wire mesh reinforcement with their respective cross-sectional areas.

Thus $$T_1 = f_{y1} A_{st1} \quad (7.4)$$

and $$T_n = f_{yn} A_{stn} \quad (7.5)$$

Where f_{y1} and f_{yn} are the yield strengths of the main reinforcement and wire mesh respectively and A_{st1} and A_{stn} are the main reinforcement and wire mesh reinforcement in ferrocement jacket, respectively. The above cross sectional areas are calculated below

$$A_{st1} = \frac{n\pi\phi^2}{4} \quad (7.6)$$

$$A_{st2} = \frac{n_i\pi\phi_1^{\,2}}{4} \quad (7.7)$$

Where

n, is number of bars as main reinforcement in beam,

n_i is number bars in wire mesh

ϕ, is diameter of main reinforcement, and

ϕ_1, is diameter of reinforcement in the ferrocement jacket.

Putting the values of *C*, T_1, T_2 etc. as calculated above, in the equation 7.1, the position of neutral axis can be calculated as below

$$0.542 b_1 f_{ck} x_u = f_{y1}\frac{n\pi\phi^2}{4} + f_{yn}\frac{n_i\pi\phi_1^{\,2}}{4} \quad (7.8)$$

The maximum moment of resistance of the section can then be calculated by taking moment of tensile forces as below.

$$M_u = T_1(d - 0.42x_u) + T_2(d_1 - 0.42x_u) + \ldots\ldots\ldots\ldots Tn(dn - 0.42x_u) \quad (7.9)$$

Where d and d_1 are the depth of section from top up to the centre of gravity (c.g) of main reinforcement and c.g of reinforcement in ferrocement jacket at soffit of retrofitted beam as shown in Fig. 7.1 and d_n is the depth of n^{th} wire mesh from the top of the beam.

The maximum load carrying capacity can thus be calculated. In case of beam subjected to two point loading the maximum load carrying capacity can be calculated from the following equation.

$$P_{max} = \frac{2M_u}{Shearspan} \quad (7.10)$$

Where, M_u is calculated using equation 7.9.

Using above methodology, the maximum load carrying capacity of the retrofitted beams used in present study is calculated and is tabulated in Table 7.1.

7.1.2 Safe Load Carrying Capacity of Beam

The safe load carrying capacity of section is defined as the load up to which the beam is satisfying the limit state of deflection i.e. the deflection in the beam is less than L/250 as specified in *IS:456-2000*.

The deflection at the centre of simply supported beam subjected to two concentrated loads at a distance of 1.0 m at the centre is given by the formula

$$\Delta = \frac{M(3L^2 - 4a^2)}{24E_c I_{eff}} \quad \text{- (7.11)}$$

Where

M is the maximum bending moment in the beam and is given by $\frac{Pa}{2}$

P is the total load acting on the beam,

a is the distance of the load from the support.

L is the centre to centre span of the beam

E_c is the modulus of elasticity of concrete and

can be calculated by using equation given in IS:456-2000

$$E_c = 5000\sqrt{f_{ck}} \quad (7.12)$$

I_{eff} is the effective moment of inertia of the beam and can be calculated by modifying the method suggested in Appendix C of *IS:456-2000*.

$$I_{eff} = \frac{I_r}{1.2 - \frac{M_r}{M}\left(1 - \frac{x_u}{3d}\right)\left(1 - \frac{x_u}{d}\right)\frac{b_w}{b_f}} \quad (7.13)$$

Where I_r is the moment of inertia of the cracked section and can be calculated using following equation

$$\frac{bx_u^{\ 3}}{3} + (1.5m - 1)A_{sc}(x_u - d')^2 + mA_{st}(d - x_u)^2$$

b_w and b_f are the width of the web and flange, respectively and in case of rectangular sections equal to width of the beam

A_{sc} Area of steel in compression

A_{st} Area of steel in tension

m modular ratio

d effective depth of beam

d' effective cover

x_u is depth of neutral axis from top

M_r is the cracking moment and is given by $\frac{f_{cr} I_{gr}}{y_t}$

f_{cr} is the modulus of rupture for RCC ferrocement composite beams is given by

$$f_{cr} = 20p' + 34 \text{ kg/cm}^2 \quad (7.14)$$

(*Singh S.K. & Kaushik S.K., 1997*)

where $$p' = A_{st2}\frac{100}{b_1 t} \quad (7.15)$$

b_1 is width of the composite section and 't' is the thickness of the ferrocement jacket.

I_{gr} is the gross moment of inertia of the composite beam and is given by

$$I_{gr} = I_{re} + I_t \quad (7.16)$$

I_{re} is the reduced moment of inertia of the original beam stressed to a particular level and calculated as effective moment of inertia of RCC beams for deflection as per method

given in *IS: 456-2000* for bending moment corresponding to the calculated load (for particular stress level)

I_t is moment of inertia of U-shaped ferrocement jacket about C.G. of section

Now applying a condition $I_r \leq I_{eff} \leq I_{gr}$, and substituting Δ = L/250, the value of P_{safe} can be calculated

7.2 VALIDATION OF MATHEMATICAL MODELS

The proposed mathematical model is verified with the help of experimental results.

7.2.1 Maximum Load Carrying Capacity

For the validation of the proposed model, the maximum load carrying capacity of the retrofitted beams in the present study is calculated using proposed method and typical example is detailed in *Appendix 'A'*

The load carrying capacities of all the retrofitted beams are calculated on the pattern explained in section 7.1.1 and demonstrated in *Appendix 'A'* and tabulated in Table 7.1. From the table it is observed that the average percentage error in maximum load calculated by the proposed method and obtained experimentally is 5.92 percent.

To further validate the model, the maximum load carrying capacity of the beams obtained by *Fahmy et al, 1997* is calculated by the proposed model. The results of the comparison are summarized in Table 7.2. These results clearly indicate that the proposed model is quite accurate in predicting the maximum load carrying capacity of the retrofitted beams. The absolute average percentage difference between the experimental and predicted results is 6%, which is quite small when one considers the expected variation associated with the behaviour of reinforced concrete structures.

Thus, it can be concluded that the maximum load carrying capacity of reinforced concrete beams retrofitted using ferrocement jackets can be calculated by the proposed method confidently.

Table 7.1: Experimental and Analytical Maximum Load Carrying Capacity of Beams Retrofitted Using Ferrocement Jacketing

S.No.	Type of Beam	P_{max} Experimental (KN)	P_{max} Analytical (KN)	Percentage Error
1	2U	31.75	33.28	4.82
2	3U	36.38	38.51	5.85
3	2B	45.92	49.7	8.23
4	3B	51.06	53.5	4.78

2U Under Reinforced section retrofitted using ferrocement jacketing reinforced with two layers of wire mesh.

3U Under Reinforced section retrofitted using ferrocement jacketing reinforced with three layers of wire mesh.

2B Balanced section retrofitted using ferrocement jacketing reinforced with two layers of wire mesh.

3B Balanced section retrofitted using ferrocement jacketing reinforced with three layers of wire mesh.

Table 7.2 Comparison Between Experimental and Calculated Maximum Load of Beams Retrofitted Using Ferrocement Jacketing

Type of Beam (*Fahmy at el. 1997*)	P_U (kN)	$P_{pred.}$ (kN)	P_{red}/P
B1	13.47	12.35	0.92
B2	13.98	12.38	0.88
B3	17.83	16.97	0.95
B4	14.4	13.66	0.95
B5	13.63	11.79	0.86
B6	15.48	13.66	0.88
B7	16.52	15.59	0.94
B8	14.08	16.12	1.14
B9	16.7	16.97	1.01

7.2.2 Safe Load Carrying Capacity

The validation of the proposed procedure for finding out the safe load carrying capacity is done by calculating the safe load carrying capacity of the retrofitted beams tested in the laboratory by the proposed procedure. Typical example of calculation of safe load carrying capacity with the proposed model is detailed in *Appendix 'B'*.

The safe load carrying capacities of all the retrofitted beams are calculated on the pattern explained in section 7.1.2 and demonstrated in *Appendix 'B'* and tabulated in Table 7.3. From the table it is observed that the average percentage error in maximum load calculated by the proposed method and obtained experimentally is –3.54 percent.

Table 7.3: Experimental and Analytical Safe Load Carrying Capacity of Beams Retrofitted Using Ferrocement Jacketing

S. No.	Type of Beam	P_s Experimental (KN)	P_s Analytical (KN)	Percentage Error
1	2U60	16.02	16.47	2.80
2	2U75	15.90	15.68	-1.38
3	2U90	15.13	15.24	0.73
4	3U60	21.2	18.42	-13.1
5	3U75	21.3	17.53	-17.7
6	3U90	20.2	17.02	-15.74
7	2B60	24.01	24.0	-0.04
8	2B75	22.43	23.20	3.43
9	2B90	22.31	22.96	2.91
10	3B60	26.01	25.84	-0.653
11	3B75	26.02	24.96	-4.07
12	3B90	24.5	24.54	0.163

2U60 *Under Reinforced section stressed to 60 percent of safe load and retrofitted using ferrocement jacketing reinforced with two layers of wire mesh.*

2U75 *Under Reinforced section stressed to 75 percent of safe load and retrofitted using ferrocement jacketing reinforced with two layers of wire mesh.*

2U90 *Under Reinforced section stressed to 90 percent of safe load and retrofitted using ferrocement jacketing reinforced with two layers of wire mesh.*

3U60 *Under Reinforced section stressed to 60 percent of safe load and retrofitted using ferrocement jacketing reinforced with two layers of wire mesh.*

3U75 *Under Reinforced section stressed to 75 percent of safe load and retrofitted using ferrocement jacketing reinforced with two layers of wire mesh.*

3U90 *Under Reinforced section stressed to 90 percent of safe load and retrofitted using ferrocement jacketing reinforced with two layers of wire mesh.*

2B60 *Balanced section stressed to 60 percent of safe load and retrofitted using ferrocement jacketing reinforced with two layers of wire mesh.*

2B75 *Balanced section stressed to 75 percent of safe load and retrofitted using ferrocement jacketing reinforced with two layers of wire mesh.*

2B90 *Balanced section stressed to 90 percent of safe load and retrofitted using ferrocement jacket having two layers of wire mesh.*

3B60 *Balanced section stressed to 60 percent of safe load and retrofitted using ferrocement jacketing reinforced with two layers of wire mesh.*

3B75 *Balanced section stressed to 75 percent of safe load and retrofitted using ferrocement jacketing reinforced with two layers of wire mesh.*

3B90 *Balanced section stressed to 90 percent of safe load and retrofitted using ferrocement jacketing reinforced with two layers of wire mesh.*

To further validate the model, the safe load carrying capacity of the beam obtained by *Singh, S.K. and Kaushik, S.K., 1997* is calculated by the proposed model. The results of the comparison are summarized in Table 7.4. These results clearly indicate that the proposed model is quite accurate in predicting the maximum load carrying capacity of the retrofitted beams. The absolute percentage difference between the experimental and predicted results is 3.57 %, which is quite small when one considers the expected variation associated with the behaviour of reinforced concrete structures.

Table 7.4 Comparison Between Experimental and Calculated Safe Load of Beams Retrofitted Using Ferrocement Jacketing

Type of Beam *(Singh S.K., and Kaushik, S.K., 1997)*	**Intial Stress Level**	**Safe Load - Experimental (kN)**	**Safe Load- Predicted (kN)**	**Error (%)**
FRB-1	Stressed upto Ultimate Load	168	174	3.57

CHAPTER -8
CONCLUSIONS

8.1 GENERAL

The effect on various parameters like maximum load carrying capacity, safe load carrying capacity, ductility ratio, and toughness of the stressed beams retrofitted with either GFRP jacketing or ferrocement jacketing have been studied in the present work. A design procedure using limit state design theory has been developed for the design of ferrocement jacketing for the retrofitting of the stressed beams. The experimental procedure developed is verified with the experimental data generated. On the basis of present study, following conclusions are drawn.

8.2 BEAMS RETROFITTED USING GFRP JACKETS

1. GFRP jackets used for retrofitting of the under reinforced beams perform better with fibres at forty-five degrees to the longitudinal axis of the beam.
2. The strength of the section decreased with an increase in the initial stress level. The maximum load carrying capacity of the beams decreased due to decrease in stiffness of section with an increase in the initial stress level.
3. The initially stressed beams retrofitted with GFRP jackets had a lesser safe load carrying capacity. This is attributed to the fact that, due to initial stress level the section loses its stiffness hence deflects more when reloaded after retrofitting.
4. GFRP jacketing leads to an improvement in the energy absorption capacity of all the beams irrespective of the type of section and orientation of fibres in the jackets. The under reinforced sections with fibres oriented at forty-five degrees performed better within the group.

8.3 BEAMS RETROFITTED USING FERROCEMENT JACKETS

1. Retrofitting of the beams with ferrocement jackets should be preferred where the strengthening of the beams is required to take care of the deficiency of the beams in flexure.

The use of ferrocement jacketing for retrofitting of initially stressed beams helps to regain the full strength of all type of beams, even if stressed up to 90 percent of the safe load.

2. Cement slurry is the most efficient bonding agent due to its low cost to strength ratio. Whereas, shear connectors with cement slurry improve the maximum load carrying capacity of the beams leading to a higher cost.

3. Welded wire mesh, with forty five degree orientation to the longitudinal axis, have a significant positive effect on the load carrying capacity of the beams, whereas, zero degree orientation is most efficient due to its low cost to strength ratio.

   Woven wire mesh used for ferrocement jacketing of beams should be preferred over welded wire mesh due to larger improvement in the load carrying capacity, ductility ratio and energy absorption.

4. The increase in the maximum load carrying capacity is higher for under reinforced beams (27-34%) as compared to balanced beams (17-20%) in case of ferrocement jackets reinforced with two layers of woven wire mesh. The corresponding increase in load carrying capacity of the beams retrofitted using ferrocement jackets reinforced with three layers of woven wire mesh, is 48-52% and 29-35% respectively.

   The percentage increase in the safe load carrying capacity is less as compared to maximum load carrying capacity because of decrease in stiffness of the section due to initial stress.

   The percentage increase in the load carrying capacity of beams retrofitted using ferrocement jacketing, increases with increase in reinforcement in the jackets.

   The percentage increase in the load carrying capacity of beams retrofitted using ferrocement jacketing, decreases with increase in initial stress.

   The percentage increase in load carrying capacity decreases with increase in tension reinforcement in the original beam.

   The maximum load carrying capacity of the retrofitted beams is independent of the thickness of the jacket.

5. Ferrocement jacketing leads to an improvement in the energy absorption capacity of all the type of beams irrespective of the type of section (under reinforced or balanced) and reinforcement in the jackets. The under reinforced

sections with higher reinforcement in the jacket performed better within the group.

6. The proposed mathematical procedure devised in the study can be efficiently used to predict the maximum and safe load carrying capacities of the initially stressed retrofitted beams.

REFRENCES

1. "A Manual of Earthquake Resistant Non-Engineered Construction," Book Published by Indian Society of Earthquake Technology, University of Roorkee, 1981, pp. 155-161.
2. "Non-Engineered Construction in Earthquake Prone Areas and Earthquake Mitigation with Special Reference to Pakistan," Project Report, Department of Civil Engineering, NED University of Engineering and Technology, Karachi, Pakistan, 1988, pp.103
3. Abdullah A, Katsuki Takiguchi, "An Investigation into the Behavior and Strength of Reinforced Concrete Columns Strengthened with Ferrocement Jackets", Cement and Concrete Composite, Vol-25, 2003, pp 233-242.
4. Abdullah and Mansur, M.A. " Effect of Mesh Orientation on Tensile Response of Ferrocement" Journal of Ferrocement: Vol. 31, No. 4, October 2001, pp 289-297.
5. ACI Committee – 549 Report " Guide for the Design, Construction and Repair of Ferrocement" ACI Structural Journal, May – June 1988, pp325-351.
6. Akhtarruzzama, A.K.M., and Pama, R.P. "Cracking Behavior of Ferrocement in Tension", Proceeding of the Third International Symposium on Ferrocement, 1988, pp.1-11.
7. Al- Sulalmani and Basunbul, I.A." Behavior of Ferrocement Material Under Direct Shear", Journal of Ferrocement: Vol. 21, No. 2, April 1991, pp 109-117.
8. Al-Farabi, M.S., Baluch, M.H., Al-Sulaimani, G.J., and Basunbul, I.A., "Repair of Damaged R/C Beams using Externally Bonded Fiber Glass Plates," Fourth International Conference Structural Failure, Durability and Retrofitting, Singapore, 1993, pp. 621-628.
9. Al-Kubaisy, M.A. " Location of the Critical Diagonal Crack in Ferrocement Beams" Journal of Ferrocement: Vol. 28, No. 2, April 1998, pp 135-146.
10. Al-Kubaisy, M.A., and Nedwell, P.J. " Behavior and Strength of Ferrocement Rectangular Beams in Shear" Journal of Ferrocement: Vol. 29, No. 1, January 1999, pp 1-15.

11. Al-Noury, S.I., and Huq, S. “Ferrocement in Axial Tension” Journal of Ferrocement, Vol. 18, No.2, 1988, pp 111-137.
12. Al-Rifaie, W.N. and Trikha, D.N. “ Effect of Arrangement and Orientation of Hexagonal Mesh on the Behaviour of Two- Way ferrocement Slabs” Journal of Ferrocement: Vol. 20, No. 3, July 1990, pp 219-230.
13. An, Wei., Saadatmanesh, Hamid, and Ehsani, Mohammad R., “RC Beams Strengthened with FRP Plates II: Analysis and Parametric Study”, Journal of Structural Engineering, Vol. 117, No. 11, November, 1991, pp 3434-3455.
14. Andrews, G., and Sharma, A.K., “Repaired Reinforced Concrete Beams” ACI, Concrete International, Detriot 1998, pp. 47-50.
15. Anwar , A,W., Nimityongskul, P., Pama, R,P., and Robles-Austriaco, L., “Method of rehabilitations of structural beam elements using ferrocement”, Journal of ferrocement, Vol 21., No3, 1991, pp 229-234.
16. Anwar, A.W., “Ferrocement for low-cost housing in Pakistan”, Journal of ferrocement, Vol 23, No 2, 1993, pp 117-123.
17. Balagurusamy, Perumalsamy N., Naaman, A.E., and Shah, Surinder P., “ Analysis and Behaviour of Ferrocement in Flexure” ASCE (Structural Division), Vol. 103, No. ST10, October 1977, pp 1937-1951.
18. Basu, P.C., “Seismic Upgradation of Buildings: An Overview”, The Indian Concrete Journal, The Associated Cements Companies Ltd., August 2002, pp. 461-475.
19. Basunbul, I.A., Husain, M., Sharif, A.M., Al-Sulaimani, G.J., and Baluch, M.H., “Repair of Shear Cracked R/C Beams with Bonded External Steel Plates”. Fourth International Conference on Structural, Failure, Durability and Retro-fitting, Singapore 1993, pp. 629-634.
20. Bonacci, J.F. and Maalej, M “ Behavioral Trends of RC Beams Strengthened with Externally Bonded FRP ” Journal of Composites for Construction, Vol. 5, No. 2, May 2001, pp 102-103.
21. Buyukozturk, Oral, and Hearing, Brain., “Failure Behavior of Precraked Concrete Beams Retrofitted with FRP”, Journal of Composites for Construction, Vol. 2, No. 3, August, 1998, pp 138-144.
22. Clarke, R.P. and Sharma, A.K. “ The Experimental Behaviour of Ferrocement Flat Plate Under Biaxial Flexure” Journal of Ferrocement: Vol. 21, No.2, April 1991, pp 127-136.

23. Colotti, Vincenzo and Spadea Giuseppe " Shear Strength of RC Beams Strengthened with Bonded Steel and FRP Plates" Journal of Structural Engineering, Vol. 127, No. 4, April 2001, pp 367-373.
24. Desayi, Prakash, Nandakumar, N., and A. El-kholy, Said. " Shear Stress of Ferrocement Trough Section Elements" Journal of Ferrocement: Vol. 24, No. 4, October 1994, pp 323-342.
25. Desia, R., "Field Shake Test Programme at Latur, Western India," News letter, Earthquake Hazard Centre, New Zealand 1999, V. 3, No.2, pp. 4-5.
26. Fahmy, Ezzat H. , Shaheen, Yousry B.I. and Korany, Yasse S. " Use of Ferrocement Laminates for Reaping Reinforced Concrete Slabs" Journal of Ferrocement: Vol. 27, No. 3, July 1997, pp 219-232.
27. Fahmy, Ezzat H. , Shaheen, Youysry B.I. and Korany Yasser, S. " Repairing Reinforced Concrete Beams by ferrocement" Journal of Ferrocement: Vol. 27, No. 1, January 1997, pp 19-32.
28. G.C. Mays and R.A. Barnes "Ferrocement Permanent Formwork as Protection to Reinforced Concrete", Journal of Ferrocement, Vol. 25, No.4, 1995, pp. 331-345.
29. GangaRao, Hota V.S., Vijay, P.V., "Bending Behavior of Concrete Beams Wrapped with Carbon Fabric", Journal of Structural Engineering, Vol. 124, No. 1, January 1998, pp 3-10.
30. Gulkan, P.; Wasti, S.T., and Karaesmen, E., "Some Aspects of Earthquake Engineering Research in Turkey," Research Report, Middle East Technical University, Ankara, Turkey 1980.
31. Hadi, M.N.S. "Retrofitting of Shear Failed Reinforced Concrete Beams", Elsevier Composite Structures, Vol. 62, 2003, pp 1-6.
32. Hossain, M.Z. and Hasgawa, T " A Comparison of the Mechanical Properties of Ferrocement in Flexure for Square and Hexagonal Meshes" Journal of Ferrocement: Vol. 28, No. 2, April 1998, pp 111-134.
33. Hussin, M.W., "Deflection and cracking of performance of fibrous ferrocement thin sheets", Journal of ferrocement, Vol 21, No. 11, 1992, pp 31-41.
34. IS: 10262-1982, Recommended Guidelines For Concrete Mix Design, Bureau of Indian Standards, New Delhi.

35. IS: 1489 (Part 1)-1991, Portland-Pozzolana Cement Specification Part 1 Fly Ash Based, Bureau of Indian Standards, New Delhi.
36. IS: 1786-1985, Specification For High Strength Deformed Steel Bars And Wires For Concrete Reinforcement, Bureau of Indian Standards, New Delhi.
37. IS: 383-1970, Specification For Coarse And Fine Aggregates From Natural Sources For Concrete, Bureau of Indian Standards, New Delhi.
38. IS: 456-2000, Indian Standard Plain and Reinforced Concrete-Code of Practice, Bureau of Indian Standards, New Delhi.
39. IS:13935-1993, Repair And Seismic Strengthening of Buildings-Guidelines, Bureau of Indian Standards, New Delhi.
40. Jai, Junhui, Boothby, Thomas E., Bakis, Charies E., and Brown, Tennisha, L. Brown, "Durabiltiy Evaluation of Glass Fiber Reinforced-Polymer-Concete Bonded Interfaces" Journal of Composites and Construction, Vol. 9, No. 4, August 1, 2005, pp 348-359.
41. Johnston, Colin D. and Mattar, Samir G. " Ferrocement - Behavior in Tension and Compression" Journal of Structural Division, ASCE, Vol. 102, No. ST5, May 1976, pp 875 –889.
42. Johnston, Colin D., Mowat, Dallas N. " Ferrocement – Material Behavior In Flexure" Journal of Structural Division, ASCE, Vol. 100, No. ST10, October 1974, pp 2053-2069.
43. Kabir, A. and Ali, S. " Strengthening of Damaged Reinforced Concrete Beams With Ferrocement Deep Beams With Ferrocement Overlays" International Seminar on Civil Engineering in the Twenty first Century, Roorkee, India, 1996, pp1667 – 1677.
44. Kachlakev, D. and McCurry, D.D., " Behavior of Full-Scale Reinforced Concrete Beams Retrofitted for Shear and Flexural with FRP Laminates", Elsevier Composite Part B: Engineering, Vol. 31, 2000, pp 445-452
45. Kadir, Mohamand Razali Abdul, Samad, Abdul, Aziz, Abdul, Muda, Zakaria Che and Ali, Abang Abdullah Abang " Flexural Behaviour of Composite Beams with Ferrocement Permanent Formwork" Journal of Ferrocement: Vol. 27, No. 3, July 1997, pp 209-214.
46. Kamasewara Rao, C.B. and Kamasundara Rao, A. " Stress Strain Relation for Ferrocement in Tension" Journal of Ferrocement: Vol. 24, No. 4, October 1994, pp 309-321.

47. Kameswara Rao,C.B., and Kamasundra Rao,A. " Stress Strain Curve in Axial Compression and Poisson's Ratio of Ferrocement", Journal of Ferrocement, 1986,Vol. 16, No.2,pp 117-128.

48. Karasudhi, P., Mathew, A.G., and Nimityongskul, P., " Fatigue of Ferrocement in Flexure" Journal of Ferrocement: Vol. 7, No. 2, October1977, pp 80-95.

49. Karunakar Rao, P., Jagannadha Rao, V. " Theory for Computation of Ultimate Moment in Ferrocement Structural Elements in Flexure" Proceedings of 3rd International Conference Ferrocement, Department of Civil Engineering, University of Roorkee, 1988, pp 83 – 89.

50. Kaushik S.K., Gupta V.K. and Singh K.T. "Behavior of Composite Slabs with Lost Formwork", Journal of Ferrocement, Vol.21, No.3, 1991, pp. 203-213.

51. Kaushik S.K., Gupta V.K., and Rahman M.K., "Efficiency of Mesh Overlaps of Ferrocement Elements", Journal of Ferrocement, Vol-17, No-4, 1987,pp-329-336.

52. Kaushik, S.K., Gupta, V.K. and Singh, K.T. " Behaviour of Composite Slabs with Lost Formwork" Journal of Ferrocement: Vol. 21, No. 3, July 1991, pp 203-213.

53. Kaushik, S.K. and Dubey, A.K. " Performance Evaluation of RC Ferrocement Composite Beams" Proceedings of Fifth International Symposium, UMIST, 1994, pp 240- 256.

54. Kaushik, S.K. and Garg, V.K. " Shear Distress of RC Beams Using Precast Ferrocement Bonded Plates", Proceedings of the Fifth International Symposium, UMIST, 1994, pp 259 – 268.

55. Kaushik, S.K., Gupta, V.K., Anuj and Singh, K.K. " Behavior and Performance of Composite Ferrocement Brick Slabs" Journal of Ferrocement: Vol. 21, No. 3, July 1991, pp 215-222.

56. Kaushik, S.K., Prakash, A. and Singh, K. K. " Inelastic Buckling of Ferrocement Encased Columns" Ferrocement: Proceedings of Fifth International Symposium, UMIST, 1994, pp 327-341.

57. Khalifa, Ahmed, and Nanni, Antonio, "Improving Shear Capacity of Existing RC T-Section Beams Using CFRP Composites", Cement and Concrete Composites, Vol. 22, No. 2, July 2000, pp 165-174.

58. Khalifa, Ahmed, Gold, William J., Nanni, Antonio, and Addel Aziz M.I., "Contribution of Externally Bonded FRP to Shear Capacity of RC Flexural Members", Journal of Composites for Construction, Vol. 2, No. 4, November, 1998, pp 195-203.

59. Khanzadi, M.K. and Ramesht, M.H. " The Effect of Cover and Arrangement of Reinforcement on The Behaviour of Ferrocement in Tension" Journal of Ferrocement: Vol. 26, No. 2, April 1996, pp 85-94.

60. Lim, C.T.E., Paramasivam, P. and Ong, K.C.G. " Pushout Shear Strength of Ferrocement – Concrete Interface" Journal of Ferrocement: Vol. 31, No. 4, October 2001, pp 299-310.

61. Lorenzis, D.L. and Nanni, A, "Shear Strengthening of Reinforced Concrete Beams with Near Surface Mounted Fibre-Reinforced Polymer Rods", ACI Structural Journal, American Concrete Institute, January-February 2001, Vol. 98, NO. 1, pp. 60-68.

62. Lorenzis, D.L. and Nanni, A., "Bond Between Near Surface Mounted Fibre-Reinforced Polymer Rods and Concrete in Structural Strengthening", ACI Structural Journal, American Concrete Institute, March-April 2002, Vol. 99, NO. 2, pp. 123-132.

63. Mansur, M.A and Abdullah. " Constitutive Law of Ferrocement Under Biaxial Tension-Compression" Journal of Ferrocement: Vol. 28, No. 1, January 1998, pp 1-25.

64. Mansur, M.A. and Ong, K.C.G. " Shear Strength of Ferrocement Beams", ACI Structural Journal, January-Februrary 1987, pp 10-17.

65. Mansur, M.A. and Ong, K.C.G. " Shear Strength of Ferrocement I- Beams", ACI Structural Journal, July- August, 1991, pp 458- 464.

66. Mansur, M.A. and Paramasivam, P. " Cracking Behavior and Ultimate Strength of Ferrocement in Flexure" Journal of Ferrocement: Vol. 16, No. 4, October 1986, pp 405-415.

67. Mansur, M.A., Tan, K.L., Naaman, A.E. and Paramasivam, P. " Design Charts for Ferrocement Structural Section in Flexure" Journal of Ferrocement: Vol. 30, No. 4, October 2000, pp 345-362.

68. Mattone, R., "Ferrocement in low-cost housing: an application proposal (use of ferrocement in rural housing projects)." Journal of ferrocement, Vol. 22, No 2,1992, pp 181-187.

69. Mays, G.C. and Barnes, R.A. " Ferrocement Permanent Formwork as Protection to Reinforced Concrete" Journal of Ferrocement: Vol. 25, No. 4, October 1995, pp 331-345.

70. Mohammad Taghi Kazemi, Reza Morshed, "Seismic Shear Strengthening of R/C Columns with Ferrocement Jacket", Cement and Concrete Composite, Article In Press, (2005).

71. Naaman, A.E., " Ferrocement and Thin Fiber Reinforced Cement Composities: Looking Back, Looking Ahead" Journal of Ferrocement, Vol. 31, No. 4, October 2001, pp 267-280.

72. Nanni, Antonio, "Flexural Behavior and Design of RC Members Using FRP Reinforcement", Journal of Structural Engineering, Vol. 119, No. 11, November, 1993, pp 3444-3459

73. Nassif, H.H., Chirravuri, G. and Sanders, M.C. " Flexural Behavior of Ferrocement / Concrete Composite Beams" Ferrocement 6: Lambot Symposium, Proceedings of the Sixth International Symposium on Ferrocement, Universty of Michigan, Michigan USA, June 1998, pp251 – 258.

74. Nassif, Hani H. and Najm, Husam, "Experimental and analytical Investigation of Ferrocement-Concrete Composite" Cement and Concrete Composite, Vol. 26, 2004, pp 787-796.

75. Nedwell, P.J. and Nakassa, A.S. " High Performance Ferrocement Using Steel Mesh and High Strength Mortar" Journal of Ferrocement: Vol. 29, No. 3, July 1999, pp 189-195.

76. Ohama, Y., and Shirai, A., "Durability of polymer-ferrocement", Journal of ferrocement, Vol 22, No1, 1992, pp 27-34.

77. Onet, Train, Magureanu, C., "Flexural Behaviour of Ferrocement Beams in Long-Term Loading" Journal of Ferrocement: Vol. 23, No. 3, July 1993, pp 199-206.

78. Onet, Train, Magureanu, C., and Vescan, V., " Aspects Concerning the Behavior of Ferrocement in Flexure" Journal of Ferrocement: Vol. 22, No. 1, January 1992, pp 1-16.

79. Papakonsatantinou, Christos G, Petrou, Michael F., and Harries, Kent A., "Fatigue Behavior of RC Beams Strengthened with GFRP Sheets", Journal of Composites for Construction, Vol. 5, No. 4, November, 2001, pp 246-253

80. Paramasivam, P., Lim, C.T.E. and, Ong, K.C.G. " Strengthening of RC Beams with Ferrocement Laminate" Cement and Concrete Composite, Vol. 20, 1998, pp 53-65.

81. Paramasivam, P.,Ong, K.C.G. and Lim, C.T.E., "Ferrocement Laminate for Strengthening of RC T-Beams" Cement and Concrete Composite, Vol. 16, 1994, pp 143-152.

82. Pham, Huy, and Al-Mahaidi, Riadh, "Assesment of available Prediction Models for the Strength of FRP Retrofitted RC Beams", Elsevier Composite Structures 2004, Vol. 66, , pp 601-610

83. Pisani, Marco A., "Evaluation of Bending Strength of RC Beams Strengthened with FRP Sheets", Journal of Composites for Construction, Vol. 10, No. 4, August, 2006, pp 313-320.

84. Prakhya, K.V.G., Rahul, T. and Adidam, S.R. " Ferrocement Plates with Light Weight Topping" Journal of Ferrocement: Vol. 18, No. 4, October 1988, pp 405-411.

85. Rafeeqi, S.F.A., Lodi, S.H., Wadalawala, Z.R. " Behaviour of Reinforced Concrete Beams Strengthened in Shear" Proceedings of the Seventh International Symposium on Ferrocement and Thin Reinforced Cement Composites, National University of Singapore, June 27-29, 2001 pp 453 – 463.

86. Rajagopalan, K. and Parameswaran, V.S. " Cracking and Ultimate Strength Characteristics of Ferrocement in Direct Tension and in Pure Bending" Indian Concrete Journal, December 1974, pp 387 – 395.

87. Ramesht, M.H., and Nedwell, P.J. " The Influence of Transverse wires on Yield and Ultimate Strength of Ferrocement in Flexure" Journal of Ferrocement: Vol. 24, No. 3, July 1994, pp 225-229.

88. Ravinderarajah, R. S. And Paramasivam, P. " Effect of Arrangement of Reinforcement on Mechanical Properties of Ferrocement" ACI Structural Journal, January – February 1988, pp 3-11.

89. Ravinderarajah, R. S. And Paramasivam, P. " Influence of Weathering on Ferrocement Properties" Journal of Ferrocement: Vol. 16, No. 1, January 1986, pp 1-11.

90. Razaqpur, A. Ghani, and Isgor, O. Burkan,, "Proposed Shear Design Method for FRP –Reinforced Concrete Members without Stirrups", ACI Structural Journal, Vol. 103, No. 1, January-February 2006, pp 93-102.

91. Ritchie, Philip A., Thomas, David A., Lu, Le-Wu and Connelly, Guy M. " External Reinforcement of Concrete Beams Using Fibre Reinforced Plastics " ACI Structural Journal, Vol. 88, No. 4, July – August 1991, pp 490--500.

92. Saadatmanesh, H., and Malek, A.M., "Design Guidelines for Flexural Strengthening of RC Beams with FRP Plates", Journal of Composites for Construction, Vol. 2, No. 4, November 1998, pp 158-164.

93. Saadatmanesh, Hamid, and Ehsani, Mohammad R., "RC Beams Strengthened with FRP Plates I: Experimental Study", Journal of Structural Engineering, Vol. 117, No. 11, November, 1991, pp 3417-3433.

94. Sehgal, V.K., Bhandari, N.M., and Kaushik, S.K., "Ferrocement Box Girder Elements for Roofs and Floors", Proc. 3rd International Conference Ferrocement, Department of Civil Engineering, University of Roorkee, 1988, pp 551-560

95. Seshu, D.R. " Flexural Behavior of Ferrocement Confined Reinforced Concrete (FCRC) Simply Supported Beams" Journal of Ferrocement: Vol. 30, No. 3, July 2000, pp 261-273.

96. Sheikh, Shamim A, DeRose, David and Mardukhi, Jamil " Retrofitting of Concrete Structures for Shear and Flexure with Fibre Reinforced Polymers" ACI Structural Journal, Vol. 99, No. 4, July- August 2002, pp 451-459.

97. Sheikh, Shamim A., "Performance of Concrete Structures Retrofitted with Fibre Reinforced Polymers", Elsevier Engineering Structures, Vol. 22, 2002, pp 869-879.

98. Singh, K.K., Kaushik, S.K. and Prakash, Anand " Ferrocement Composite Columns" Proceedings of 3rd International Conference Ferrocement, Department of Civil Engineering, University of Roorkee, 1988, pp 296 – 305.

99. Singh, S.K., Kaushik, S.K., "Flexural Strengthening of Reinforced Concrete Beams By Ferrocement", Maharshtra India Chapter of ACI, 1997, pp 17-24.

100. Singh, K.K., Kaushik, S.K., and Prakash, A., "Strengthening of Brick Masonry Columns by Ferrocement," Proceedings of the Third International Symposium on Ferrocement, University of Roorkee, 1998, pp. 306-315.

101. SP: 16, Design Aids for Reinforced Concrete to IS: 456-1978, Bureau of Indian Standard, New Delhi.

102. Takiguchi, K. and Abdullah " Ferrocement as Strengthening and Repairing Material for R/C Columns" Seventh International Symposium on Ferrocement and Thin Reinforced Cement Composites, National University of Singapore, 27-29, June 2001, pp 441- 452.

103. Teng J.G., Chen J.F., Smith, S.T., "FRP Strengthened RC Structures" John Wiley Publications, 2002

104. Teng, J.G., lam, L., Chan, W., and Wang, J., "Retrofitting of Deficient RC Cantilever Slabs Using GFRP Strips", Journal of Composites for Construction, Vol. 4, No. 2, May, 2000, pp 75-84

105. Toutanji, Houssam A. and Gomez, William " Durability Characteristics of Concrete Beams Externally Bonded with FRP Composite Sheets" Cement and Concrete Composite, Vol 19, 1997, pp 351-358.

106. Triantafillou, Thanasis C., "Shear Strengthening of Reinforced Concrete Beams Using Epoxy-Bonded FRP Composites", ACI Structural Journal, Vol. 95, No. 2, March-April 1998, pp 107-115

107. Tsai, Hsiang-Chuan and Lin, Guan-Cheng (1993), "Optimum Tuned-Mass dampers for Minimizing Steady-State Response of Support –Excited and Damped System", Earthquake Engineering and Structural Dynamics, Vol. 22, pp 957-973.

108. Vidivelli, B., Antiny Jeyasehar, C., and Srividya, P.R., " Repair and Rehablitation of Reinforced Concrete Beams by Ferrocement" Seventh International Symposium on Ferrocement and Thin Reinforced Cement Composites, National University of Singapore, 27-29, June 2001, pp 465- 471.

109. Wang, Y.C., "Analytical and Experimental Study on Seismic Performance of RC T-Beams with design Deficiency in Steel Bar Curtailment ", Elsevier Engineering Structures, Vol. 25, 2003, pp 215-227

110. Wasti, S.T., Erberik, M.A., Sucuoglu, H.., and Kaur, C., "Studies on Strengthening of Rural Structures Damaged in the 1995 Dinar Earthquakes," Proceedings of the Eleventh European Conference on Earthquake Engineering, Paris, France (1998).

111. White, R.N. (1995), "Seismic Rehabilitation of Non-Ductile Reinforced Concrete Frames – A Summary of issues, Methods and Needs", Proceedings,

Workshop on the Seismic Rehabilitation of Lightly Reinforced Concrete Frames, Gaithersburg, USA, June 12 –13, National Institute of Standards and Technology, pp 39-71

112. Xiong, Guangjing, Liu, Jinwei and Xie, Huicai " Flexural Behavior of Reinforced Concrete Beams with Unbonded Repair Patch" ACI Structural Journal, Vol. 97, No. 5, September – October 2000, pp 783-786.

APPENDIX A

MAXIMUM LOAD CARRYING CAPACITY OF THE RETROFITTED BEAMS

The calculation of maximum load carrying capacity of balanced beam section retrofitted using ferrocement jacket having two layers of woven wire mesh as reinforcement using the procedure described in section 7.1.1 is shown below

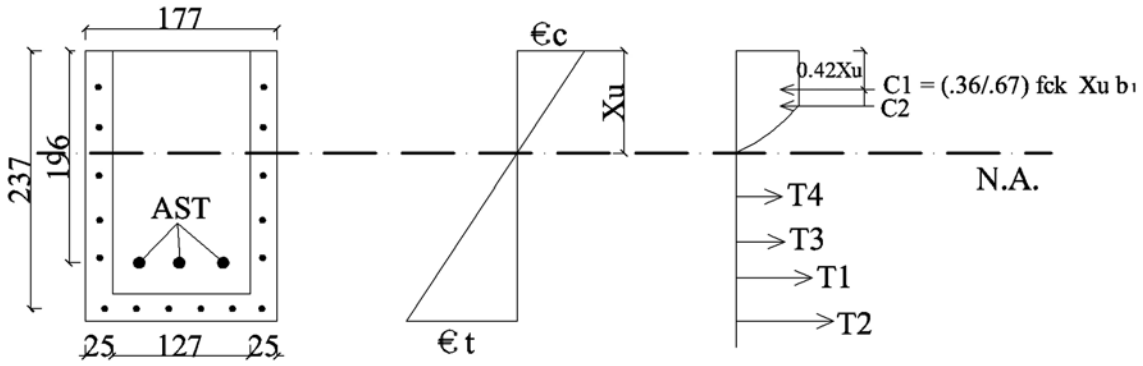

t = 25 mm

b_1 = 127 + 25 +25 = 177 mm

f_{ck} = 28 N/mm^2

$A_{st1} = \frac{3x\pi x12^2}{4}$ = 339.29 mm^2

f_y = 452 N/mm^2 (For 12 mm diameter bars)

$A_{st2} = \frac{2x6x\pi x2.4^2}{4}$ = 54.28 mm^2

f_y = 451 N/mm^2 (For wire)

$\Sigma C = 0.542 b_1 f_{ck} x_u + \Sigma (A_{wsc}) \times f_y$

$= 0.542x177x28x_u + 451 \times 9.05 \times 2$

$\Sigma T = T_1 + T_2 + T_3 \ldots\ldots$

$= 339.29 \times 452 + 451 \times 54.28 + 9.05 \times 2 (5 \times 451)$

Equating $\Sigma C = \Sigma T$

$0.542x177x28x_u$ + 451 x 9.05 x 2 = 339.29 x 452 + 451 x 54.28 + 9.05 x 2 (5 x 451)

x_u = 78.35 mm

Now Ultimate moment of resistance M_u is given by

$M_u = T_1(d - 0.42x_u) + T_2(d_1 - 0.42x_u) + Tn(d_n - 0.42x_u)$

= 452 x 339.29 x (196 –0.42 x 78.35) + 451 x 54.28 x (237 – 0.42x 78.35)
+ 451 x 2 x 9.05 x (174.09+144.09+114.09+84.09)

= 34.22 KNm

So $P_u = \frac{2M_u}{Shearspan}$

$= \frac{2x34.22}{1.375}$

P_{max} = 49.7 kN

APPENDIX B

SAFE LOAD CARRYING CAPACITY OF THE RETROFITTED BEAMS

The calculation of safe load carrying capacity of balanced section initially stressed to 60 percent of the safe load and retrofitted with ferrocement laminate having two layers of woven wire mesh by the proposed procedure as described in section 7.1.2 is given below

Firstly the effective moment of inertia of reinforced cement concrete balanced section at 60 percent of safe load carrying capacity of the control beam is calculated as per procedure specified

Safe Load carrying Capacity of Balanced Section = 19.875 KN

60 percent of Safe Load Carrying Capacity = 11.925 KN

Bending Moment in beam = 1.375 x 11.925x 0.5

= 8.19 KNm

$I_{gr} = \frac{127x227^3}{12}$

$= 1.238 \times 10^8$ mm^4

$E_c = 5000\sqrt{f_{ck}} = 5000\sqrt{28}$

$= 26457.51$ N/mm^2

$E_s = 215000$ N/mm^2

$m = \frac{E_s}{E_c} = 8.14$

$f_{cr} = 0.7\sqrt{f_{ck}} = 0.7\sqrt{28}$

$= 3.7$ N/mm^2

$y_t = \frac{D}{2} = \frac{227}{2}$

$M_r = \frac{f_{cr} x I_{gr}}{y_t} = \frac{3.7x1.238x10^8 x2}{227}$

$= 4.035$ KNm

assuming $\frac{d'}{d} = 0.15$

$p_c = \frac{2x50.26}{127x227} = 0.349$ percent

$p_t = \frac{113.097x3}{127x227} = 1.177$ percent

$\frac{p_c(m-1)}{p_t m} = 0.26$

$p_t m = 9.58$

Using table 89 of SP-16

$\frac{I_r}{I_{gr}} = 0.6684$

$I_r = 0.6684 \times 1.238 \times 10^8$

$= 8.274 \times 10^7$ mm^4

Using table 93 of SP-16

$\frac{x}{d} = 0.3416$

$1-\frac{x}{d} = 0.6584$

$1-\frac{x}{3d} = 0.886$

So $I_{eff} = \frac{I_r}{1.2-\frac{M_r}{M}\left(1-\frac{X_u}{3d}\right)\left(1-\frac{X_u}{d}\right)\frac{b_w}{b_f}}$

$\frac{I_{eff}}{I_r} = \frac{1}{1.2-\frac{4.035}{8.19}x0.886x0.6584x1}$

$I_{eff} = 92921521$ mm^4

Now gross area of the beam intiaaly stressed to 60 percent of safe load and retrofitted using ferrocement Jacketing having two layers of woven wire mesh is

I_{gr} = Effective MOI of control beam at 60 percent of safe load (i.e. 11.925 KN)

\+ MOI of U-shaped laminate about an axis passing through d'/2

Now

Effective MOI of control beam at 60 percent of safe load (i.e. 11.925 KN)

= 92921521 mm^4

MOI of U-shaped 25 mm thick ferrocement laminate about an axis passing through d'/2

= 1.077×10^8 mm^4

So I_{gr} = $92921521 + 1.077 \times 10^8$

= 2.01×10^8 mm^4

f_{cr} is the modulus of rupture for RCC ferrocement composite beams is given by

f_{cr} = $20p' + 34$ kg/cm^2 (S.K. Singh & S.K. Kaushik)

where p' = $A_{st2} \times \frac{100}{b't}$

= $\frac{2x27.14x100}{177x25}$

= 1.227 percent

f_{cr} = $20 \times 1.227 + 34$ kg/cm^2

= 5.74 N/mm^2

M_r is the cracking moment and is given by $\frac{f_{cr} I_{gr}}{y_t}$

M_r = $\frac{5.74x2.01x10^8}{126}$

= 9.15 KNm

assuming $\frac{d'}{d}$ = 0.15

p_c = $\frac{2x50.26}{177x252}$ = 0..225 percent

p_t = $\frac{113.097x3 + 2x27.14}{177x252}$ = 0.882 percent

$\frac{p_c(m-1)}{p_t m}$ = 0.224

$p_t m$ = 7.18

Using table 89 of SP-16

$\frac{I_r}{I_{gr}}$ = 0.5336

I_r = $0.5336 \times 2.01 \times 10^8$

$$= \quad 1.07 \times 10^8 \text{ mm}^4$$

Using table 93 of SP-16

$$\frac{x}{d} = 0.367$$

$$1-\frac{x}{d} = 0.633$$

$$1-\frac{x}{3d} = 0.878$$

So $$I_{eff} = \frac{I_r}{1.2-\frac{M_r}{M}\left(1-\frac{X_u}{3d}\right)\left(1-\frac{X_u}{d}\right)\frac{b_w}{b_f}}$$

$$\frac{I_{eff}}{I_r} = \frac{1}{1.2-\frac{9.15}{Px0.6875}x0.878x0.633x1}$$

$$I_{eff} = \frac{1.07x10^8}{1.2-\frac{9.15}{Px0.6875}x0.878x0.633x1} \qquad I_r \le I_{eff} \le I_{gr}$$

$$\Delta = \frac{M(3L^2-4a^2)}{24E_cI_{eff}}$$

Now substituting the value of I_{eff} in the equation given above the value of 'P' corresponding to Δ equal to L/250 i.e. 15mm can be calculated. In this case it comes out to be

$$\mathbf{P_{safe} = 24.0\ KN}$$

APPENDIX C

IDEALIZATION OF LOAD DEFLECTION CURVE

The load deflection data obtained from the testing of the beams is plotted and the load deflection curve thus obtained is idealized as quadri-linear curve for the purpose of calculating ductility ratio and toughness of the beam. The ductility ratio is defined as the ratio of deflection at ultimate load (defined as 0.85 of maximum load) to the deflection at yield load. Whereas, toughness is the area under the idealized load deflection curve upto the ultimate load.

The idealized load deflection curve is obtained by linearly joining four points starting from the origin. Each of these four points are located on the curve as explained below.

1. Elastic load point (P_E), is the load upto which load deflection curve is linear.
2. Yield load point (P_Y), is the load at which the yielding of the beam starts, which is obtained by drawing a tangent to the elastic load point and maximum load point on the curve.
3. Maximum load point (P_{max}), and
4. Ultimate load point (P_U), defined as the point at which the load drops to 85% of the maximum load.

The calculation of above parameters for one such idealized curve, shown on the next page, are as below.

P_E	=	32 kN	Δ_E	=	27.79 mm
P_Y	=	36 kN	Δ_Y	=	32.8 mm
P_{max}	=	37 kN	Δ_{max}	=	38.66 mm
P_U	=	31.45 kN	Δ_U	=	54.68 mm

The toughness is given by the area under the idealized curve and is equal to

$$\text{Toughness} = A_1 + A_2 + A_3 + A_4$$

Where

$$A_1 = \frac{1}{2} x 27.79 x 32 = 444.64 \text{ kN-mm}$$

$A_2 = \frac{1}{2} x(32+36)x(32.8-27.79) = 170.34$ kN-mm

$A_3 = \frac{1}{2} x(36+37)x(38.66-32.8) = 213.89$ kN-mm

$A_4 = \frac{1}{2} x(37+31.45)x(54.68-38.66) = 548.28$ kN-mm

So,

Toughness = 444.64 + 170.34 + 213.89 + 548.28 = 1377.15 kN-mm

and ductility ratio is given by

Δ_U / Δ_Y = 54.68 / 32.8 = 1.67